NIST SPECIAL PUBLICATION 260-121

U.S. DEPARTMENT OF COMMERCE/Technology Administration
National Institute of Standards and Technology

Standard Reference Materials:

Certification of a Standard Reference Material for the Determination of Interstitial Oxygen Concentration in Semiconductor Silicon by Infrared Spectrophotometry

Brian G. Rennex

The National Institute of Standards and Technology was established in 1988 by Congress to "assist industry in the development of technology . . . needed to improve product quality, to modernize manufacturing processes, to ensure product reliability . . . and to facilitate rapid commercialization . . . of products based on new scientific discoveries."

NIST, originally founded as the National Bureau of Standards in 1901, works to strengthen U.S. industry's competitiveness; advance science and engineering; and improve public health, safety, and the environment. One of the agency's basic functions is to develop, maintain, and retain custody of the national standards of measurement, and provide the means and methods for comparing standards used in science, engineering, manufacturing, commerce, industry, and education with the standards adopted or recognized by the Federal Government.

As an agency of the U.S. Commerce Department's Technology Administration, NIST conducts basic and applied research in the physical sciences and engineering and performs related services. The Institute does generic and precompetitive work on new and advanced technologies. NIST's research facilities are located at Gaithersburg, MD 20899, and at Boulder, CO 80303. Major technical operating units and their principal activities are listed below. For more information contact the Public Inquiries Desk, 301-975-3058.

Technology Services
- Manufacturing Technology Centers Program
- Standards Services
- Technology Commercialization
- Measurement Services
- Technology Evaluation and Assessment
- Information Services

Electronics and Electrical Engineering Laboratory
- Microelectronics
- Law Enforcement Standards
- Electricity
- Semiconductor Electronics
- Electromagnetic Fields[1]
- Electromagnetic Technology[1]

Chemical Science and Technology Laboratory
- Biotechnology
- Chemical Engineering[1]
- Chemical Kinetics and Thermodynamics
- Inorganic Analytical Research
- Organic Analytical Research
- Process Measurements
- Surface and Microanalysis Science
- Thermophysics[2]

Physics Laboratory
- Electron and Optical Physics
- Atomic Physics
- Molecular Physics
- Radiometric Physics
- Quantum Metrology
- Ionizing Radiation
- Time and Frequency[1]
- Quantum Physics[1]

Manufacturing Engineering Laboratory
- Precision Engineering
- Automated Production Technology
- Robot Systems
- Factory Automation
- Fabrication Technology

Materials Science and Engineering Laboratory
- Intelligent Processing of Materials
- Ceramics
- Materials Reliability[1]
- Polymers
- Metallurgy
- Reactor Radiation

Building and Fire Research Laboratory
- Structures
- Building Materials
- Building Environment
- Fire Science and Engineering
- Fire Measurement and Research

Computer Systems Laboratory
- Information Systems Engineering
- Systems and Software Technology
- Computer Security
- Systems and Network Architecture
- Advanced Systems

Computing and Applied Mathematics Laboratory
- Applied and Computational Mathematics[2]
- Statistical Engineering[2]
- Scientific Computing Environments[2]
- Computer Services[2]
- Computer Systems and Communications[2]
- Information Systems

---

[1] At Boulder, CO 80303.
[2] Some elements at Boulder, CO 80303.

NIST Special Publication 260-121

Standard Reference Materials:

Certification of a Standard Reference Material for the Determination of Interstitial Oxygen Concentration in Semiconductor Silicon by Infrared Spectrophotometry

Brian G. Rennex

Semiconductor Electronics Division
Electronics and Electrical Engineering Laboratory
National Institute of Standards and Technology
Gaithersburg, MD 20899-0001

U.S. DEPARTMENT OF COMMERCE, Ronald H. Brown, Secretary
TECHNOLOGY ADMINISTRATION, Mary L. Good, Under Secretary for Technology
NATIONAL INSTITUTE OF STANDARDS AND TECHNOLOGY, Arati Prabhakar, Director

Issued August 1994

National Institute of Standards and Technology Special Publication 260–121
Natl. Inst. Stand. Technol. Spec. Publ. 260–121, 81 pages (Aug. 1994)
CODEN: NSPUE2

U.S. GOVERNMENT PRINTING OFFICE
WASHINGTON: 1994

For sale by the Superintendent of Documents, U.S. Government Printing Office, Washington, DC 20402–9325

Preface

Standard Reference Materials (SRMs) as defined by the National Institute of Standards and Technology (NIST) are well-characterized materials, produced in quantity and certified for one or more physical or chemical properties. They are used to assure the accuracy and compatibility of measurements throughout the Nation. SRMs are widely used as primary standards in many diverse fields in science, industry, and technology, both within the United States and throughout the world. They are also used extensively in the fields of environmental and clinical analysis. In many applications, traceability of quality control and measurement processes to the national measurement system is carried out through the mechanism and use of SRMs. For many of the Nation's scientists and technologists, it is therefore of more than passing interest to know the details of the measurements made at NIST in arriving at the certified values of the SRMs produced. The NIST Special Publication 260 Series is a series of papers reserved for this purpose.

The 260 Series is dedicated to the dissemination of information on different phases of the preparation, measurement, certification, and use of NIST SRMs. In general, much more detail will be found in these papers than is generally allowed, or desirable, in scientific journal articles. This enables the user to assess the validity and accuracy of the measurement processes employed, to judge the statistical analysis, and to learn details of techniques and methods utilized for work entailing greatest care and accuracy. These papers also should provide sufficient additional information so SRMs can be utilized in new applications in diverse fields not foreseen at the time the SRM was originally issued.

Inquiries concerning the technical content of this paper should be directed to the author(s). Other questions concerned with the availability, delivery, price, and so forth, will receive prompt attention from:

Standard Reference Materials Program
Bldg. 202, Rm. 204
National Institute of Standards and Technology
Gaithersburg, MD 20899
Telephone: (301) 975-6776
FAX: (301) 948-3730

Thomas E. Gills, Chief
Standard Reference Materials Program

ACKNOWLEDGMENTS

The following contributions to this report are gratefully acknowledged: A. Baghdadi, R. I. Scace, and E. J. Walters for their preparation of the report for the Grand Round Robin which laid the ground-work for this report; A. Baghdadi for early contributions to the test methods for measurement of oxygen in silicon and for envisioning and beginning the current work; J. J. Filliben of the NIST Statistical Engineering Division for review of the statistical treatment of data; D. R. Ricks and J. M. Thomas of the NIST Semiconductor Electronics Division for specimen preparation; the Materials Technology Group of the Semiconductor Electronics Division for support of the SRM development; N. M. Trahey and T. E. Gills of the NIST Office of Standards Reference Materials for funding support; J. P. Ehrstein for constant feedback and careful review of the various ideas of value to the study; and J. C. Geist for many insightful remarks on experimental aspects of the project.

OTHER NIST PUBLICATIONS IN THIS SERIES

Trahey, N.M., ed., NIST Standard Reference Materials Catalog 1992-93, NIST Spec. Publ. 260 (February 1992). SN003-003-03146-1*

Michaelis, R.E., and Wyman, L.L., Standard Reference Materials: Preparation of White Cast Iron Spectrochemical Standards, NBS Misc. Publ. 260-1 (June 1964). COM74-11061**

Michaelis, R.E., Wyman, L.L., and Flitsch, R., Standard Reference Materials: Preparation of NBS Copper-Base Spectrochemical Standards, NBS Misc. Publ. 260-2 (October 1964). COM74-11063**

Michaelis, R.E., Yakowitz, H., and Moore, G.A., Standard Reference Materials: Metallographic Characterization of an NBS Spectrometric Low-Alloy Steel Standard, NBS Misc. Publ. 260-3 (October 1964). COM74-11060**

Hague, J.L., Mears, T.W., and Michaelis, R.E., Standard Reference Materials: Sources of Information, Publ. 260-4 (February 1965). COM74-11059**

Alvarez, R., and Flitsch, R., Standard Reference Materials: Accuracy of Solution X-Ray Spectrometric Analysis of Copper-Base Alloys, NBS Misc. Publ. 260-5 (February 1965). PB168068**

Shultz, J.I., Standard Reference Materials: Methods for the Chemical Analysis of White Cast Iron Standards, NBS Misc. Publ. 260-6 (July 1965). COM74-11068**

Bell, R.K., Standard Reference Materials: Methods for the Chemical Analysis of NBS Copper-Base Spectrochemical Standards, NBS Misc. Publ. 260-7 (October 1965). COM74-11067**

Richmond, M.S., Standard Reference Materials: Analysis of Uranium Concentrates at the National Bureau of Standards, NBS Misc. Publ. 260-8 (December 1965). COM74-11066**

Anspach, S.C., Cavallo, L.M., Garfinkel, S.B., et al., Standard Reference Materials: Half Lives of Materials Used in the Preparation of Standard Reference Materials of Nineteen Radioactive Nuclides Issued by the National Bureau of Standards, NBS Misc. Publ. 260-9 (November 1965). COM74-11065**

Yakowitz, H., Vieth, D.L., Heinrich, K.F.J., et al., Standard Reference Materials: Homogeneity Characterization of NBS Spectrometric Standards II: Cartridge Brass and Low-Alloy Steel, NBS Misc. Publ. 260-10 (December 1965). COM74-11064**

Napolitano, A., and Hawkins, E.G., Standard Reference Materials: Viscosity of Standard Lead-Silica Glass, NBS Misc. Publ. 260-11** (November 1966).

Yakowitz, H., Vieth, D.L., and Michaelis, R.E., Standard Reference Materials: Homogeneity Characterization of NBS Spectrometric Standards III: White Cast Iron and Stainless Steel Powder Compact, NBS Misc. Publ. 260-12 (September 1966).

Spijkerman, J.J., Snediker, D.K., Ruegg, F.C., et al., Standard Reference Materials: Mossbauer Spectroscopy Standard for the Chemical Shift of Iron Compounds, NBS Misc. Publ. 260-13** (July 1967).

Menis, O., and Sterling, J.T., Standard Reference Materials: Determination of Oxygen in Ferrous Materials (SRMs 1090, 1091, 1092), NBS Misc. Publ. 260 14** (September 1966).

Passaglia, E. and Shouse, P.J., Standard Reference Materials: Recommended Method of Use of Standard Ligh-Sensitive Paper for Calibrating Carbon Arcs Used in Testing Testiles for Colorfastness to Light, NBS Spec. Publ. 260-15 (July 1967). Superseded by SP 260-41.

Yakowitz, H., Michaelis, R.E., and Vieth, D.L., Standard Reference Materials: Homogeneity Characterization of NBS Spectrometric Standards IV: Preparation and Microprobe Characterization of W-20% Mo Alloy Fabricated by Powder Metallurgical Methods, NBS Spec. Publ. 260-16 (January 1969). COM74-11062**

Catanzaro, E.J., Champion, C.E., Garner, E.L., et al., Standard Reference Materials: Boric Acid; Isotopic, and Assay Standard Reference Materials, NBS Spec. Publ. 260-17 (February 1970). PB189457**

Geller, S.B., Mantek, P.A., and Cleveland, N.G., Calibration of NBS Secondary Standards Magnetic Tape. Computer Amplitude Reference Amplitude Measurement "Process A", NBS Spec. Publ. 260-18 (November 1969). Superseded by SP 260-29.

Paule, R.C., and Mandel, J., Standard Reference Materials: Analysis of Interlaboratory Measurements on the Vapor Pressure of Gold (Certification of SRM 745). NBS Spec. Publ. 260-19 (January 1970). PB190071**

260-20: Unassigned

Paule, R.C., and Mandel, J., Standard Reference Materials: Analysis of Interlaboratory Measurements on the Vapor Pressures of Cadmium and Silver, NBS Spec. Publ. 260-21 (January 1971). COM74-11359**

Yakowitz, H., Fiori, C.E., and Michaelis, R.E., Standard Reference Materials: Homogeneity Characterization of Fe-3 Si Alloy, NBS Spec. Publ. 260-22 (February 1971). COM74-11357**

Napolitano, A., and Hawkins, E.G., Standard Reference Materials: Viscosity of a Standard Borosilicate Glass, NBS Spec. Publ. 260-23 (December 1970). COM71-00157**

Sappenfield, K.M., Marinenko, G., and Hague, J.L., Standard Reference Materials: Comparison of Redox Standards, NBS Spec. Publ. 260-24 (January 1972). COM72-50058**

Hicho, G.E., Yakowitz, H., Rasberry, S.D., et al., Standard Reference Materials: A Standard Reference Material Containing Nominally Four Percent Austenite, NBS Spec. Publ. 260-25 (February 1971). COM74-11356**

Martin, J.F., Standard Reference Materials: NBS-U.S. Steel Corp. Joint Program for Determining Oxygen and Nitrogen in Steel, NBS Spec. Publ. 260-26 (February 1971). PB 81176620**

Garner, E.L., Machlan, L.A., and Shields, W.R., Standard Reference Materials: Uranium Isotopic Standard Reference Materials, NBS Spec. Publ. 260-27 (April 1971). COM74-11358**

Heinrich, K.F.J., Myklebust, R.L., Rasberry, S.D., et al., Standard Reference Materials: Preparation and Evaluation of SRMs 481 and 482 Gold-Silver and Gold-Copper Alloys for Microanalysis, NBS Spec. Publ. 260-28 (August 1971). COM71-50365**

Geller, S.B., Standard Reference Materials: Calibration of NBS Secondary Standard Magnetic Tape (Computer Amplitude Reference) Using the Reference Tape Amplitude Measurement "Process A-Model 2," NBS Spec. Publ. 260-29 (June 1971). COM71-50282** Supersedes Measurement System in SP 260-18.

Gorozhanina, R.S., Freedman, A.Y., and Shaievitch, A.B., (translated by M.C. Selby), Standard Reference Materials: Standard Samples Issued in the USSR (A Translation from the Russian), NBS Spec. Publ. 260-30 (June 1971). COM71-50283**

Hust, J.G., and Sparks, L.L., Standard Reference Materials: Thermal Conductivity of Electrolytic Iron SRM 734 from 4 to 300 K, NBS Spec. Publ. 260-31 (November 1971). COM71-50563**

Mavrodineanu, R., and Lazar, J.W., Standard Reference Materials: Standard Quartz Cuvettes for High Accuracy Spectrophotometry, NBS Spec. Publ. 260-32 (December 1973). COM74-50018**

Wagner, H.L., Standard Reference Materials: Comparison of Original and Supplemental SRM 705, Narrow Molecular Weight Distribution Polystyrene, NBS Spec. Publ. 260-33 (May 1972). COM72-50526**

Sparks, L.L., and Hust, J.G., Standard Reference Material: Thermoelectric Voltage of Silver-28 Atomic Percent Gold Thermocouple Wire, SRM 733, Verses Common Thermocouple Materials (Between Liquid Helium and Ice Fixed Points), NBS Spec. Publ. 260-34 (April 1972). COM72-50371**

Sparks, L.L., and Hust, J.G., Standard Reference Materials: Thermal Conductivity of Austenitic Stainless Steel, SRM 735 from 5 to 280 K, NBS Spec. Publ. 260-35 (April 1972). COM72-50368**

Cali, J.P., Mandel, J., Moore, L.J., et al., Standard Reference Materials: A Reference Method for the Determination of Calcium in Serum NBS SRM 915, NBS Spec. Publ. 260-36 (May 1972). COM72-50527**

Shultz, J.I., Bell, R.K., Rains, T.C., et al., Standard Reference Materials: Methods of Analysis of NBS Clay Standards, NBS Spec. Publ. 260-37 (June 1972). COM72-50692**

Richard, J.C., and Hsia, J.J., Standard Reference Materials: Preparation and Calibration of Standards of Spectral Specular Reflectance, NBS Spec. Publ. 260-38 (May 1972). COM72-50528**

Clark, A.F., Denson, V.A., Hust, J.G., et al., Standard Reference Materials: The Eddy Current Decay Method for Resistivity Characterization of High-Purity Metals, NBS Spec. Publ. 260-39 (May 1972). COM72-50529**

McAdie, H.G., Garn, P.D., and Menis, O., Standard Reference Materials: Selection of Differential Thermal Analysis Temperature Standards Through a Cooperative Study (SRMs 758, 759, 760), NBS Spec. Publ. 260-40 (August 1972) COM72-50776**

Wood. L.A., and Shouse, P.J., Standard Reference Materials: Use of Standard Light-Sensitive Paper for Calibrating Carbon Arcs Used in Testing Textiles for Colorfastness to Light, NBS Spec. Publ. 260-41 (August 1972). COM72-50775**

Wagner, H.L., and Verdier, P.H., eds., Standard Reference Materials: The Characterization of Linear Polyethylene, SRM 1475, NBS Spec. Publ. 260-42 (September 1972). COM72-50944**

Yakowitz, H., Ruff, A.W., and Michaelis, R.E., Standard Reference Materials: Preparation and Homogeneity Characterization of an Austenitic Iron-Chromium-Nickel Alloy, NBS Spec. Publ. 260-43 (November 1972). COM73-50760**

Schooley, J.F., Soulen, R.J., Jr., and Evans, G.A., Jr., Standard Reference Materials: Preparation and Use of Superconductive Fixed Point Devices, SRM 767, NBS Spec. Publ. 260-44 (December 1972). COM73-50037**

Greifer, B., Maienthal, E.J., Rains, T.C., et al., Standard Reference Materials: Development of NBS SRM 1579 Powdered Lead-Based Paint, NBS Spec. Publ. 260-45 (March 1973). COM73-50226**

Hust, J.G., and Giarratano, P.J., Standard Reference Materials: Thermal Conductivity and Electrical Resistivity Standard Reference Materials: Austenitic Stainless Steel, SRMs 735 and 798, from 4 to 1200 K, NBS Spec. Publ. 260-46 (March 1975). COM75-10339**

Hust, J.G., Standard Reference Materials: Electrical Resistivity of Electrolytic Iron, SRM 797, and Austenitic Stainless Steel, SRM 798, from 5 to 280 K, NBS Spec. Publ. 260-47 (February 1974). COM74-50176**

Mangum, B.W., and Wise, J.A., Standard Reference Materials: Description and Use of Precision Thermometers for the Clinical Laboratory, SRM 933 and SRM 934, NBS Spec. Publ. 260-48 (May 1974). Superseded by NIST Spec. Publ. 260-113. COM74-50533**

Carpenter, B.S., and Reimer, G.M., Standard Reference Materials: Calibrated Glass Standards for Fission Track Use, NBS Spec. Publ. 260-49 (November 1974). COM74-51185**

Hust, J.G., and Giarratano, P.J., Standard Reference Materials: Thermal Conductivity and Electrical Resistivity Standard Reference Materials: Electrolytic Iron, SRMs 734 and 797 from 4 to 1000 K, NBS Spec. Publ. 260-50 (June 1975). COM75-10698**

Mavrodineanu, R., and Baldwin, J.R., Standard Reference Materials: Glass Filters As a SRM for Spectrophotometry-Selection, Preparation, Certification, and Use-SRM 930 NBS Spec. Publ. 260-51 (November 1975). COM75-10339**

Hust, J.G., and Giarratano, P.J., Standard Reference Materials: Thermal Conductivity and Electrical Resistivity SRMs 730 and 799, from 4 to 3000 K, NBS Spec. Publ. 260-52 (September 1975). COM75-11193**

Durst, R.A., Standard Reference Materials: Standardization of pH Measurements, NBS Spec. Publ. 260-53 (December 1978). Superseded by SP 260-53 Rev. 1988 Edition. PB88217427**

Burke, R.W., and Mavrodineanu, R., Standard Reference Materials: Certification and Use of Acidic Potassium Dichromate Solutions as an Ultraviolet Absorbance Standard, NBS Spec. Publ. 260-54 (August 1977). PB272168**

Ditmars, D.A., Cezairliyan, A., Ishihara, S., et al., Standard Reference Materials: Enthalpy and Heat Capacity; Molybdenum SRM 781, from 273 to 2800 K, NBS Spec. Publ. 260-55 (September 1977). PB272127**

Powell, R.L., Sparks, L.L., and Hust, J.G., Standard Reference Materials: Standard Thermocouple Material, Pt-67: SRM 1967, NBS Spec. Publ. 260-56 (February 1978). PB277172**

Cali, J.P., and Plebanski, T., Standard Reference Materials: Guide to United States Reference Materials, NBS Spec. Publ. 260-57 (February 1978). PB277173**

Barnes, J.D., and Martin, G.M., Standard Reference Materials: Polyester Film for Oxygen Gas Transmission Measurements SRM 1470, NBS Spec. Publ. 260-58 (June 1979). PB297098**

Chang, T., and Kahn, A.H., Standard Reference Materials: Electron Paramagnetic Resonance Intensity Standard: SRM 2601; Description and Use, NBS Spec. Publ. 260-59 (August 1978). PB292097**

Velapoldi, R.A., Paule, R.C., Schaffer, R., et al., Standard Reference Materials: A Reference Method for the Determination of Sodium in Serum, NBS Spec. Publ. 260-60 (August 1978). PB286944**

Verdier, P.H., and Wagner, H.L., Standard Reference Materials: The Characterization of Linear Polyethylene (SRMs 1482, 1483, 1484), NBS Spec. Publ. 260-61 (December 1978). PB289899**

Soulen, R.J., and Dove, R.B., Standard Reference Materials: Temperature Reference Standard for Use Below 0.5 K (SRM 768), NBS Spec. Publ. 260-62 (April 1979). PB294245**

Velapoldi, R.A., Paule, R.C., Schaffer, R., et al., Standard Reference Materials: A Reference Method for the Determination of Potassium in Serum, NBS Spec. Publ. 260-63 (May 1979). PB297207**

Velapoldi, R.A., and Mielenz, K.D., Standard Reference Materials: A Fluorescence SRM Quinine Sulfate Dihydrate (SRM 936), NBS Spec. Publ. 260-64 (January 1980). PB80132046**

Marinenko, R.B., Heinrich, K.F.J., and Ruegg, F.C., Standard Reference Materials: Micro-Homogeneity Studies of NBS SRM, NBS Research Materials, and Other Related Samples, NBS Spec. Publ. 260-65 (September 1979). PB300461**

Venable, W.H., Jr., and Eckerle, K.L., Standard Reference Materials: Didymium Glass Filters for Calibrating the Wavelength Scale of Spectrophotometers (SRMs 2009, 2010, 2013, 2014). NBS Spec. Publ. 260-66 (October 1979). PB80104961**

Velapoldi, R.A., Paule, R.C., Schaffer, R., et al., Standard Reference Materials: A Reference Method for the Determination of Chloride in Serum, NBS Spec. Publ. 260-67 (November 1979). PB80110117**

Mavrodineanu, R., and Baldwin, J.R., Standard Reference Materials: Metal-On-Quartz Filters as a SRM for Spectrophotometry SRM 2031, NBS Spec. Publ. 260-68 (April 1980). PB80197486**

Velapoldi, R.A., Paule, R.C., Schaffer, R., et al., Standard Reference Materials: A Reference Method for the Determination of Lithium in Serum, NBS Spec. Publ. 260-69 (July 1980). PB80209117**

Marinenko, R.B., Biancaniello, F., Boyer, P.A., et al., Standard Reference Materials: Preparation and Characterization of an Iron-Chromium-Nickel Alloy for Microanalysis: SRM 479a, NBS Spec. Publ. 260-70 (May 1981). SN003-003-02328-1*

Seward, R.W., and Mavrodineanu, R., Standard Reference Materials: Summary of the Clinical Laboratory Standards Issued by the National Bureau of Standards, NBS Spec. Publ. 260-71 (November 1981). PB82135161**

Reeder, D.J., Coxon, B., Enagonio, D., et al., Standard Reference Materials: SRM 900, Anti-epilepsy Drug Level Assay Standard, NBS Spec. Publ. 260-72 (June 1981). PB81220758

Interrante, C.G., and Hicho, G.E., Standard Reference Materials: A Standard Reference Material Containing Nominally Fifteen Percent Austenite (SRM 486), NBS Spec. Publ. 260-73 (January 1982). PB82215559**

Marinenko, R.B., Standard Reference Materials: Preparation and Characterization of K-411 and K-412 Mineral Glasses for Microanalysis: SRM 470, NBS Spec. Publ. 260-74 (April 1982). PB82221300**

Weidner, V.R., and Hsia, J.J., Standard Reference Materials: Preparation and Calibration of First Surface Aluminum Mirror Specular Reflectance Standards (SRM 2003a), NBS Spec. Publ. 260-75 (May 1982). PB82221367**

Hicho, G.E., and Eaton, E.E., Standard Reference Materials: A Standard Reference Material Containing Nominally Five Percent Austenite (SRM 485a), NBS Spec. Publ. 260-76 (August 1982). PB83115568**

Furukawa, G.T., Riddle, J.L., Bigge, W.G., et al., Standard Reference Materials: Application of Some Metal SRMs as Thermometric Fixed Points, NBS Spec. Publ. 260-77 (August 1982). PB83117325**

Hicho, G.E., and Eaton, E.E., Standard Reference Materials: Standard Reference Material Containing Nominally Thirty Percent Austenite (SRM 487), NBS Spec. Publ. 260-78 (September 1982). PB83115576**

Richmond, J.C., Hsia, J.J., Weidner, V.R., et al., Standard Reference Materials: Second Surface Mirror Standards of Specular Spectral Reflectance (SRMs 2023, 2024, 2025), NBS Spec. Publ. 260-79 (October 1982). PB84203447**

Schaffer, R., Mandel, J., Sun, T., et al., Standard Reference Materials: Evaluation by an ID/MS Method of the AACC Reference Method for Serum Glucose, NBS Spec. Publ. 260-80 (October 1982). PB84216894**

Burke, R.W., and Mavrodineanu, R., Standard Reference Materials: Accuracy in Analytical Spectrophotometry, NBS Spec. Publ. 260-81 (April 1983). PB83214536**

Weidner, V.R., Standard Reference Materials: White Opal Glass Diffuse Spectral Reflectance Standards for the Visible Spectrum (SRMs 2015 and 2016), NBS Spec. Publ. 260-82 (April 1983). PB83220723**

Bowers, G.N., Jr., Alvarez, R., Cali, J.P., et al., Standard Reference Materials: The Measurement of the Catalytic (Activity) Concentration of Seven Enzymes in NBS Human Serum (SRM 909), NBS Spec. Publ. 260-83 (June 1983). PB83239509**

Gills, T.E., Seward, R.W., Collins, R.J., et al., Standard Reference Materials: Sampling, Materials Handling, Processing, and Packaging of NBS Sulfur in Coal SRMs 2682, 2683, 2684, and 2685, NBS Spec. Publ. 260-84 (August 1983). PB84109552**

Swyt, D.A., Standard Reference Materials: A Look at Techniques for the Dimensional Calibration of Standard Microscopic Particles, NBS Spec. Publ. 260-85 (September 1983). PB84112648**

Hicho, G.E., and Eaton, E.E., Standard Reference Materials: A SRM Containing Two and One-Half Percent Austenite, SRM 488, NBS Spec. Publ. 260-86 (December 1983). PB84143296**

Mangum, B.W., Standard Reference Materials: SRM 1969: Rubidium Triple-Point - A Temperature Reference Standard Near 39.30° C, NBS Spec. Publ. 260-87 (December 1983). PB84149996**

Gladney, E.S., Burns, C.E., Perrin, D.R., et al., Standard Reference Materials: 1982 Compilation of Elemental Concentration Data for NBS Biological, Geological, and Environmental Standard Reference Materials, NBS Spec. Publ. 260-88 (March 1984). PB84218338**

Hust, J.G., Standard Reference Materials: A Fine-Grained, Isotropic Graphite for Use as NBS Thermophysical Property RMs from 5 to 2500 K, NBS Spec. Publ. 260-89 (September 1984). PB85112886**

Hust, J.G., and Lankford, A.B., Standard Reference Materials: Update of Thermal Conductivity and Electrical Resistivity of Electrolytic Iron, Tungsten, and Stainless Steel, NBS Spec. Publ. 260-90 (September 1984). PB85115814**

Goodrich, L.F., Vecchia, D.F., Pittman, E.S., et al., Standard Reference Materials: Critical Current Measurements on an NbTi Superconducting Wire SRM, NBS Spec. Publ. 260-91 (September 1984). PB85118594**

Carpenter, B.S., Standard Reference Materials: Calibrated Glass Standards for Fission Track Use (Supplement to NBS Spec. Publ. 260-49), NBS Spec. Publ. 260-92 (September 1984). PB85113025**

Ehrstein, J.R., Standard Reference Materials: Preparation and Certification of SRM for Calibration of Spreading Resistance Probes, NBS Spec. Publ. 260-93 (January 1985). PB85177921**

Gills, T.E., Koch, W.F., Stolz, J.W., et al., Standard Reference Materials: Methods and Procedures Used at the National Bureau of Standards to Certify Sulfur in Coal SRMs for Sulfur Content, Calorific Value, Ash Content, NBS Spec. Publ. 260-94 (December 1984). PB85165900**

Mulholland, G.W., Hartman, A.W., Hembree, G.G., et al., Standard Reference Materials: Development of a 1mm Diameter Particle Size Standard, SRM 1690, NBS Spec. Publ. 260-95 (May 1985). PB86113693**

Carpenter, B.S., Gramlich, J.W., Greenberg, R.R., et al., Standard Reference Materials: Uranium-235 Isotopic Abundance Standard Reference Materials for Gamma Spectrometry Measurements, NBS Spec. Publ. 260-96 (September 1986). PB87108544**

Mavrodineanu, R., and Gills, T.E., Standard Reference Materials: Summary of the Coal, Ore, Mineral, Rock, and Refactory Standards Issued by the National Bureau of Standards, NBS Spec. Publ. 260-97 (September 1985). PB86110830**

Hust, J.G., Standard Reference Materials: Glass Fiberboard SRM for Thermal Resistance, NBS Spec. Publ. 260-98 (August 1985). SN003-003-02674-3*

Callanan, J.E., Sullivan, S.A., and Vecchia, D.F., Standard Reference Materials: Feasibility Study for the Development of Standards Using Differential Scanning Calorimetry, NBS Spec. Publ. 260-99 (August 1985). PB86106747**

Taylor, J.K., Trahey, N.M., ed., Standard Reference Materials: Handbook for SRM Users, NBS Spec. Publ. 260-100 (February 1993). PB93183796**

Mangum, B.W., Standard Reference Materials: SRM 1970, Succinonitrile Triple-Point Standard: A Temperature Reference Standard Near 58.08° C, NBS Spec. Publ. 260-101 (March 1986). PB86197100**

Weidner, V.R., Mavrodineanu, R., Mielenz, K.D., et al., Standard Reference Materials: Holmium Oxide Solution Wavelength Standard from 240 to 640 nm - SRM 2034, NBS Spec. Publ. 260-102 (July 1986). PB86245727**

Hust, J.G., Standard Reference Materials: Glass Fiberblanket SRM for Thermal Resistance, NBS Spec. Publ. 260-103 (September 1985). PB86109949**

Mavrodineanu, R., and Alvarez, R., Standard Reference Materials: Summary of the Biological and Botanical Standards Issued by the National Bureau of Standards, NBS Spec. Publ. 260-104 (November 1985). PB86155561**

Mavrodineanu, R., and Rasberry, S.D., Standard Reference Materials: Summary of the Environmental Research, Analysis, and Control Standards Issued by the National Bureau of Standards, NBS Spec. Publ. 260-105 (March 1986). PB86204005**

Koch, W.F., ed., Standard Reference Materials: Methods and Procedures Used at the National Bureau of Standards to Prepare, Analyze, and Certify SRM 2694, Simulated Rainwater, and Recommendations for Use. NBS Spec. Publ. 260-106 (July 1986). PB86247483**

Hartman, A.W., and McKenzie, R.L., Standard Reference Materials: SRM 1965, Microsphere Slide (10 μm Polystyrene Spheres), NBS Spec. Publ. 260-107 (November 1988). PB89153704**

Mavrodineanu, R., and Gills, T.E., Standard Reference Materials: Summary of Gas Cylinder and Permeation Tube Standard Reference Materials Issued by the National Bureau of Standards, NBS Spec. Publ. 260-108 (May 1987). PB87209953**

Candela, G.A., Chandler-Horowitz, D., Novotny, D.B., et al., Standard Reference Materials: Preparation and Certification of an Ellipsometrically Derived Thickness and Refractive Index Standard of a Silicon Dioxide Film (SRM 2530), NIST Spec. Publ. 260-109 (October 1988). PB89133573**

Kirby, R.K., and Kanare, H.M., Standard Reference Materials: Portland Cement Chemical Composition Standards (Blending, Packaging, and Testing), NBS Spec. Publ. 260-110 (February 1988). PB88193347**

Gladney, E.S., O'Malley, B.T., Roelandts, I., et al., Standard Reference Materials: Compilation of Elemental Concentration Data for NBS Clinical, Biological, Geological, and Environmental Standard Reference Materials, NBS Spec. Publ. 260-111 (November 1987). PB88156708**

Marinenko, R.B., Blackburn, D.H., and Bodkin, J.B., Standard Reference Materials: Glasses for Microanalysis: SRMs 1871-1875, NIST Spec. Publ. 260-112 (February 1990). PB90215807**

Mangum, B.W., and Wise, J.A., Standard Reference Materials: Description and Use of a Precision Thermometer for the Clinical Laboratory, SRM 934, NIST Spec. Publ. 260-113 (June 1990). PB90257643**

Vezzetti, C.F., Varner, R.N., and Potzick, J.E., Standard Reference Materials: Bright-Chromium Linewidth Standard, SRM 476, for Calibration of Optical Microscope Linewidth Measuring Systems, NIST Spec. Publ. 260-114 (January 1991). PB91167163**

Williamson, M.P., Willman, N.E., and Grubb, D.S., Standard Reference Materials: Calibration of NIST SRM 3201 for 0.5 in. (12.65 mm) Serial Serpentine Magnetic Tape Cartridge, NIST Spec. Publ. 260-115 (February 1991). PB91187542**

Mavrodineanu, R., Burke, R.W., Baldwin, J.R., et al., Standard Reference Materials: Glass Filters as a Standard Reference Material for Spectrophotometry - Selection, Preparation, Certification and Use of SRM 930 and SRM 1930, NIST Spec. Publ. 260-116 (March 1994). SN003-00303256-5*

Vezzetti, C.F., Varner, R.N., and Potzick, J.E., Standard Reference Materials: Anti-reflecting-Chromium Linewidth Standard, SRM 475, for Calibration of Optical Microscope Linewidth Measuring Systems, NIST Spec. Publ. 260-117 (January 1992). PB92-149798**

Williamson, M.P., Standard Reference Materials: Calibration of NIST Standard Reference Material 3202 for 18-Track, Parallel, and 36-Track, Parallel Serpentine, 12.65 mm (0.5 in), 1491 cpmm (37871 cpi), Magnetic Tape Cartridge, NIST Spec. Publ. 260-118 (July 1992). PB92-226281**

Vezzetti, C.F., Varner, R.N., and Potzick, Standard Reference Materials: Antireflecting-Chromium Linewidth Standard, SRM 473, for Calibration of Optical Microscope Linewidth Measuring System, NIST Spec. Publ. 260-119 (September 1992).

Caskey, G.W., Philips, S.D., Borchardt., et al., Standard Reference Materials: A Users' Guide to NIST SRM 2084: CMM Probe Performance Standard, NIST Spec. Publ. 260-120 (1994).

Rennex, B.G., Standard Reference Materials: Certification of a Standard Reference Material for the Determination of Interstitial Oxygen Concentration in Semiconductor Silicon by Infrared Spectrophotometry, NIST Spec. Publ. 260-121 (1994).

*Send order with remittance to: Superintendent of Documents, U.S. Government Printing Office, Washington, DC 20102. Remittance from foreign countries should include an additional one fourth of the purchase price for postage.

**May be ordered from: National Technical Information Services (NTIS), Springfield, VA 22161.
For information phone (703-487-4650)
To Place an Order with PB# phone (800-553-6847)

TABLE OF CONTENTS

LIST OF FIGURES[1]

[1]Throughout the figure and table captions it should be understood that the term oxygen concentration refers to oxygen number fraction. When multiplied by 10^6, it is referred to as ppma by convention.

LIST OF FIGURES (continued)

LIST OF TABLES

Standard Reference Materials:

CERTIFICATION OF A STANDARD REFERENCE MATERIAL FOR THE DETERMINATION OF INTERSTITIAL OXYGEN CONCENTRATION IN SEMICONDUCTOR SILICON BY INFRARED SPECTROPHOTOMETRY

Brian G. Rennex
Semiconductor Electronics Division
National Institute of Standards and Technology
Gaithersburg, MD 20899, USA

ABSTRACT

A Standard Reference Material, SRM-2551, has been prepared, measured, and certified for the determination of interstitial oxygen number fraction (commonly referred to as the oxygen concentration) in semiconductor silicon. This SRM is intended for calibration of infrared spectrophotometers used to measure the 1107 cm^{-1} interstitial oxygen peak in silicon. Its purpose is to enable its users to improve their measurement agreement. The expanded SRM uncertainty is 0.17% for the low-oxygen specimens, 0.13% for the medium-oxygen specimens, and 0.12% for the high-oxygen specimens. The certifying instrument was a Fourier-transform infrared spectrophotometer which measured the oxygen peak height. Specimens from an earlier international Grand Round Robin (GRR) were used to convert these infrared values to oxygen number fraction (concentration) values. A major source of uncertainty had been measurement drift; this was largely compensated using a control specimen. The remaining sources of uncertainty were instrument reproducibility, nonuniformity in oxygen concentration and thickness over the specimen area, and variation in residual oxygen in the SRM float-zone specimens, each of which float-zone specimens served as the zero-oxygen reference for a measurement. These sources were combined in quadrature to arrive at the above-quoted 2σ estimate of expanded SRM uncertainty. This SRM uncertainty applies to a "derived" oxygen number fraction which is first measured by an infrared technique and which is then converted to an oxygen number fraction. The oxygen number fraction previously measured in the GRR has a much larger uncertainty than the expanded SRM uncertainty.

Key words: oxygen; silicon; FTIR; Standard Reference Materials.

I. INTRODUCTION

A. SRM OBJECTIVE

This report documents the development of Standard Reference Material (SRM) 2551 for the measurement of interstitial oxygen number fraction (commonly referred to as oxygen concentration) in silicon. This SRM was produced at the National Institute of Standards and Technology (NIST). The purpose of SRM 2551 is to provide a basis for measurement consistency throughout the semiconductor industry. That is, this standard is intended to enable a group of its users to have agreement among their measurements. The expanded SRM uncertainty ranges from 0.12% to 0.17% for three oxygen levels. These values are much lower than the uncertainty for absolute oxygen measurements in which case the interlaboratory variability can be as large as 10 to 30% [1-5]. Improvement in measurement consistency is more useful to users for quality control or comparison than is reliance on the uncertainty of absolute oxygen determination. This report shows that the measurement consistency achievable with SRM 2551 is based primarily on the reproducibility of the certifying infrared instrument. Therefore, the emphasis of this work was to document thoroughly the NIST instrument reproducibility. It is important to note that even though the certified parameter and its expanded uncertainty are given in units of oxygen number fraction (concentration), the certified parameter is a "derived" oxygen number fraction first measured by a relative infrared technique and then converted to an oxygen number fraction. The directly measured oxygen number fraction cannot be determined by this infrared technique, nor can it be measured with the quoted expanded SRM uncertainty.

B. BACKGROUND

The measurement of the interstitial oxygen number fraction of semiconductor silicon has long been of scientific interest, and it is important for manufacturers of silicon and of semiconductor devices. The concentration of oxygen in silicon affects the formation of Si-O precipitates which serve as gettering sites for unwanted fast-diffusing impurities. It also affects, by a precipitation-hardening mechanism, distortions of silicon wafers during the thermal treatments they experience during integrated circuit manufacture. Both of these practical considerations require highly reproducible measurements for control of oxygen levels by both suppliers and users of silicon wafers.

Customary semiconductor industry practice expresses "oxygen concentration" in several kinds of units. The unit "ppma" expresses it as a number fraction of interstitial oxygen atoms with respect to the total number of atoms in a volume of silicon bulk material, the unit "mg/kg" or ppm (wt) expresses it as a mass fraction, and the unit "10^{17} atoms/cm^3" expresses it as a concentration of interstitial oxygen atoms in a cubic centimeter of silicon. The preferred quantity in this report is the number fraction. Strictly speaking, this quantity is just a number, but the commonly used unit (ppma) will be shown in parentheses to avoid confusion with ppm (wt). In this report, when the term oxygen or oxygen value is used for brevity, it refers to interstitial oxygen number fraction. Conversions among these units are given in the SRM certificate in appendix A, and an explanation of the conversions among these units is given in appendix E.

Measurement of the oxygen number fraction is commonly made by infrared spectrophotometry in which the height of the strongest spectral oxygen peak, at 1107 cm^{-1}, is determined. The database and test method for this infrared measurement are well established [1-7]. It is a relative technique that relies on Beer's Law which states that interstitial oxygen number fraction is proportional to the infrared oxygen absorption coefficient peak height. Industry uses the infrared technique for measurement of this oxygen

peak height because it is quick, precise, nondestructive, and inexpensive, while the direct measurement of oxygen number fraction is destructive, difficult, expensive, and imprecise.

Absolute (direct) oxygen measurements must be performed to determine the conversion coefficient between infrared measurements and absolute oxygen measurements. These include charged-particle activation analysis using cyclotron-accelerated alpha particles, high-energy photon activation using ~30 MeV electrons to create xrays, and gas fusion techniques. Over the years, several different conversion coefficients have been adopted by various standards-writing organizations, depending on the state of the measurement art at the time. There were significant discrepancies among the early values, but more recent work has produced conversion coefficients in much better agreement with the current internationally accepted value. That number is the result of the Grand Round Robin (GRR), a major worldwide experiment completed in 1988 [1,2]; it has been adopted by all of the major standards-writing organizations active in the semiconductor field.[1] More recently, a European (BCR) reference material for oxygen in silicon was completed in 1991 [3-5].

The GRR report is a sister document to this report. The GRR produced interlaboratory data for both infrared peak height and absolute oxygen measurements. The certification procedure for SRM 2551 utilized a subset of GRR specimens for which a determination of absolute oxygen concentration had been made.

C. SRM DESCRIPTION

Appendix A is a sample SRM 2551 Certificate which contains the following: an SRM Set description, a summary of the test method for the infrared measurement and the optical peak height calculation, a summary of uncertainties, recommendations for calibration of a user instrument with an SRM set, and instructions for handling SRM specimens. Note that the term total SRM precision in the certificate corresponds to the term expanded SRM uncertainty in this report. Briefly, an SRM set consists of a float-zone specimen with a nominal zero oxygen concentration and three Czochralski silicon specimens with oxygen number fractions (concentrations) at nominal values of 17×10^{-6}, 23×10^{-6}, and 26×10^{-6} (17, 23, and 26 ppma). These specimens have nominal thicknesses of 2 mm; they are squares with nominal side values of 25 mm×25 mm.

D. OVERVIEW

A brief overview of the report is given here as a road map for readers as they proceed through the more detailed discussion to follow.

1) The primary SRM goal is to provide a basis for consistent measurement of oxygen in silicon for the semiconductor industry. This goal can be best accomplished with a reproducible infrared instrument for development of the SRM and with reproducible infrared instruments calibrated with the SRM [appendix A].

2) The infrared measurement is of a spectral oxygen absorption coefficient peak height [sec. II and appendix B].

---

[1]American Society for Testing and Materials, Deutsches Institut für Normung, Guo Biao (State Standards of China), and Japan Electronic Industry Development Association.

3) An SRM conversion coefficient for the NIST spectrometer was determined using a procedure to convert infrared values used for certification to an oxygen scale based on the GRR [sec. III and IV and appendix C].

4) A control specimen was used to monitor drift during all measurements. Data for this control specimen were then used to compensate for drift. This compensation improved instrument reproducibility by about a factor of 3 [sec. V].

5) Performance evaluation runs were made after each group of four SRM sets had been measured. These runs provided data for an estimate of instrument reproducibility both before and after drift compensation [sec. VI].

6) Production runs were made on the SRM sets; each set comprised three oxygen specimens (each at a different oxygen level) and a nominally zero-oxygen specimen [appendix D].

7) The main sources of uncertainty were determined and combined in quadrature to estimate the expanded SRM uncertainty. The four significant sources of uncertainty in the infrared measurement are drift, which is largely compensated; instrument repeatability along with random effects due to specimen changing, which lead to any random variation that remains after drift compensation; nonuniformity in the oxygen concentration and the specimen thickness over the area of specimen subtended by the FTIR beam; and variation in the small amount of residual oxygen in the SRM float-zone specimens, each of which serves as the zero reference for the determination of α, for a particular SRM set [sec. VII].

8) The result is a 2σ estimate of expanded SRM uncertainty which varies from 0.17% for the low-oxygen specimens to 0.12% for high-oxygen specimens. This value meets projected IC industry requirements into the next century [sec. VIII].

II. APPARATUS

A Fourier Transform Infrared spectrophotometer (FTIR) was used to measure infrared transmittance through silicon specimens; Figure 1 shows schematically the optical configuration of the NIST FTIR. This instrument operated at the 4 cm^{-1} resolution required by the ASTM test method for determination of oxygen in silicon, and its small size and rigid construction contribute to good quantitative repeatability [6].

Appendix B explains the derivation of the spectral absorption coefficient peak height, α, from the transmittance peak height. This α is independent of specimen thickness since it is the quotient of the absorbance and the specimen thickness. Figures 2 and 3 show typical spectra in the region of the 1107 cm^{-1} oxygen peak.

It was discovered that the measured α was extremely sensitive to the angular orientation of the silicon wafer in the FTIR, possibly due to the high index of refraction of silicon. Changes in orientation due to specimen removal and reloading caused sufficient specimen rotation to, in turn, cause large and abrupt offsets in α (of about 0.5%). A possible explanation for this error would be that both the infrared beam and the infrared detector are nonuniform, and a tiny shift of the beam with respect to the detector results

in a significant shift in the measured intensity. Also, the just-mentioned abrupt shifts in α were not eliminated by the drift compensation to be discussed in section V.

This error was eliminated by use of a light cone which made the focused beam position on the detector less sensitive to the orientation of the specimen. Losses within the light cone resulted in a loss of about half the signal intensity, but the error in reproducibility was completely eliminated. This was proven in section VI (as is shown in figs. 14 to 17), where it can be seen that any shifts in α, which occurred when the performance evaluation specimens were replaced, occurred in all specimens and, hence, could be drift compensated. That is, the shifts in α occurred in a proportionate manner for all specimens; this behavior is referred to in this report as "tracking" of the time plots among the measured specimens. Before the light cone was employed, the shifts for different specimens did not track, indicating that the cause of the shifts was somehow dependent on what had happened to an individual specimen.

The light cone used at the detector was a gold-plated, f/4 light cone with the following dimensions: length = 6 mm; entry diameter = 2 mm; and exit diameter = 1 mm. The multiple reflections in the light cone scrambled the beam in the sense that a particular original direction of a beam ray would not determine its final position on the detector in a manner corresponding to simple geometrical optics.

The NIST FTIR is housed in a room which was temperature-controlled to 21 $\pm$ 0.5 °C. Temperature control was important because temperature fluctuations appeared to be the primary cause of measurement drift. The temperature at the sample holder was 27.8 $\pm$ 0.5 °C. Temperature stability within the sample chamber was ensured by waiting an hour following sample loading, before measurement began.

To automatically measure many specimens, a sample holder was used. Up to nine specimens were loaded in this 3×3 (position) sample holder, which could be repositioned to within better than a micrometer by an automatic x-y positioner. The alignment procedure was first to align the center of the sample holder with the infrared beam, using an IR sensitive film. Then an iris, located 50 mm before the sample chamber focal point, was centered, via a manual x-y positioner, onto the center of the sample holder; the iris was adjusted so that the beam diameter at the specimen was 5 mm. The specimen was located 50 mm behind the sample chamber focal point. The infrared beam was normal to the specimen surface. The NIST FTIR instrument allows normal incidence because light reflected from the detector or the specimen back into the interferometer cannot result in a spurious contribution to the modulated signal. This is because the corner-cube size is 2.5 times the beam size, and the beam illuminates only one side of the corner cube. The result is that the beam is translated laterally in such a way that it cannot return to the detector. A 2-mm-diameter deuterated-triglycine-sulfate (DTGS) detector was used at the same temperature as that of the sample chamber temperature. This minimized any spurious effects due to background blackbody radiation. To confirm that there was no error due to blackbody radiation from components in the optical path, the IR source was turned off, at which time there was no measurable interferogram or spectrum whatsoever.

A manual x-y positioner was used to locate the light cone optimally over the detector, and a manual x-y-z positioner was used to optimize the signal by moving the detector in all three directions while monitoring the detector signal. This alignment was done whenever the open-beam signal decreased below a certain threshold, which was roughly 96% of the maximum signal. This monitoring was done throughout the period of SRM tests.

III. ABSOLUTE OXYGEN MEASUREMENTS

Calibration of the NIST FTIR instrument was based on infrared measurements of a set of eight specimens for which a determination of absolute oxygen concentration had previously been made in the Grand Round Robin (GRR) [1,2]. This eight-specimen set is a subset of 20 specimens (from 20 ingots at 20 distinct levels of oxygen) used in the GRR, and it is referred to here as the eight-specimen calibration set. Eight specimens were used since only eight specimens (plus a float-zone specimen) could be accommodated on the instrument sample holder at one time. The GRR determination of absolute oxygen was based on data from charged particle activation analysis. These oxygen measurements were made on specimens that had originally been adjacent to the wafers reserved for optical measurements. There were two such wafers from each of 20 ingots (at 20 oxygen levels), and each wafer provided four specimens for the optical measurements by GRR participants.

The uncertainties for these absolute techniques are not well characterized, but their uncertainty is much larger than the expanded SRM uncertainty, which is less than 0.2%. The spread of data among the different laboratories which made the absolute oxygen measurements was 10 to 30% [1,2]. In a subsequent BCR study, the intra-laboratory reproducibility of absolute measurements was $\pm 4\%$, and a propagation of errors estimate of absolute uncertainty was $\pm 6\%$ [3-5]. Since these absolute oxygen uncertainties, which are the best currently possible due to the limitations of the existing measurement techniques, are large, one must use these data (averaged over a number of specimens and laboratories) simply to arrive at a scaling factor for the measured optical parameter. This scaling is achieved with the conversion coefficient to be discussed in the next section.

Using only GRR data, a comparison was made between the GRR conversion coefficient based on specimens at all 20 GRR oxygen levels, as well as the conversion coefficient based on the eight-specimen subset used as the NIST calibration set. The GRR conversion coefficient for the 20-specimen regression is 3.575 mg/(kg·cm) [6.275 ppma/cm] versus 3.549 mg/(kg·cm) [6.230 ppma/cm] for the eight-specimen subset. The respective standard deviations of these coefficients are 0.6% and 1.2%. The eight-specimen set yields a conversion coefficient that is 0.72% less than that from the full 20-specimen GRR set. The T-factor for comparison of these two slopes or conversion coefficients is 0.52, indicating that they are not statistically different. Nevertheless, to ensure that the certified oxygen values are as representative as possible of all the GRR data for absolute oxygen, the original oxygen values of the eight specimens have been scaled up by 0.72%. These adjusted oxygen values appear in table 1.

IV. DETERMINATION OF SRM CONVERSION COEFFICIENT

As stated in the introduction, the basic strategy of this SRM certification is to take advantage of a precise infrared measurement technique to provide an SRM with high internal consistency. This is accomplished by the determination of an SRM conversion coefficient for the NIST FTIR to convert precisely measured values of α to certified values in oxygen units. This was done using mean absolute oxygen values from the GRR work. Then, even though the absolute uncertainty of any particular oxygen value is large, the measurement consistency or reproducibility of the certified values within the SRM is good.

There were two requirements for determination of the SRM conversion coefficient. First, in the previous section, there was an explanation of the provisions taken to make the absolute oxygen values of the eight-specimen set representative of the GRR. Second, the conversion coefficient must be specific to the NIST FTIR.

The conversion coefficient specific to the NIST FTIR was used for this SRM certification to eliminate any bias between the NIST FTIR and the mean response of all infrared instruments used to determine the GRR conversion coefficient. That is, the internationally recognized conversion coefficient determined in the GRR is an average based on measurements by many infrared laboratories, each of which had a bias with respect to the group average. The set of laboratory bias values can be quantified by a standard deviation, namely the interlaboratory variability. The 1σ interlaboratory variability for the GRR was 2.7%. Although the current NIST FTIR was not used in the GRR, it would also be expected to have a laboratory bias.

If the GRR conversion coefficient were used for the SRM certification, the calculated oxygen values would be biased from the results of the GRR by the amount of the NIST FTIR laboratory bias. For clarity, this point is explained in mathematical terms in appendix C. The conclusion is that the conversion coefficient measured with the NIST FTIR should be used as the SRM conversion coefficient in this work, and this, in turn, will enable the SRM users to also achieve measured oxygen values consistent with the GRR.

The absorption coefficient values (shown in table 1 and figs. 4 and 5) for the conversion coefficient determination were taken by the NIST FTIR in a 6-day test run for the eight-specimen calibration set mentioned in the previous section (III). Absorption coefficient oxygen peak heights were measured 55 times, with each data point being the average of 300 scans. These eight specimens covered a range of nominal oxygen number fraction values between 9×10^{-6} and 29×10^{-6} (9 ppma and 29 ppma); these specimens and a GRR float-zone (zero oxygen) specimen were mounted simultaneously in the specimen holder. The sequence of measurements for each repeat was open beam, float-zone, and then each of the eight specimens. Acquisition of these 55 sets of data points resulted in a total test time of 6 days, which can be seen by inspection of figures 6 to 13 to be sufficient to achieve good statistics and to achieve a good evaluation of the drift compensation, to be explained below.

A conversion coefficient is determined by a linear regression fit to data for absolute oxygen concentration versus α. The absolute oxygen values representative of the Grand Round Robin study described in section III are shown in table 1, which also has the mean α values from the test run on the eight-specimen calibration set. The resulting plot is fitted with a straight line which passes through the origin as shown in figure 4. The slope of this line is $M_{nist} = 0.1612\times10^{6}$ cm^{-1} [0.1612 (ppma·cm)$^{-1}$] which corresponds to an SRM conversion coefficient of 6.205×10^{-6} cm (ppma·cm). In figure 5, if the straight line is not constrained to pass through the origin, the oxygen intercept value is -0.074 cm^{-1} and the slope is 0.1670×10^{6} cm^{-1} [(ppma·cm)$^{-1}$]. Because of the large scatter of absolute oxygen number fraction values about the fitted line, the assumption of the line passing through the origin is not unreasonable. Also, this assumption was used in the determination of the GRR conversion coefficient.

V. DRIFT COMPENSATION

The above-mentioned time plots on the eight-specimen calibration set can also be used to evaluate drift compensation. Figure 6 shows these time plots as percent changes (from the mean) of α for all eight specimens; that is, the values plotted are divided by the average over the entire run, and this quotient is then multiplied by 100. These curves are offset by 0.4% with increasing oxygen value, for clarity of viewing. They track one to another, which means that any drift causes the same approximate percent changes for each curve. The specimen (third from the top in fig. 6) closest to the center of the SRM

oxygen range [at 24×10^{-6} (24 ppma)] was used here as a control specimen for drift compensation. This same specimen was used as the control specimen for the production runs and for the performance evaluation runs discussed later.

The formula for drift compensation is the following.

$$\alpha_{i,j}' = \alpha_{i,j}(\alpha_{cmean}/\alpha_{c,j}) \quad .$$

Here, "i" refers to a test specimen, and "c" refers to the control specimen. The equation applies to a set of single data points "j" taken in concurrent test runs. Here, $\alpha_{i,j}'$ is the compensated α, $\alpha_{i,j}$ is the uncompensated α, both for the test specimen; $\alpha_{c,j}$ is the uncompensated α for the control specimen, and α_{cmean} is the mean of all the α values for the control specimen. If the drift compensation worked exactly, the set of j values of $\alpha_{i,j}'$ would have a constant value. In fact, this set has a distribution characterized by a mean and a standard deviation, and the latter gives the drift-compensated reproducibility. Other data plots related to drift compensation are shown in section VI on performance evaluation runs and in section VII on uncertainty estimates.

Figures 7 to 13 show, for each of the seven other calibration specimens, time plots of the measured α and of the drift-compensated α. The "x" indicates a measured point, and the "c" indicates a compensated point. Figures 7 and 8, for the lowest oxygen levels, show that drift compensation is not complete because the corrected curve is not flat. Even so, there is substantial compensation, and the percent standard deviation of the corrected points of the curve about its mean is reduced by a factor of two over that of the uncorrected points. As the oxygen level increases to the range of the SRM [17×10^{-6} to 26×10^{-6} (17 ppma to 26 ppma)], the corrected curve is very flat and the percent standard deviation values, i.e., the instrument repeatability values, are improved by a factor of 3 to 4 over those of the time plots of uncompensated data. The empirical conclusion is that drift in α is substantially reduced in the oxygen range covered by the oxygen SRM.

VI. PERFORMANCE EVALUATION RUNS

Performance evaluation runs were taken concurrently (i.e., overnight) with the SRM production runs to monitor the instrument and to acquire the data needed to estimate the instrument reproducibility over the entire period of these production runs. Performance evaluation runs were taken every day after two production runs had been taken (during that same 24-h period). The approximate timing was two consecutive 8-h production runs, followed by a 7-h performance evaluation run, with about an hour for specimen changing. Even though the performance evaluation runs were concurrent and alternating with the production runs, they are discussed before the production runs. This is because the performance evaluation provides an estimate of instrument reproducibility which is needed for the discussion of the uncertainty associated with production runs, which is given in the next section.

The performance evaluation set was taken from specimens used in the Grand Round Robin study. [1,2] This set was similar to those of the SRM production runs because it used the same control specimen, and it had a float-zone specimen and specimens at three comparable levels of oxygen. Its protocol was also the same as that for the production runs except that it was measured twice as frequently. The production run protocol is given in appendix D.

The purpose of performance evaluation runs was twofold. First, they verified that the measured peak heights of all specimens tracked. The term "tracking" means that temporal percent changes in all measured oxygen or α values were roughly the same. Second, the performance evaluation runs produced a large database for determination of instrument reproducibility, and this database covered the entire period of time over which the productions runs were made. Here, reproducibility is distinguished from repeatability, which refers to repeated measurements when the specimen holder has been moved, but when the specimens have not been removed from the specimen holder. Reproducibility refers to the case when specimens have been unloaded from and reloaded into the specimen holder, and it provides information regarding the equivalence of the measurement for all SRM sets measured over the course of the certification. As is seen in section VII on uncertainties, the NIST FTIR reproducibility is the largest contributor to the expanded SRM uncertainty.

The performance evaluation data plots described next are time plots of α, the parameter determined in test runs by the NIST FTIR. Figure 14 shows normalized (percent of average value) plots of α for the performance evaluation specimens. The symbols L, M, H, and C refer to the low, medium, high, and control specimens, respectively, and each curve is offset by 0.5%. Specimen C was used as the control specimen for both performance evaluation and production runs because it is centrally located in terms of oxygen level. The term normalized means that each curve represents percent changes from its own mean value over time. Note that the number of points in each run may vary. A symbol "0" below the curve indicates the first of several single points (4 to 20) in a run. As was stated earlier, there was actually a time gap (typically of about 17 h or more for the two production runs) immediately before each "0" point. The data points in figure 14 were not compensated for drift. It is evident that the curves track according to the drift, and this corroborates the use of a control specimen for drift compensation.

Drift compensated curves for the three oxygen specimens are shown in figures 15 to 17, and their distributions are shown in figures 18 to 20. These distributions are reasonably gaussian. Values averaged over the three specimens are used to estimate standard deviation values from the three compensated and the three uncompensated curves, and these average percent values are adjusted to correspond to the average value of oxygen number fraction [21.2×10^{-6} (21.2 ppma)] for these three specimens. The average standard deviation for the uncompensated curves in figures 15 to 17 is 0.147% or 0.499 cm^{-1}. The average standard deviation (referred to as σ_{rep} where "rep" refers to reproducibility) for the compensated curves in figures 18 to 20 is 0.185 cm^{-1} or 0.055%. This is an improvement by a factor of 2.7 over the standard deviation values for the uncompensated data.

As can be seen from table 6 (discussed later), the three nominal oxygen levels are 17×10^{-6}, 23×10^{-6}, and 26×10^{-6} (17, 23, and 26 ppma). The percent value of σ_{rep} of 0.055% (0.0115×10^{-6} [0.0115 ppma)] corresponded to an average oxygen value of 21.2×10^{-6} (21.2 ppma). Using this value to estimate σ_{rep} for the three SRM levels results in values of σ_{rep} equal to 0.068% for 17×10^{-6} (17 ppma), 0.050% for 23×10^{-6} (23 ppma), and 0.044% for 26×10^{-6} (26 ppma). These values are components of the SRM uncertainty discussed in section VII.

Comparison of the set of figures 15 to 17 with the set of figures 10 to 13 reveals another important result, namely, that the repeatability and the reproducibility for drift-compensated points are virtually the same. This means that reloading specimens does not result in significant additional errors in the FTIR measurement. This was not the case until the light-cone detector assembly discussed in section II was used.

VII. UNCERTAINTY ESTIMATES

In this section, the various sources of uncertainty are discussed in detail. These values are then combined in quadrature and multiplied by two to arrive at the estimate of expanded SRM uncertainty to be reported with the certified SRM values. The four significant sources of uncertainty in the infrared measurement are drift, which is largely compensated; instrument reproducibility, which is the random variation that remains after drift compensation; the variation in the small amount of residual oxygen in the SRM float-zone specimens, each of which serves as the zero reference for the determination of α, for a particular SRM set; and nonuniformity in the oxygen concentration and the specimen thickness over the area of specimen subtended by the FTIR beam.

The measurement consistency achievable with SRM 2551 is based primarily on the reproducibility of the certifying infrared instrument. The stated uncertainty is an expanded (2σ) uncertainty with which the oxygen scale obtained from the eight-specimen calibration set is reproduced in each of the SRM sets. Therefore, the emphasis of this work was to document thoroughly the NIST instrument reproducibility which is determined with a type A evaluation in ISO terminology [8]. It is important to note that even though the certified parameter and its uncertainty are given in units of oxygen number fraction (concentration), the certified parameter is a value first measured by an infrared technique and then converted to oxygen number fraction units. Absolute oxygen number fraction cannot be directly measured by this infrared technique nor can it be measured with the quoted expanded SRM uncertainty.

The first significant uncertainty is the reproducibility of the optical measurement of the absorption coefficient. The measurement protocol for production runs is described in appendix D. It explains that all specimens in two SRM sets and a control specimen were measured consecutively and repeatedly and that an α value for each specimen is the average of four (single) test points taken over a period of 8 hours. Also, a check was made that the transmittance at 2000 cm^{-1} was within 2% of the expected value of 54% [6,7].

Drift compensation was used for all production runs because they took place over many weeks, and there was drift over this period of time that was several times larger than any random variation. With reference to the expression for drift compensation in section V, the adjustment of each α point for each specimen of each SRM set was accomplished as follows. Mean α values for a particular production run, based on four or more points or repeats, were calculated for each of the three SRM set specimens, α_i, and for the control specimen, α_c. Compensated mean SRM values α_i' were then calculated using a grand mean value, α_{cmean}, for the control specimen based on data taken over the entire period of SRM measurement, along with the mean values α_i and α_c.

For each SRM specimen, four repeats were made to ensure that the instrument was in steady state and that there was no chance of using a single outlier value for the SRM. It would have been desirable to take statistical advantage of the fact that there were four test points. If these points had been uncorrelated, the estimate of uncertainty in the mean α would have equaled the standard deviation divided by the square root of the four points taken for each run.

The requirement of no correlation is equivalent to the requirement that all drift has been compensated. To test for correlation of mean values of compensated α from each performance evaluation run for three levels of oxygen, figures 21 to 23 show that drift has been reduced from that seen in figures 15 to 17 for the compensated α values. Note that the figures 15 to 17 differ from the other figures in that they show every point in a run rather than just the mean values (of all the points in each run). Even though the drift

has been reduced, it is clearly still present in the plot of mean values shown in figure 21 for low oxygen, it is less evident in figure 22 for medium oxygen, and it is virtually gone in figure 23 for high oxygen. That is, in figure 21, the same drift pattern as that seen in figure 15 is reduced but still apparent. Note that the standard deviations in figures 15 to 17 are based on a population of individual test points, not on a population of already averaged values of test points. Thus, if drift had been successfully compensated (i.e., if the resulting distribution were random), the standard deviation values (of the means) of figures 15 to 17 would have been reduced over those in figures 21 to 23 [by $1/(n^{0.5})$, where n was about 6]. The reduction in σ-values is insignificant for the low oxygen specimens, somewhat significant for the medium oxygen specimens, and significant for the high oxygen specimens. That is, the actual values decrease from 0.059% to 0.055% for low oxygen, from 0.059% to 0.047% for medium oxygen, and from 0.046% to 0.028% for high oxygen. This indicates that drift is slightly reduced for low oxygen, somewhat improved for medium oxygen, and significantly improved for high oxygen.

Even so, a conservative approach was taken — not to divide by 2, but rather to use the above-quoted values of standard deviation of the population, σ_{rep}, to estimate the standard deviation of the means. That is, the standard deviation is used for the standard deviation of the mean; its values are 0.068% for 17×10^{-6} (17 ppma), 0.050% for 23×10^{-6} (23 ppma), and 0.044% for 26×10^{-6} (26 ppma).

The second significant source of uncertainty is the variation of oxygen among the SRM 2551 float-zone specimens. The float-zone specimen in each SRM set is used to subtract the phonon or silicon structure from the measured absorption coefficient spectrum to arrive at the pure oxygen peak. These float-zone specimens used in the SRM sets are assumed to have zero oxygen. In fact, they have a small and variable amount of residual oxygen. This variation would cause a first SRM user (with a first float-zone specimen) to differ in a measured unknown oxygen value from a second SRM user (with a second float-zone specimen) who had measured the same unknown specimen. This systematic difference in the measured oxygen values would be equal to the difference between the two float-zone oxygen values.

To estimate this component of uncertainty, a series of test runs were made in which each SRM float-zone specimen was measured with reference to the GRR float-zone specimen. The distribution of the difference between the SRM float-zones and the GRR float-zone is shown in figure 24. The mean value was 0.0112×10^{-6} (0.0112 ppma). That is, the GRR float-zone specimen was 0.0112×10^{-6} (0.0112 ppma) less than the mean of the SRM float-zone specimens. The standard deviation was 0.007×10^{-6} (0.007 ppma), which includes the actual variation in float-zone oxygen levels, as well as the instrument reproducibility for this measurement.

This instrument reproducibility was determined by measuring the same specimen throughout the course of all float-zone tests. The histogram for this measurement is shown in figure 25, and it has a standard deviation of 0.006 $x10^{-6}$ (0.006 ppma). If this reproducibility had been significantly smaller than the above-mentioned standard deviation of 0.007×10^{-6} (0.007 ppma), it would have been possible to adjust each SRM float-zone oxygen number fraction (concentration) to a common value. However, the two values (0.006 and 0.007) were comparable, and no adjustments for individual specimens were made. Instead, the overall standard deviation value of 0.007×10^{-6} (0.007 ppma) is used to estimate the uncertainty due to float-zone variation.

Also, since the GRR float-zone oxygen number fraction (concentration) was 0.0112×10^{-6} (0.0112 ppma) lower than the mean value for all SRM float-zone values, each reported oxygen value in table 6 has been increased by 0.0112×10^{-6} (0.0112 ppma) over the value arrived at by multiplying the SRM conversion coefficient by the measured oxygen absorption coefficient peak height. Thus, even though it is not

possible to measure the actual oxygen content of a single float-zone specimen with the infrared technique, the lowest value available, namely that of the GRR float-zone specimen, was used as the best approximation of the zero oxygen level.

Other SRM uncertainties are due to (1) the thickness measurement and (2) variation of oxygen concentration and thickness over the illuminated area of the specimen. The combination is the total material nonuniformity uncertainty.

Thickness appears in the expression for absorption coefficient; its uncertainty has two aspects. First, the uncertainty of a single thickness measurement is 0.2 μm, or 0.01% of the 2-mm thickness for the SRM specimens. Second, a single point was used to estimate the average thickness over the 6-mm circle sampled by the infrared beam, and this single value is not perfectly representative of the average value because the specimen is not perfectly flat. This discrepancy is called the thickness representativeness uncertainty, and it was estimated as follows. Comparisons were made on several specimens between a center point and an average of five points, one at the center and the other four near the four corners of a 5×5 mm square. These comparisons gave a value of 0.015% as the average absolute difference and 0.03% as an upper limit (2σ value) for these difference values. Thus, the thickness representativeness standard deviation equals 0.015%.

Another error arises from differences in the positioning of an SRM specimen with respect to the FTIR beam, in conjunction with any nonuniformity of oxygen concentration and thickness across a specimen. That is, this measurement had uncertainty contributions from both thickness and oxygen nonuniformity. To estimate this combined uncertainty, repeated points were taken at different positions of the FTIR beam on a specimen.

It was estimated that 1 mm would be an upper limit on the uncertainty in positioning of the FTIR beam at the center of the specimen. The beam was moved twice this distance, or 2 mm, to get better statistics by working with a larger discrepancy. Ten repeated measurements were made with the specimen in the original position and then in a position 2 mm away. The conservative assumption was made that errors due to half the offset, namely 1 mm, would be half of those for the 2-mm offset. This is conservative because this error depends on the lack of overlap between two beam positions, and this lack of overlap does not depend linearly on the beam displacement due to the circular beam geometry. Beam-offset measurements were made on four specimens taken from each of the three levels of oxygen, or on a total of 12 specimens.

Table 2 and figure 26 show data for the positioning uncertainty study. The α data is presented in sets of three for each specimen, one at an original position and two at positions 2 mm away from the original position. The second column gives the percent difference in α between the original position and the two offset positions. The third column gives the standard deviation in α for each of the ten repeats at a particular position. The average of all standard deviation values for these repeats was 0.031%, and the range of standard deviation values is also shown in table 2.

To decide if the differences due to repositioning are caused by material nonuniformity or instrument repeatability, note that the uncertainty in the mean value at each position is estimated as 0.031% divided by the square root of 10, or roughly 0.01%. The upper limit on the percent differences (column 2 of table 2) due to repositioning was 0.10%. This value is significantly larger than the just-described

uncertainty of the mean of 0.01% at a particular position, and therefore there is good confidence that any measured difference larger than 0.01% is due to a difference in oxygen concentration and/or thickness at the two positions.

The upper limit estimate of the material nonuniformity uncertainty (a 2σ value due to a 1-mm offset), as distinguished from the 2-mm offset used in the test, was one-half this value, or 0.05%. The standard deviation for the material nonuniformity (σ_{mu}) is 0.025%. This 0.025% figure is added in quadrature to the single-point thickness uncertainty of 0.01% and the thickness representativeness uncertainty of 0.015%, to arrive at 0.031% for the total material nonuniformity uncertainty which is rounded to 0.03%.

The combined SRM uncertainty for the FTIR measurement was calculated by combining in quadrature (1) the reproducibility standard deviation, (2) the float-zone standard deviation, and (3) the total material nonuniformity standard deviation. The expanded SRM uncertainty was calculated as twice the combined SRM uncertainty. This gives the following values for expanded SRM uncertainty for the low, medium, and high levels of oxygen: 0.17% for 17×10^{-6} (17 ppma), 0.13% for 23×10^{-6} (23 ppma), and 0.12% for 26×10^{-6} (26 ppma). The corresponding values in oxygen number fraction (ppma) are: 0.029×10^{-6} (0.029 ppma) for 17×10^{-6} (17 ppma), 0.030×10^{-6} (0.030 ppma) for 23×10^{-6} (23 ppma), and 0.031×10^{-6} (0.031 ppma) for 26×10^{-6} (26 ppma). Table 3 gives a summary of how the various individual uncertainties contribute to the expanded SRM uncertainty. The terms combined and expanded uncertainty are consistent with the new ISO terminology, and all of the component uncertainties were arrived at with a type A evaluation, meaning that repeated values were taken to establish a statistical basis for the various estimates [8].

A total of seven SRM sample sets (21 specimens) were remeasured to check this expanded SRM uncertainty estimate, and all remeasured values lay within the tolerance interval defined by this estimate. These data are shown in table 4. The standard deviation of these percent differences is 0.044% which is comparable to the FTIR reproducibility (0.044% to 0.068%), and the mean offset was 0.05% which indicated that a small amount of drift had occurred over the period of 3 months between the original measurements and the later repeat measurements.

In a second check, three remeasurements were made for a pair of SRM sample sets in which the specimens were put into several different locations in the specimen holder. This was to check for any anomalous effects due to either specimen position or order of specimen measurement within the holder. Again, all remeasured values lay within the tolerance equal to the expanded SRM uncertainty. Table 5 shows these data, and the standard deviation of these percent differences was 0.049%.

VIII. RESULTS AND CONCLUSIONS

The certified derived oxygen number fraction values, as scaled to the GRR, for each SRM 2551 set are given in table 6. The estimate of expanded SRM uncertainty is summarized in table 3, thickness values are given in table 7, and appendix A consists of a sample SRM 2551 Certificate Report. Appendix E derives the conversions among the various units of oxygen number fraction (concentration).

Key features of the SRM measurements were the following:

1) The FTIR instrument reproducibility of 0.05% was an improvement over typical previous values which ranged from about one-half to several percent. The 2σ values of expanded SRM uncertainty for the low, medium, and high oxygen levels were 0.17%, 0.13%, and 0.12%.

2) Ample statistics show that the expanded SRM uncertainty applied over the entire period of SRM measurements and over all SRM sets.

3) Improved accuracy resulted from four factors: a small, rigid instrument was used; an x-y positioner was used to obtained automatic repeats over long periods of time; a control specimen was used to compensate for drift; and a light-cone with an x-y-z positioning capability was used to avoid errors due to specimen positioning.

4) A test method and computer program with some new features was used to calculate the absorption coefficient peak height [appendix 2].

5) The measured absorption coefficient peak height varies with temperature in this range with a coefficient of 0.0016 K^{-1} [7,9], while the actual oxygen number fraction (concentration) remains constant. This means that the certified estimate of oxygen number fraction (concentration) can be used without adjustment even if a user's measurement temperature is different from the value used in the SRM 2551 work. However, the user must expect his own oxygen conversion coefficient (explained in sec. IV and appendix 3) to vary with temperature according to the above temperature coefficient.

6) Finally, the purpose of this SRM is to provide a standard which enables, in principle, a group of SRM users to have agreement within twice the expanded SRM uncertainty. The quoted expanded SRM uncertainty was achieved by a strategy to utilize an FTIR instrument to measure highly precise and relatively consistent values of an optical parameter proportional to oxygen number fraction (concentration). Our belief is that the measurement consistency so achieved is more relevant to user needs for quality control and interlaboratory comparison than any statement referring only to the uncertainty of a direct or absolute determination of oxygen number fraction (concentration).

ADDENDUM - The following additional information is given here in view of a recent publication [11]. All SRM 2551 specimens are n-type. This means that there there is no measurable error due to free-carrier absorption in the vicinity of the 1107 cm^{-1} oxygen peak [12].

REFERENCES

[1] A. Baghdadi, R.I. Scace, and E.J. Walters, *Semiconductor Measurement Technology:* Database for and Statistical Analysis of the Interlaboratory Determination of the Conversion Coefficient for the Measurement of the Interstitial Oxygen Content of Silicon by Infrared Absorption, NIST Special Publication 400-82 (1989).

[2] A. Baghdadi, W.M. Bullis, M.C. Croarkin, L. Yue-Zhen, R.I. Scace, R.W. Series, P. Stallhofer, and M. Watanabe, Interlaboratory Determination of Calibration Factor for the Measurement of the Interstitial Oxygen Content of Silicon by Infrared Absorption, *J. Electrochem. Soc.* **136** (7), 2015-2024 (July 1989).

[3] S. Vandendriessche, B. Griepink, H. Marchandise, and K. Strijckmans, The Certification of Low Oxygen Content in Semiconductor Silicon (CRM 368), BCR Information Report EUR 12927 EN (1990). Published by the Commission of European Communities, Directorate-General, Telecommunications, Information Industries and Innovation, L-2920 Luxembourg, Catalogue number: CD-NA-12927-EN-C.

[4] S. Vandendriessche, B. Griepink, H. Marchandise, B. Pajot, R. Murray, K. Graff, and K. Strijckmans, The Certification of a Reference Material for the Determination of Oxygen in Semiconductor Silicon by Infra-Red Spectrometry (CRM 369), BCR Information Report EUR 12928 EN (1991). Published by the Commission of European Communities, Directorate-General, Telecommunications, Information Industries and Innovation, L-2920 Luxembourg, Catalogue number: CD-NA-12928-EN-C.

[5] R. Murray, K. Graff, B. Pajot, K. Strijckmans, S. Vandendriessche, B. Griepink, and H. Marchandise, Interlaboratory Determination of Oxygen in Silicon for Certified Reference Materials, *J. Electrochem. Soc.* **139** (12), 3582 (1992).

[6] ASTM Standard F 1188, Standard Test Method for Interstitial Atomic Oxygen Content of Silicon by Infrared Absorption, ASTM, Philadelphia, PA (1990).

[7] DIN Standard 50 438/1, Determination of Impurity Content in Silicon by Infrared Absorption: Oxygen, Beuth Verlag GmbH, Burggrafenstrasse 4-10, D-1000 Berlin 30, Federal Republic of Germany. [In German. An English translation is published in the Annual Book of ASTM Standards, Vol. 10.05, ASTM, Philadelphia, PA (1993).]

[8] Guide to the Expression of Uncertainty in Measurement, ISO, Geneva Switzerland, 1993. Available from Bureau International des Poids et Mesures, Pavilon de Breteuil, F-92312 Sevres Cedex, France.

[9] F. Schomann and K. Graff, Correction Factors for the Determination of Oxygen in Silicon by IR-Spectrometry, *J. Electrochem. Soc.* **136**, 2025 (1989).

[10] R.D. Deslattes, Annual Review of Physical Chemistry 31, 435 (1980).

[11] Kitagawara, Y., Tamatsuka, M., Takenaka, T., "Accurate Evaluation of Interstitial Oxygen Concentrations in Medium-Resistivity Si Crystals" J. Electrochem. Soc. 141 (5), 1362-1364 (May 1994).

[12] Gladden, W.K., Baghdadi, A., "Free Carrier Absorption and Interstitial Oxygen Measurements," Emerging Semiconductor Technology, ASTM STP 960, D.C. Gupta and P.H. Langer, Eds., American Society for Testing and Materials (1986).

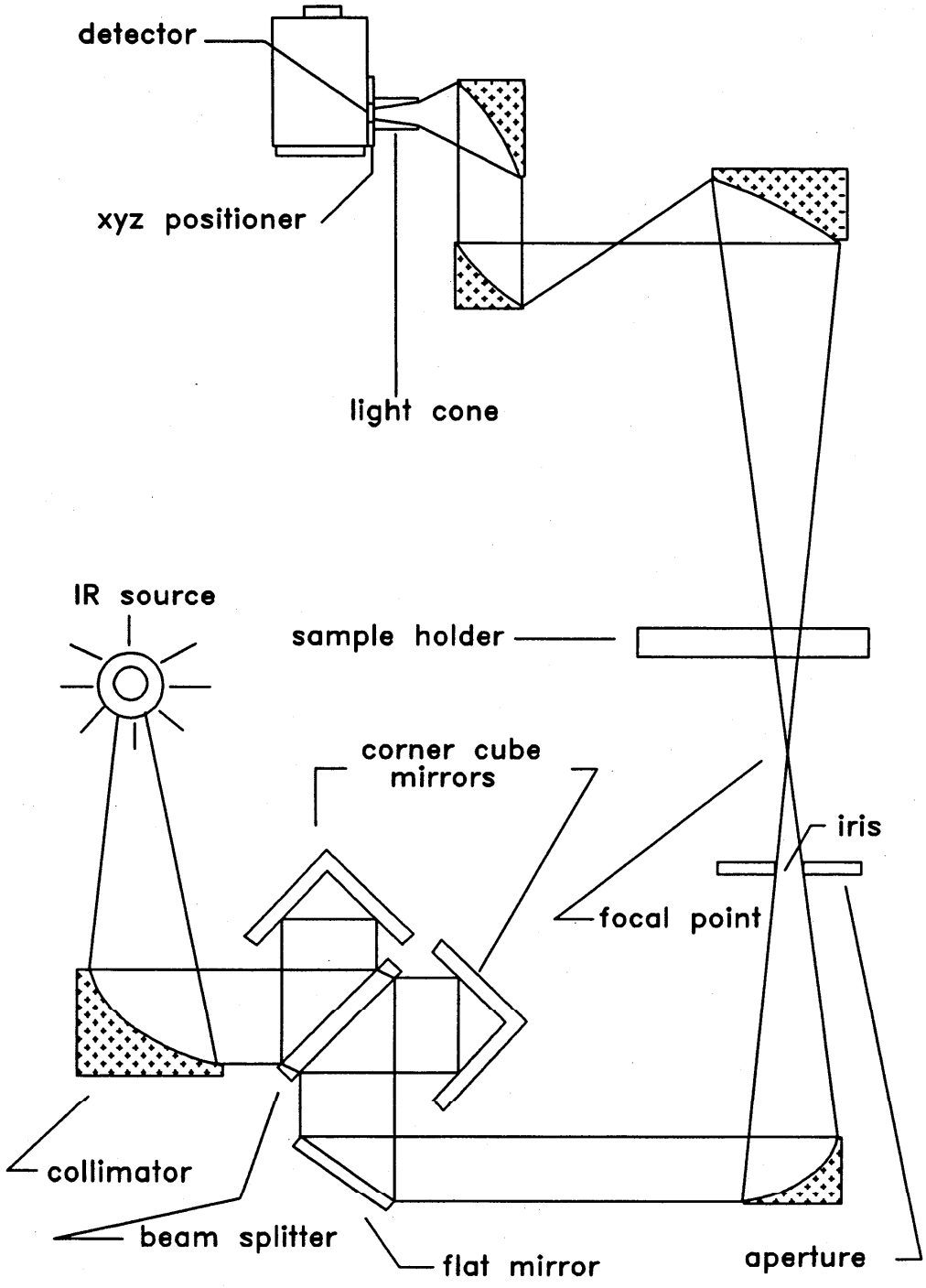

Figure 1. NIST FTIR configuration.

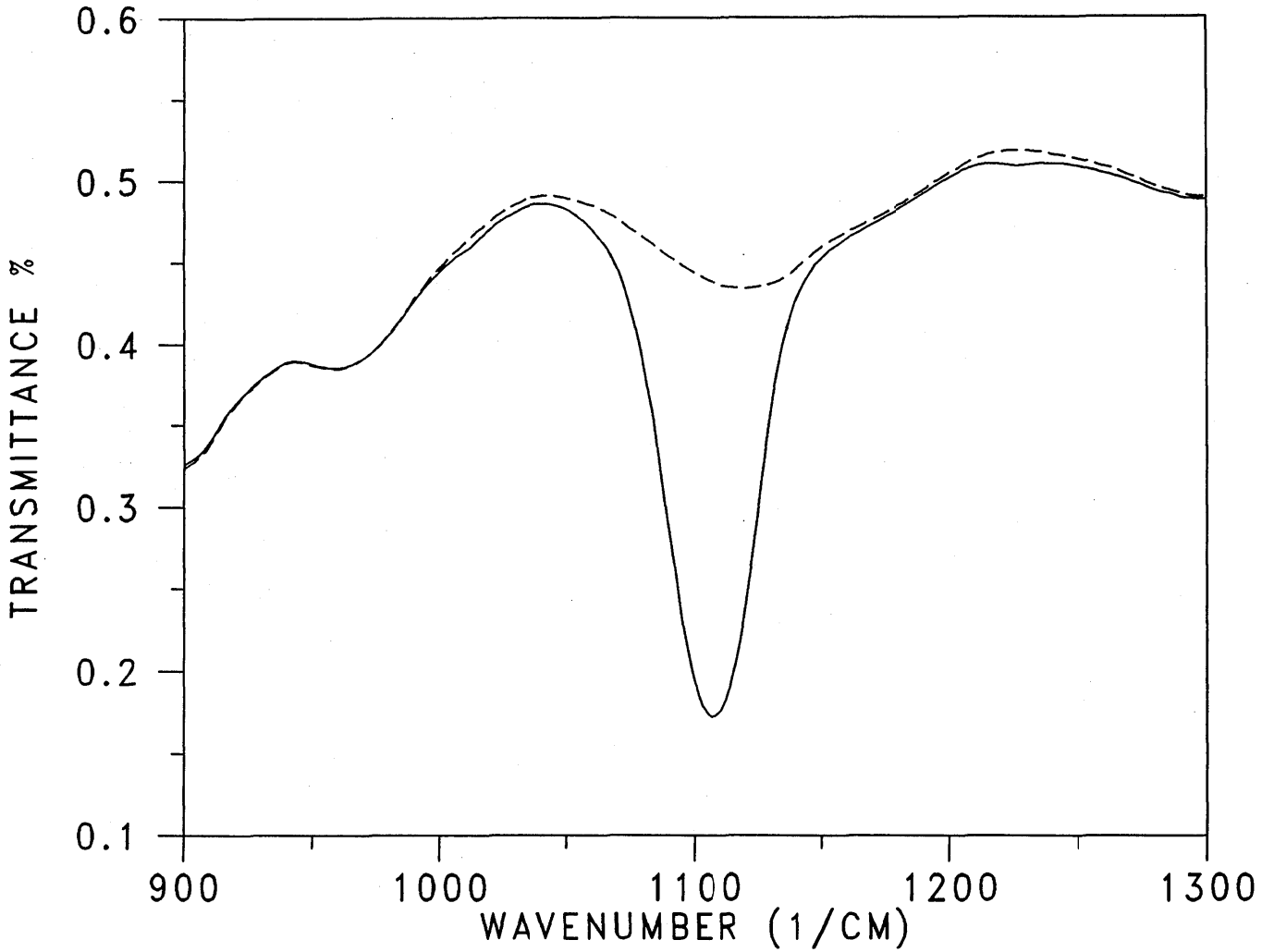

Figure 2. Transmittance spectra for oxygen and float-zone specimens. Solid line for oxygen only and dashed line for float-zone specimen.

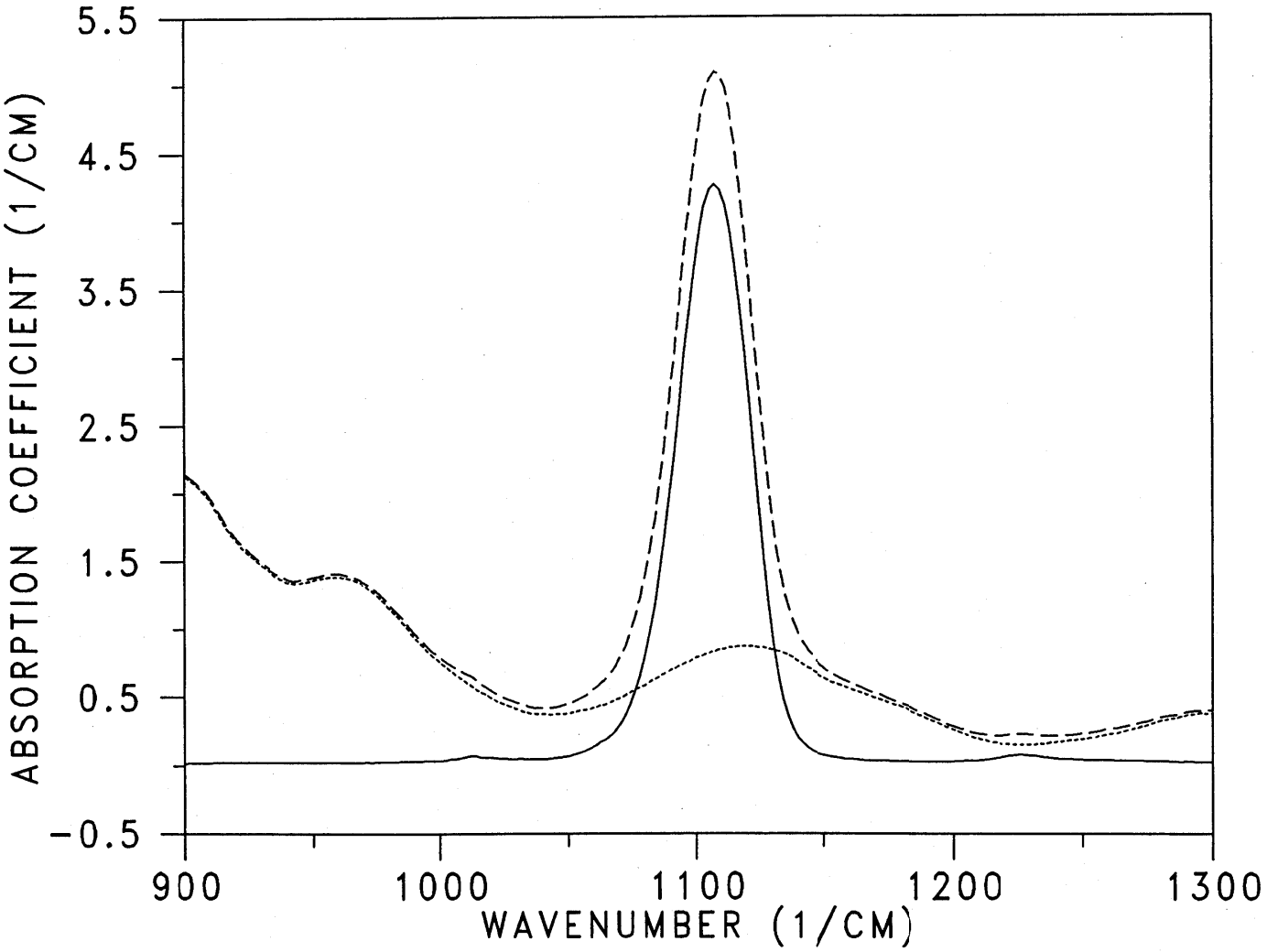

Figure 3. Absorption coefficient spectra for both oxygen and float-zone specimens, and the difference spectrum between them. Solid line for oxygen only, dashed line for oxygen specimen, and dotted line for float-zone specimen.

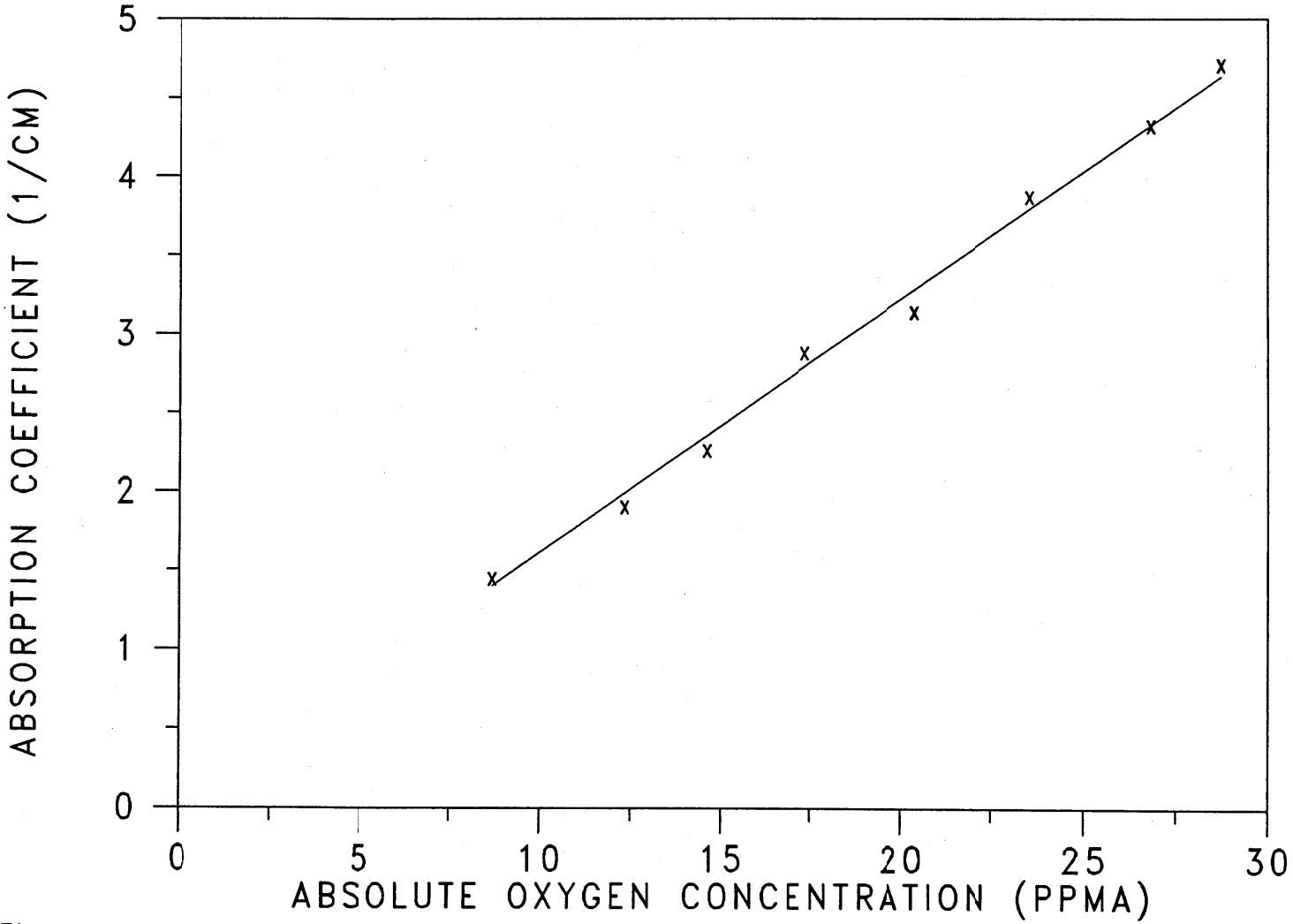

Figure 4. Absorption coefficient versus absolute oxygen concentration with the conversion coefficient (6.205 ppma-cm) equal to the inverse of the slope (0.1612/ppma-cm) for the case where the regression line is constrained to pass through the origin.

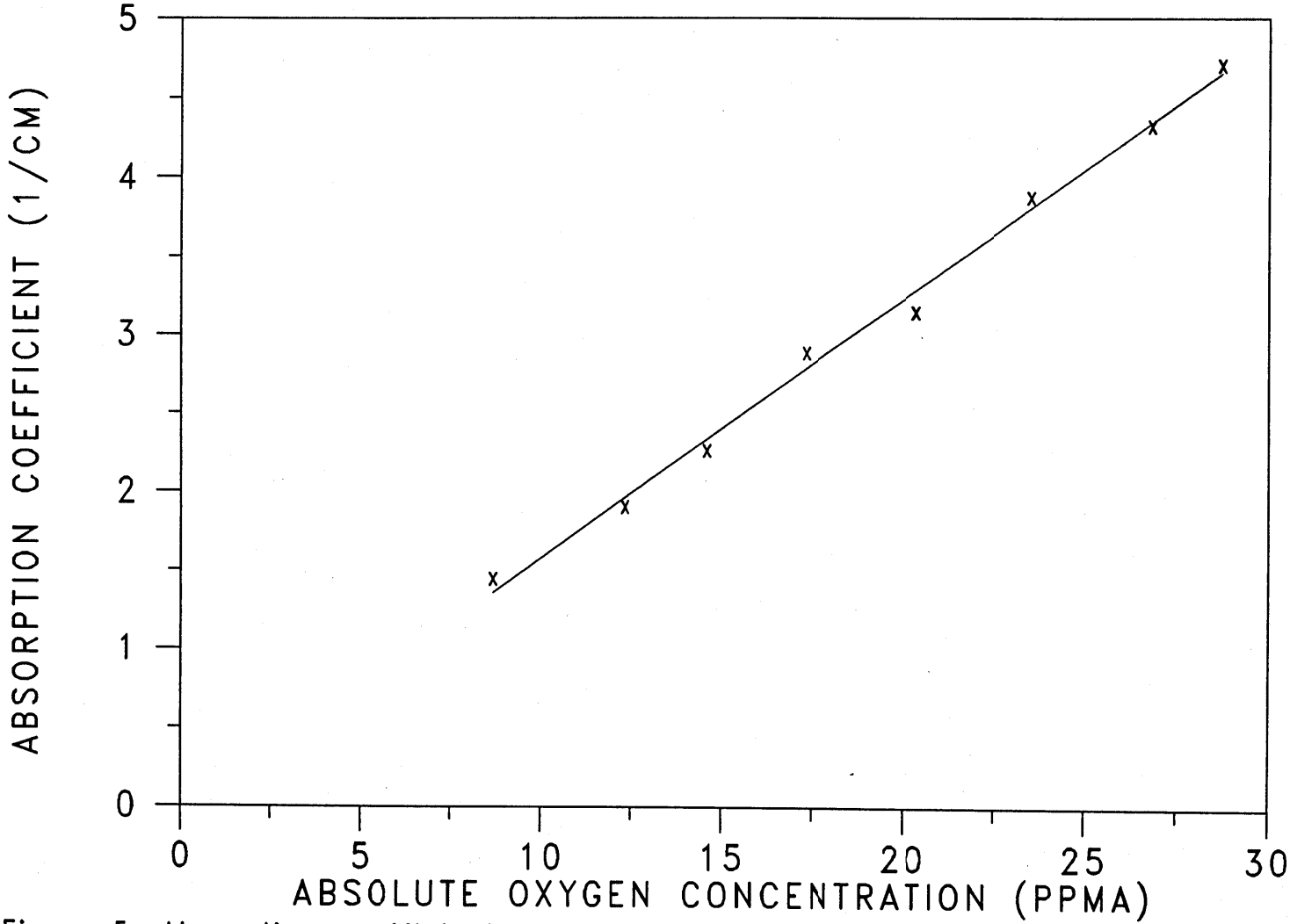

Figure 5. Absorption coefficient versus absolute oxygen concentration with a slope of 0.1646/ppma-cm and an intercept of -0.074/cm for the case where the regression line is not constrained to pass through the origin.

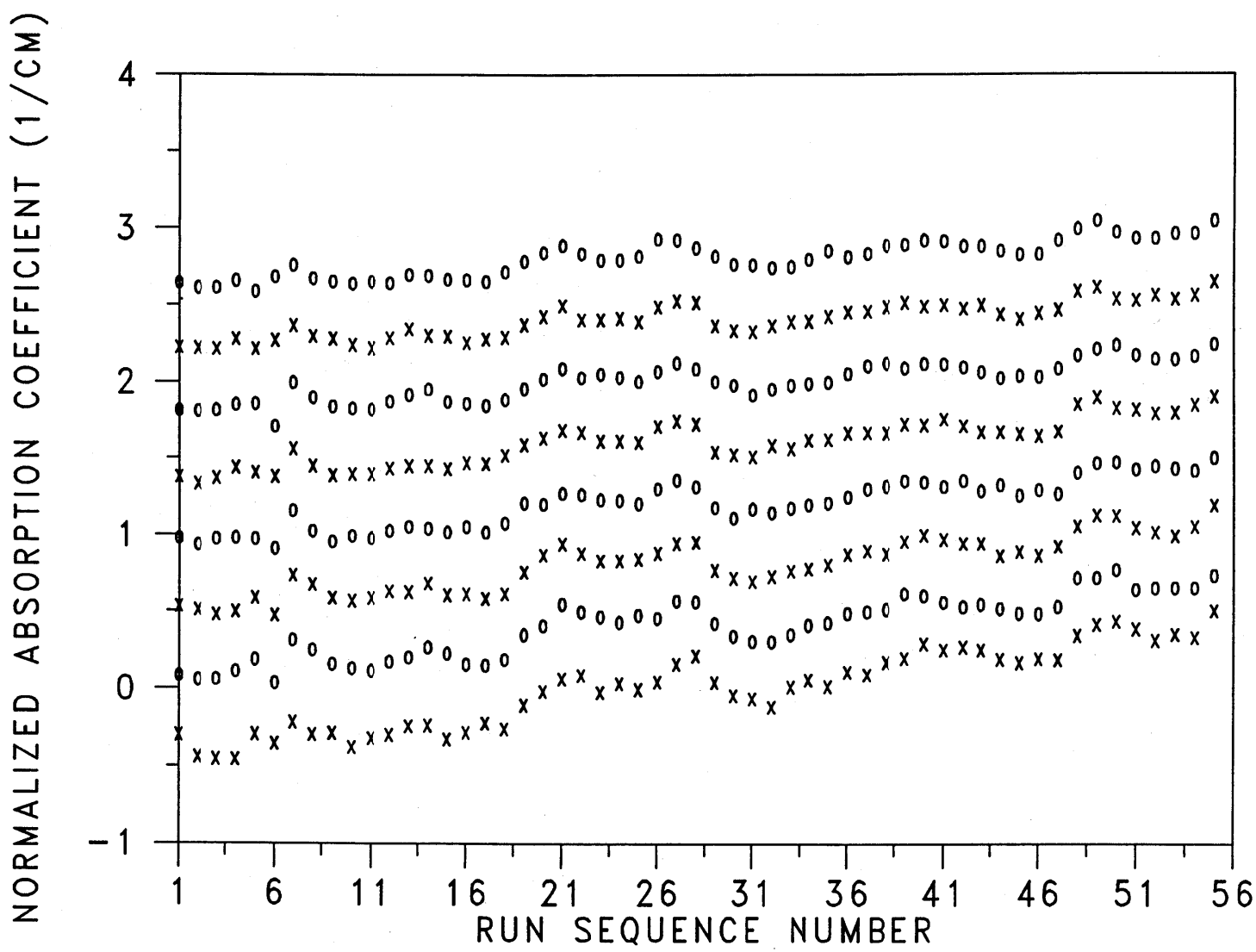

Figure 6. Time plots of normalized absorption coefficient peak heights for the eight-specimen calibration set (1/cm vs chronological test points occurring roughly once every three hours).

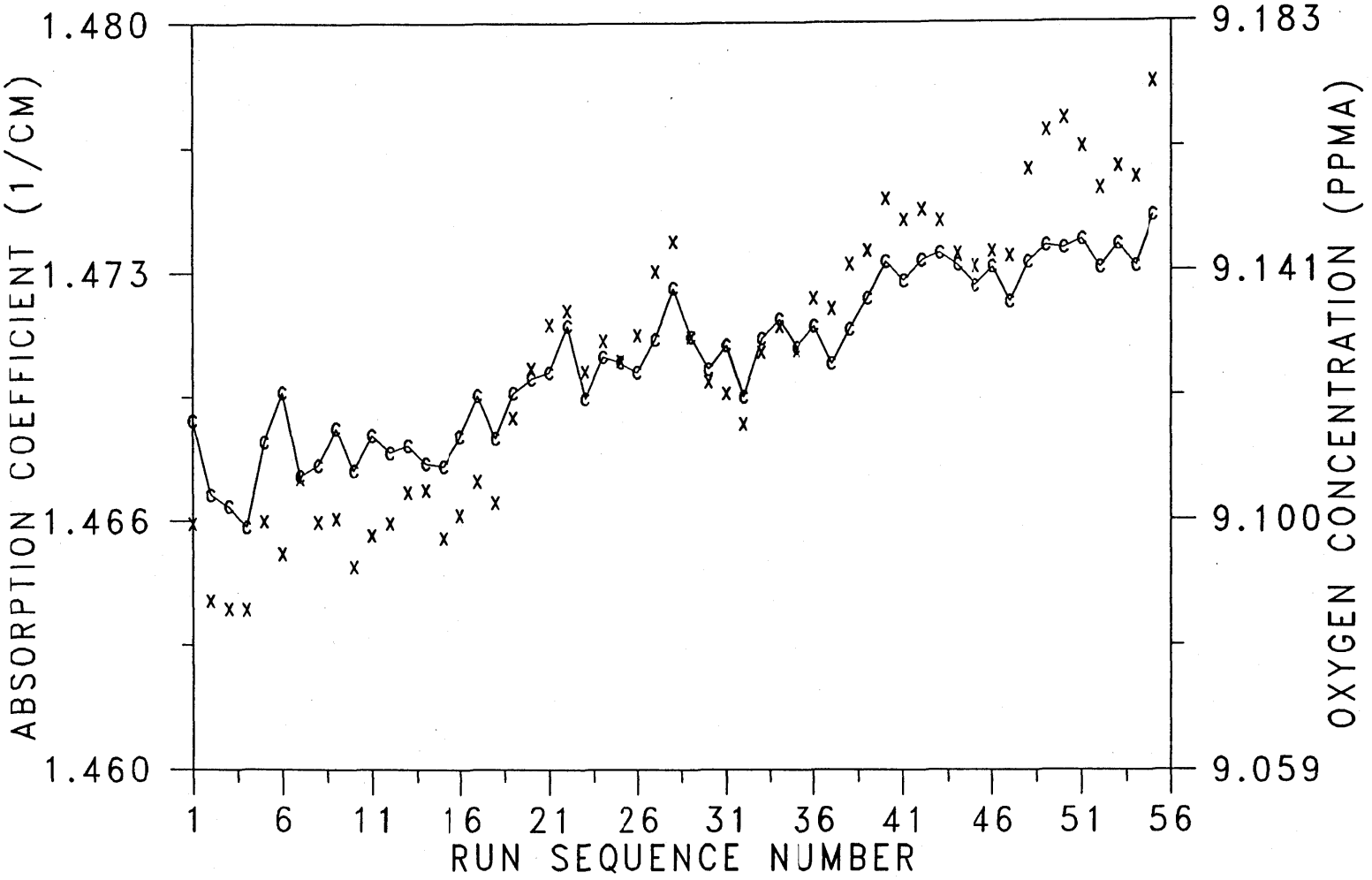

Figure 7. Time plots of absorption coefficient peak heights for specimen 1 of the eight-specimen calibration set. The "c" points are drift compensated, and the "x" points are not. The mean of each curve is 1.47/cm. The percent standard deviation values are 0.263% for the measured values and 0.148% for the compensated values.

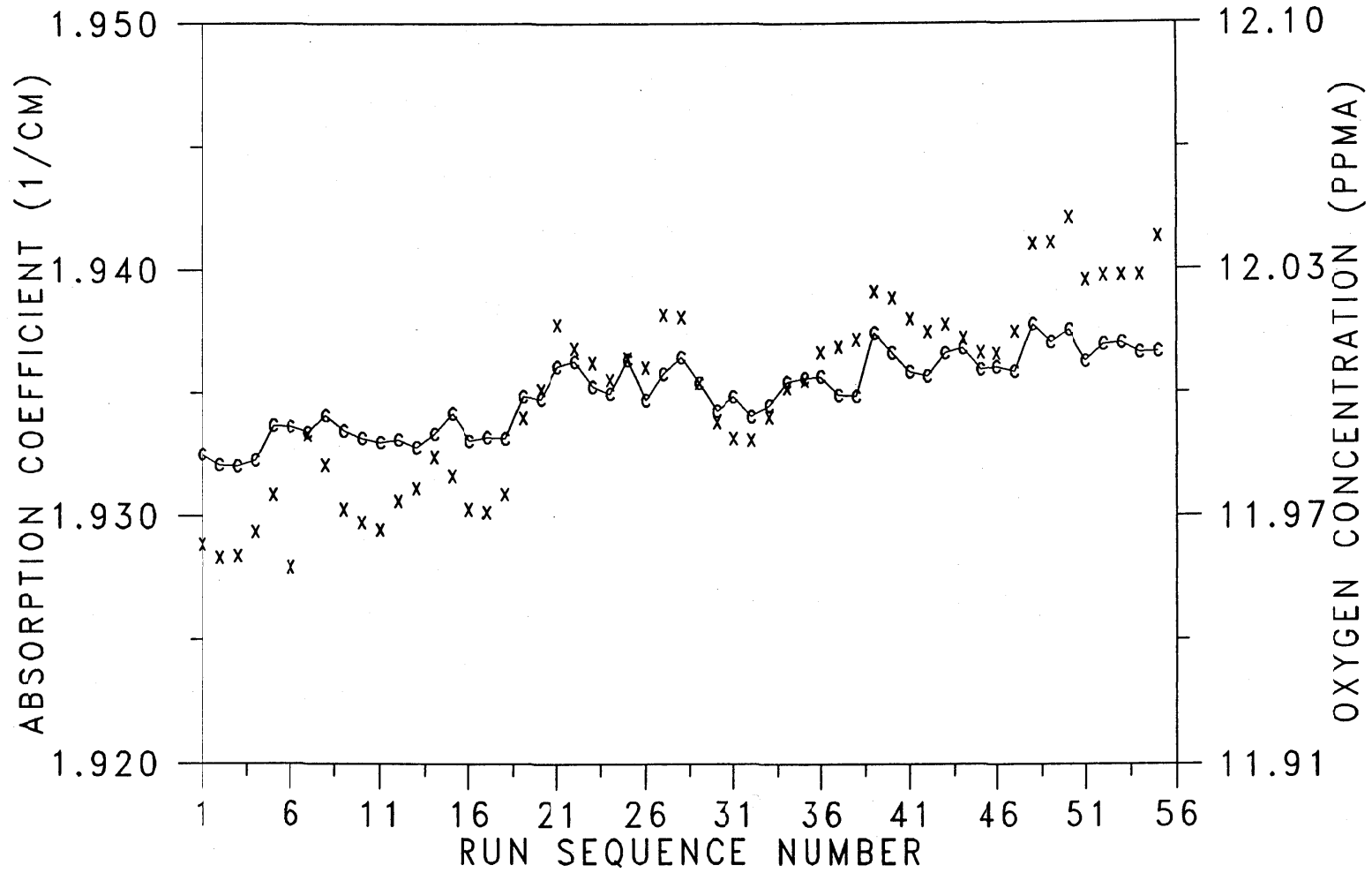

Figure 8. Time plots of absorption coefficient peak heights for specimen 2 of the eight-specimen calibration set. The "c" points are drift compensated, and the "x" points are not. The mean of each curve is 1.94/cm. The percent standard deviation values are 0.200% for the measured values and 0.081% for the compensated values.

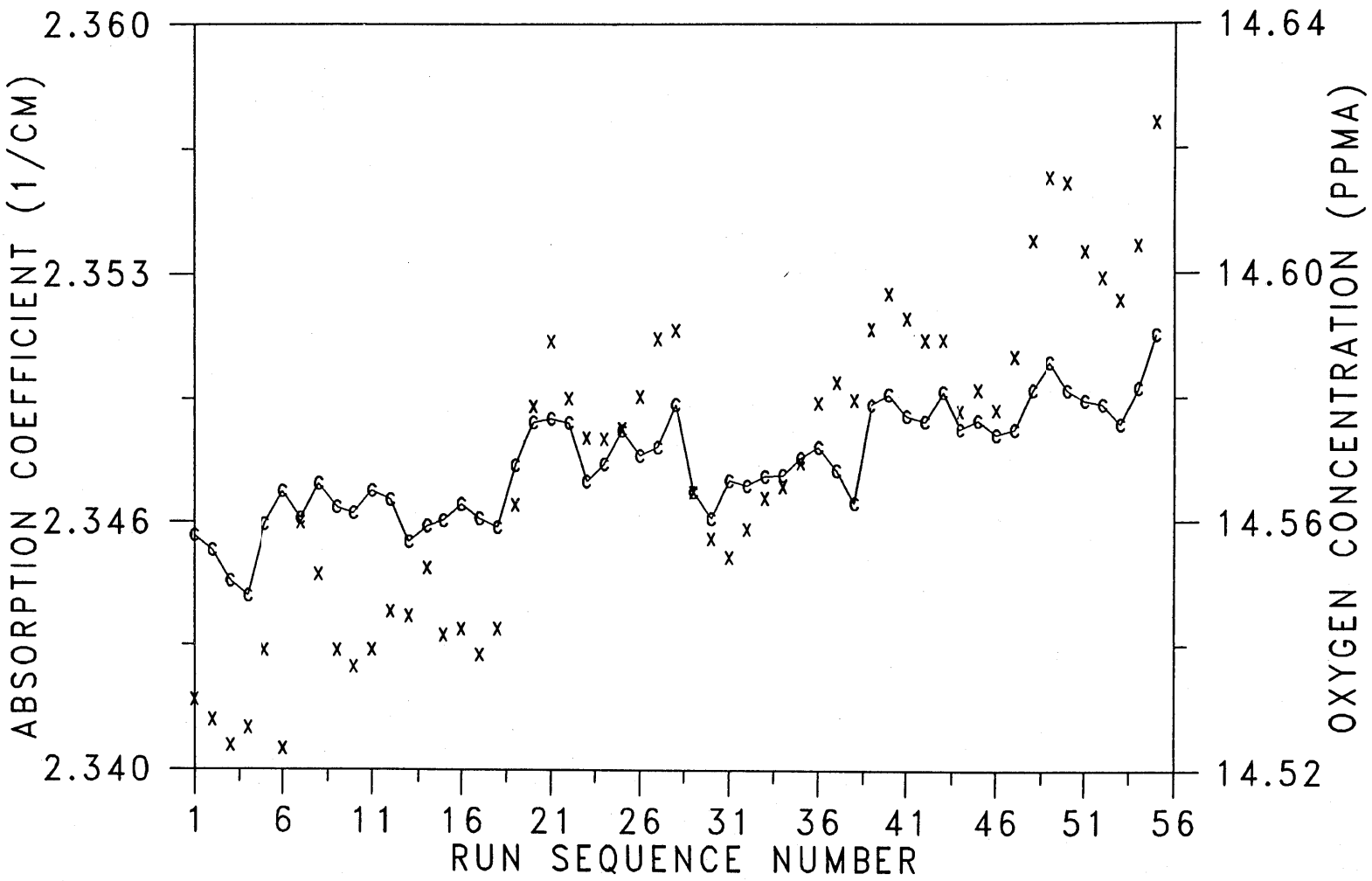

Figure 9. Time plots of absorption coefficient peak heights for specimen 3 of the eight-specimen calibration set. The "c" points are drift compensated, and the "x" points are not. The mean of each curve is 2.35/cm. The percent standard deviation values are 0.184% for the measured values and 0.081% for the compensated values.

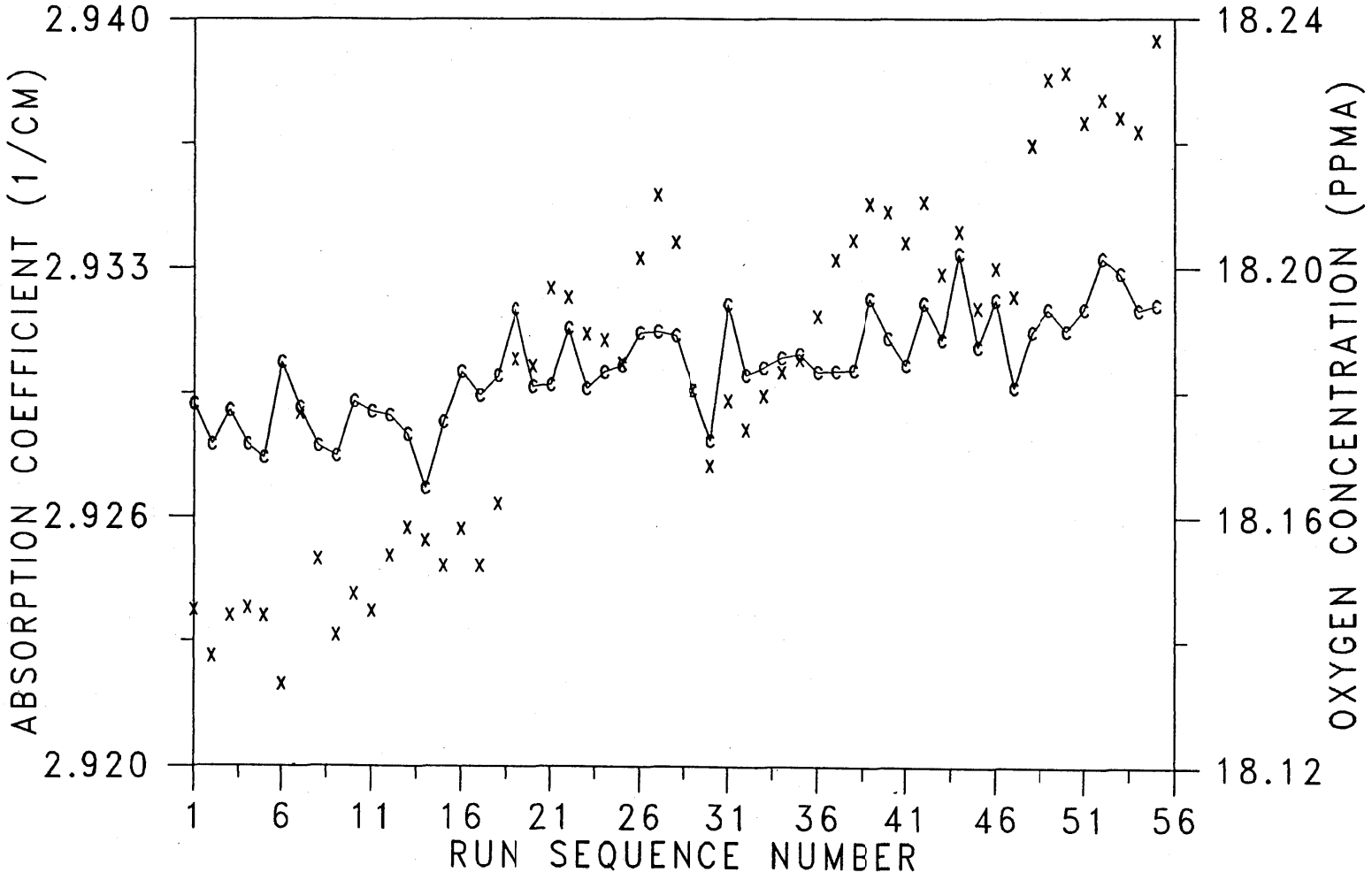

Figure 10. Time plots of absorption coefficient peak heights for specimen 4 of the eight-specimen calibration set. The "c" points are drift compensated, and the "x" points are not. The mean of each curve is 2.93/cm. The percent standard deviation values are 0.162% for the measured values and 0.048% for the compensated values.

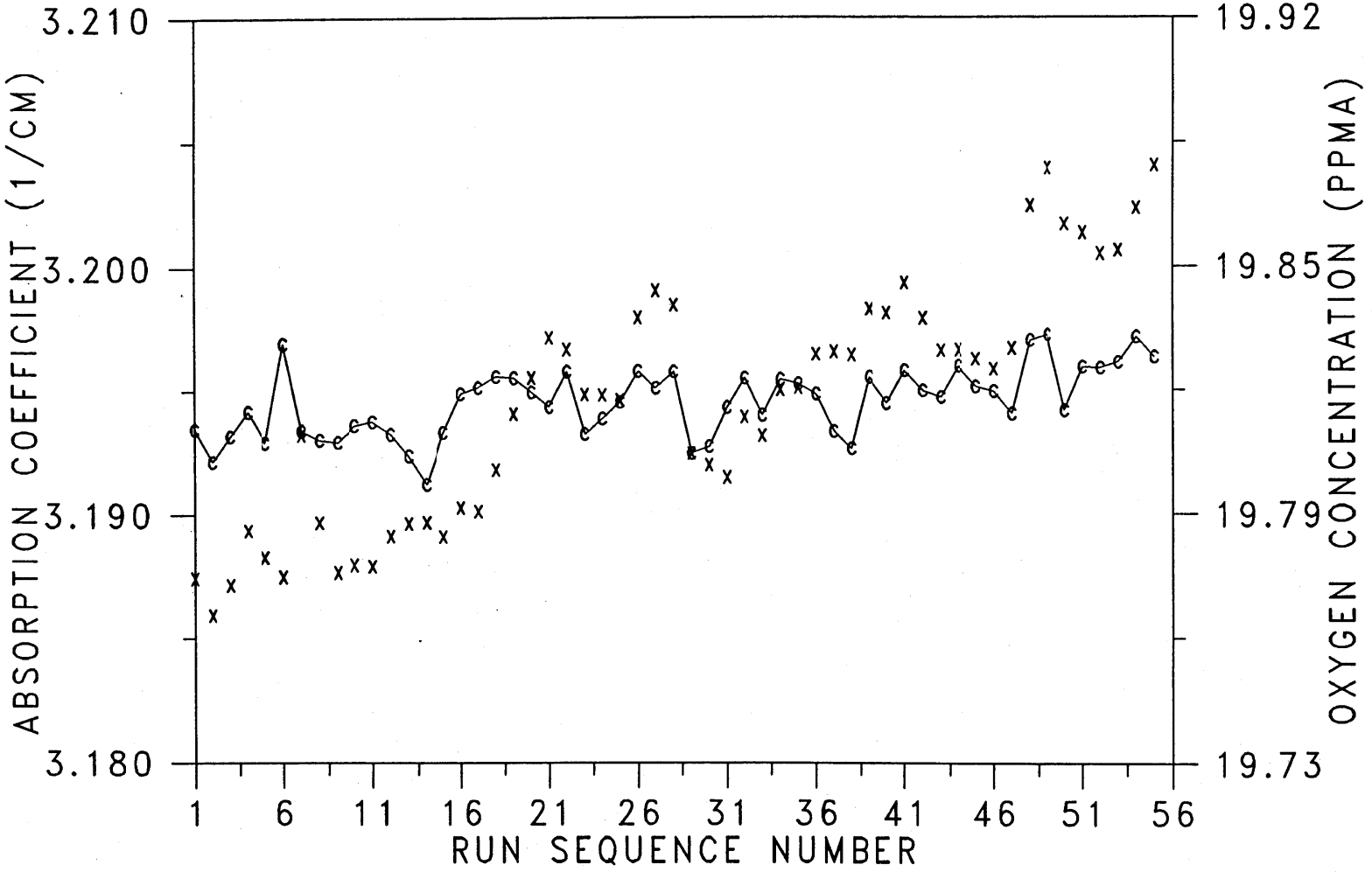

Figure 11. Time plots of absorption coefficient peak heights for specimen 5 of the eight-specimen calibration set. The "c" points are drift compensated, and the "x" points are not. The mean of each curve is 3.19/cm. The percent standard deviation values are 0.151% for the measured values and 0.043% for the compensated values.

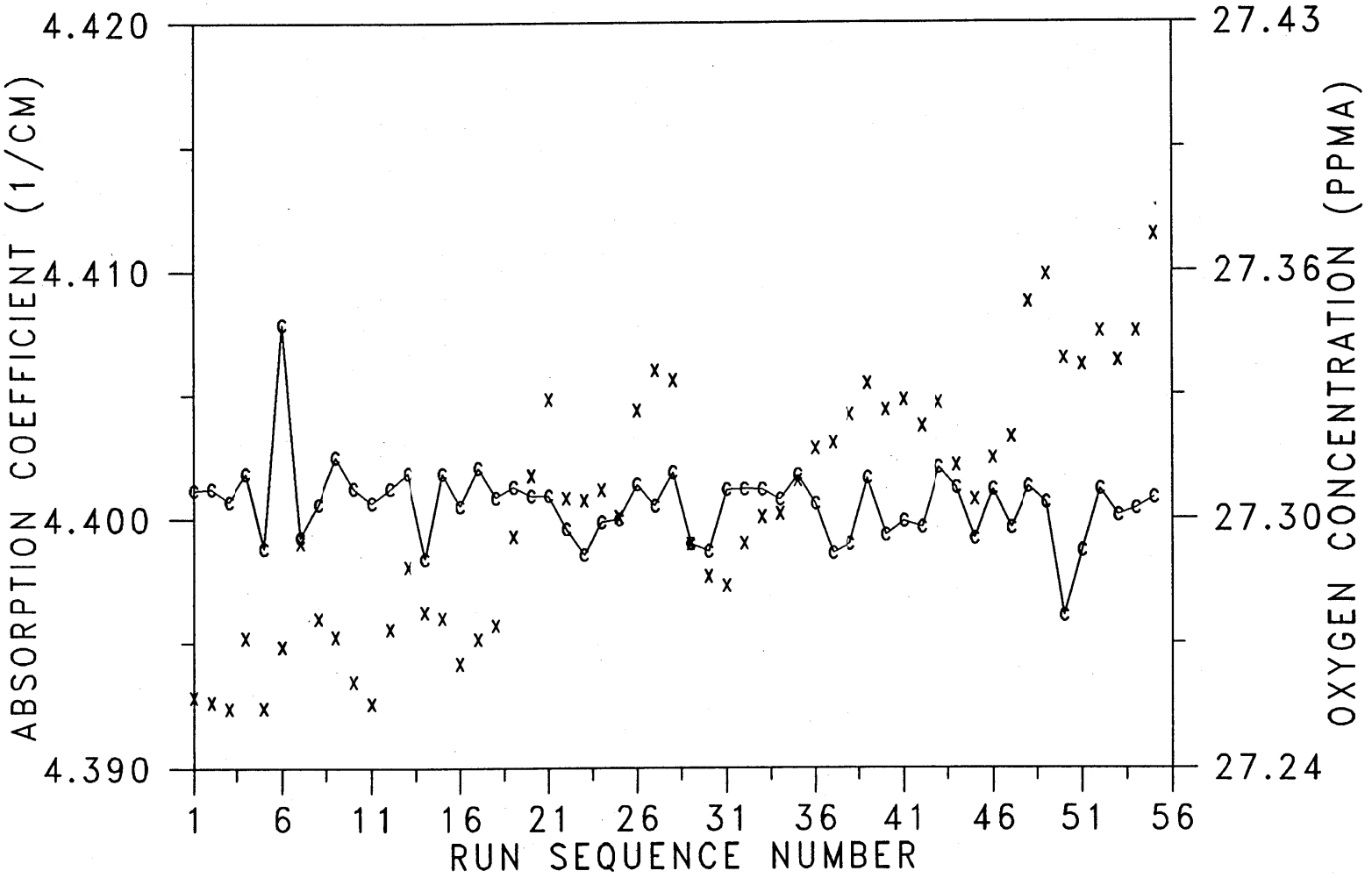

Figure 12. Time plots of absorption coefficient peak heights for specimen 7 of the eight-specimen calibration set. The "c" points are drift compensated, and the "x" points are not. The mean of each curve is 4.40/cm. The percent standard deviation values are 0.114% for the measured values and 0.036% for the compensated values.

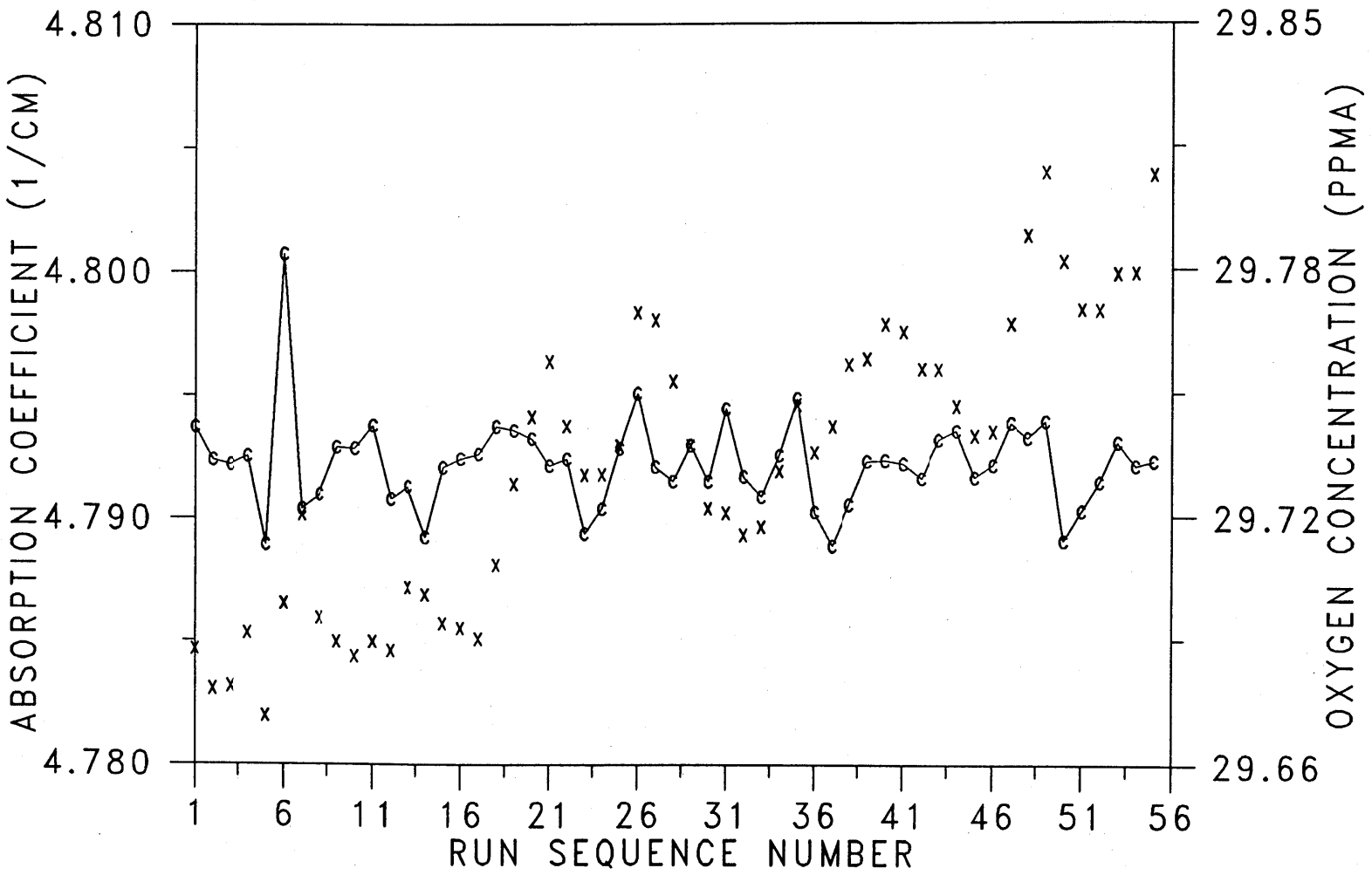

Figure 13. Time plots of absorption coefficient peak heights for specimen 8 of the eight-specimen calibration set. The "c" points are drift compensated, and the "x" points are not. The mean of each curve is 4.79/cm. The percent standard deviation values are 0.120% for the measured values and 0.039% for the compensated values.

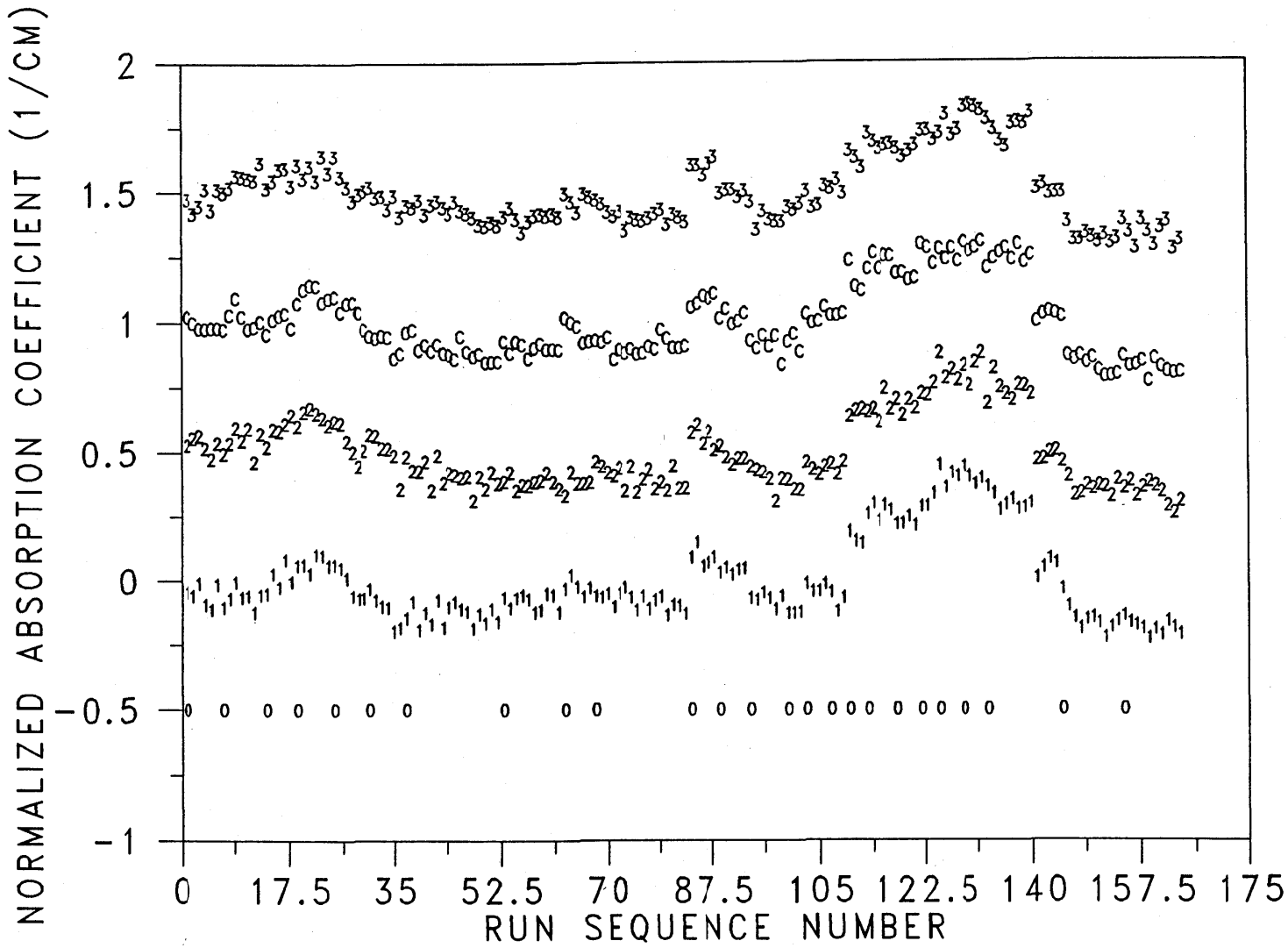

Figure 14. Time plots of normalized absorption coefficient peak heights for performance evaluation set. Test points are spaced by approximately an hour within a daily run. There are time gaps of 17 hours before the beginning of each run, indicated by "0".

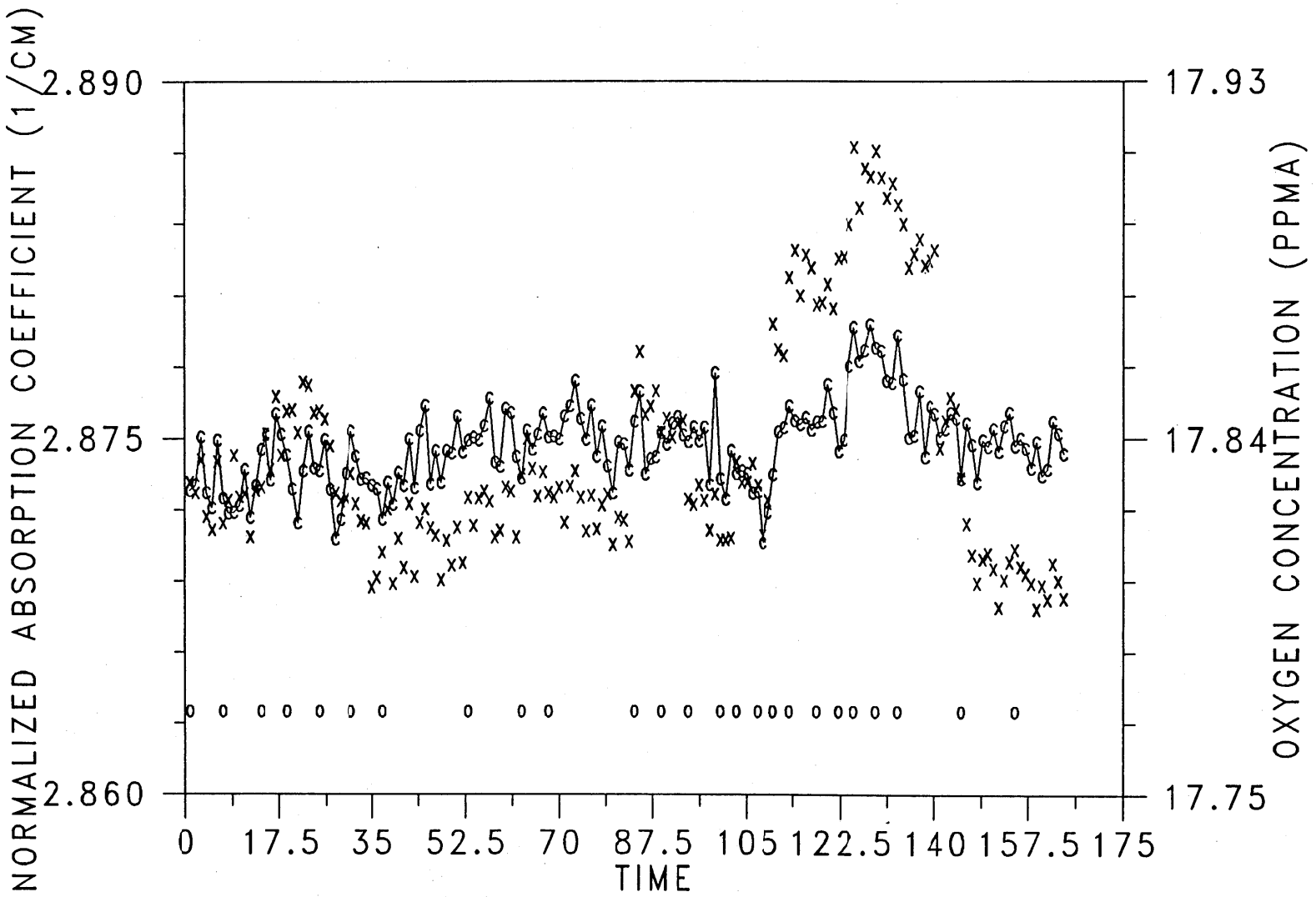

Figure 15. Time plots of absorption coefficient peak heights for the low-oxygen specimen of the performance evaluation set. The "c" points are drift compensated, and the "x" points are not. The mean of each curve is 2.874. The percent standard deviation values are 0.166% for the measured values and 0.059% for the compensated values.

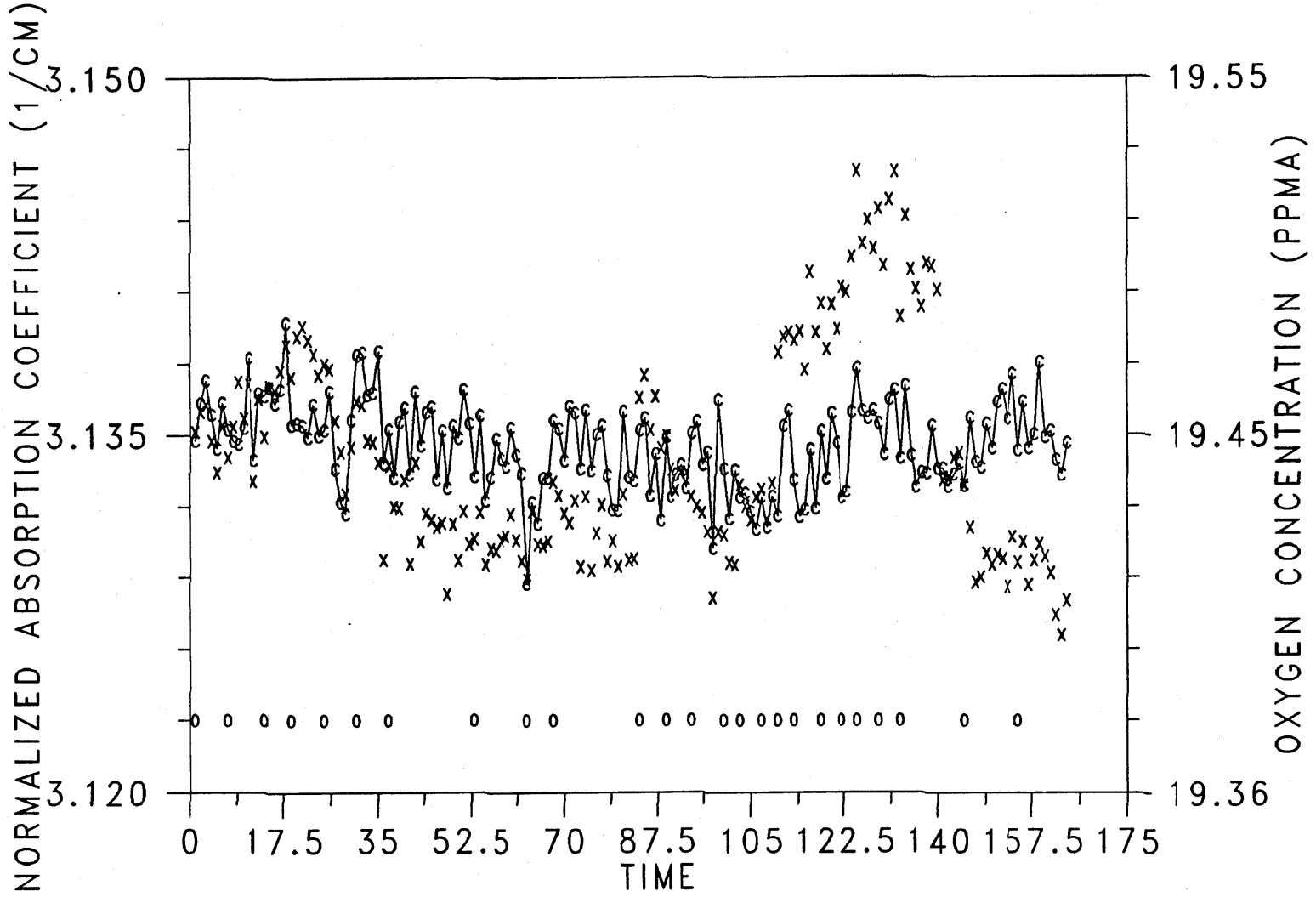

Figure 16. Time plots of absorption coefficient peak heights for the mid-oxygen specimen of the performance evaluation set. The "c" points are drift compensated, and the "x" points are not. The mean of each curve is 3.134. The percent standard deviation values are 0.142% for the measured values and 0.059% for the compensated values.

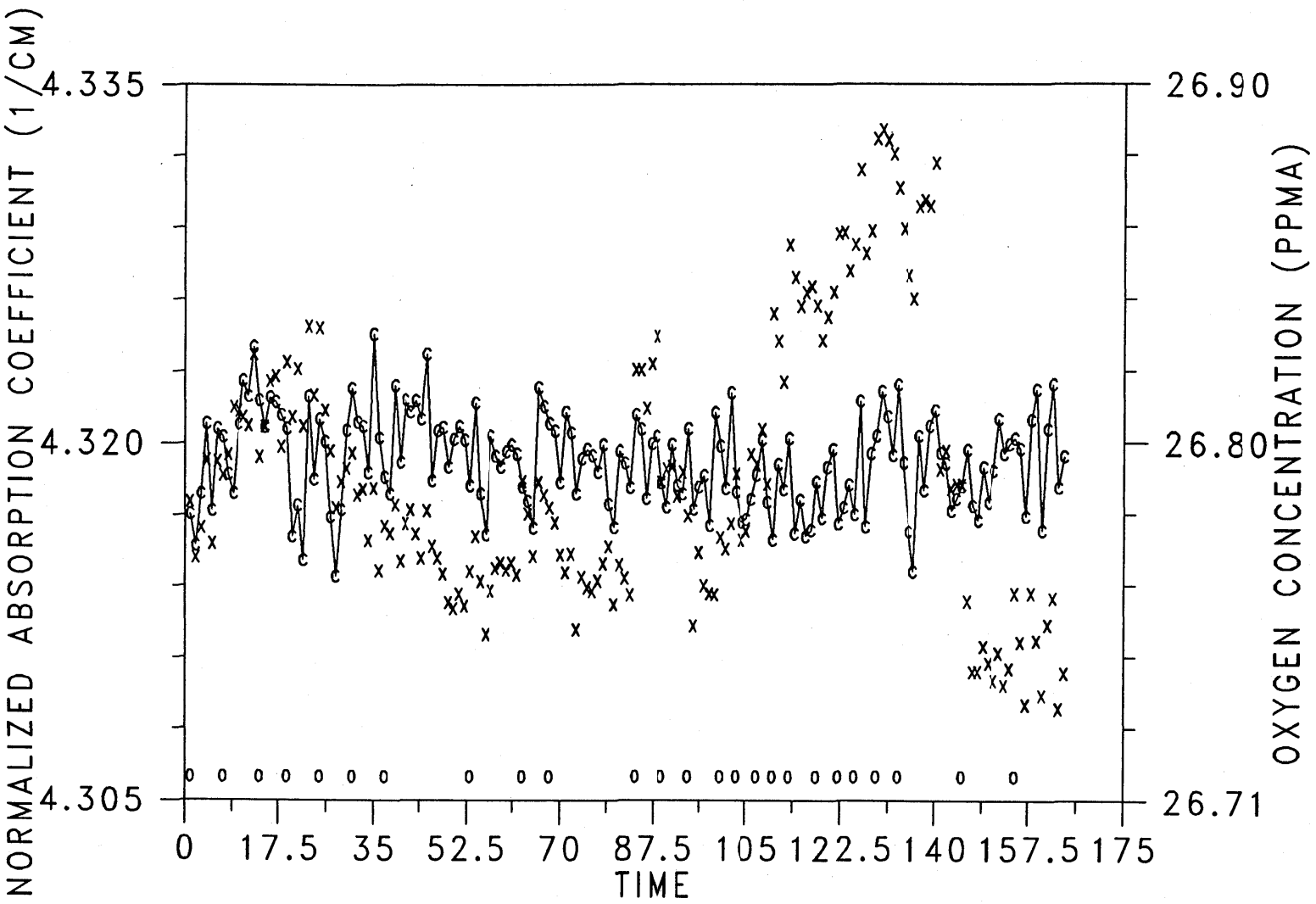

Figure 17. Time plots of absorption coefficient peak heights for the high-oxygen specimen of the performance evaluation set. The "c" points are drift compensated, and the "x" points are not. The mean of each curve is 4.319. The percent standard deviation values are 0.133% for the measured values and 0.046% for the compensated values.

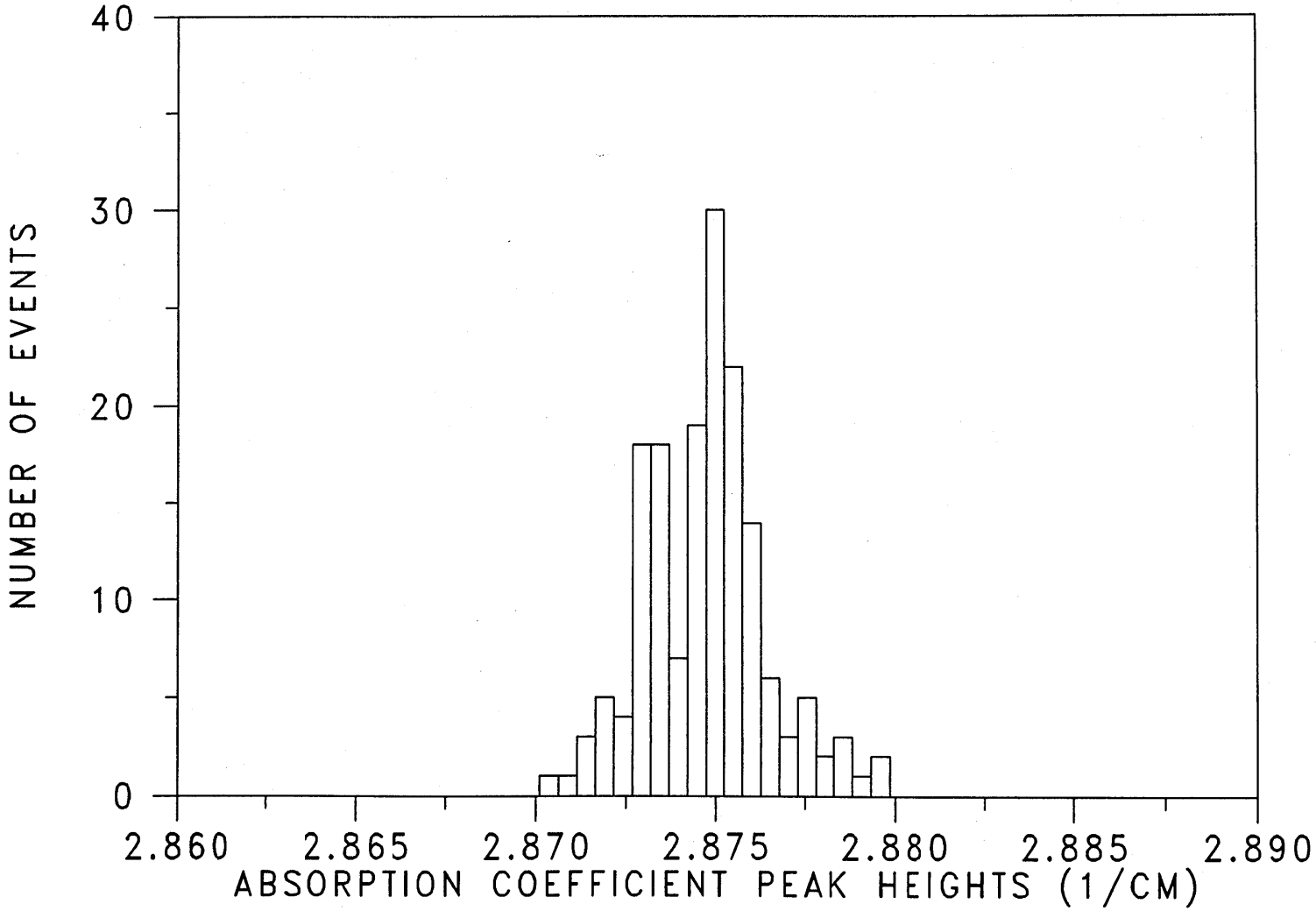

Figure 18. Histogram for time plots of absorption coefficient peak heights for the low-oxygen specimen of the performance evaluation set. The mean value is 2.875, and the percent standard deviation is 0.059%.

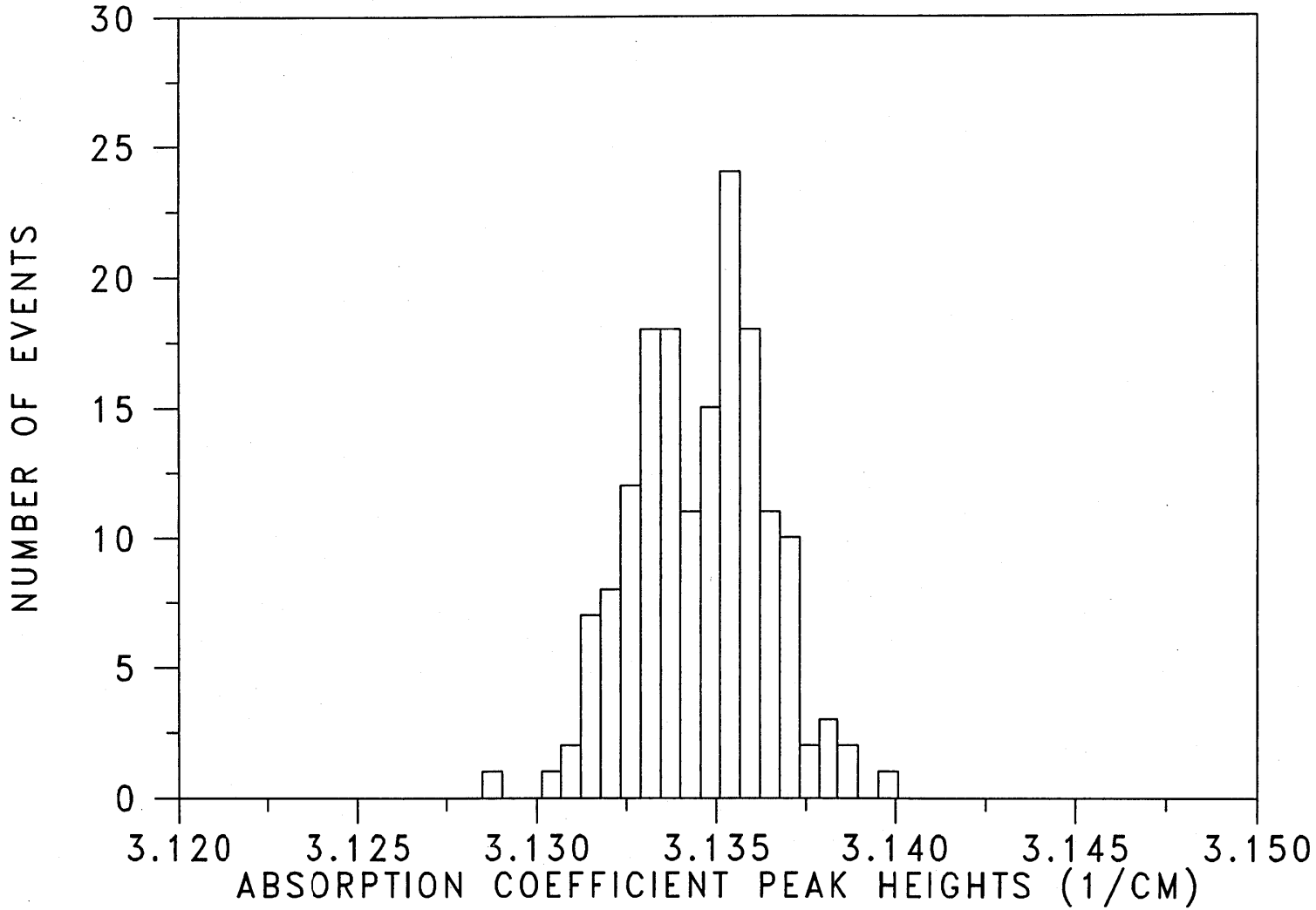

Figure 19. Histogram for time plots of absorption coefficient peak heights for the medium-oxygen specimen of the performance evaluation set. The mean value is 3.135, and the percent standard deviation is 0.059%.

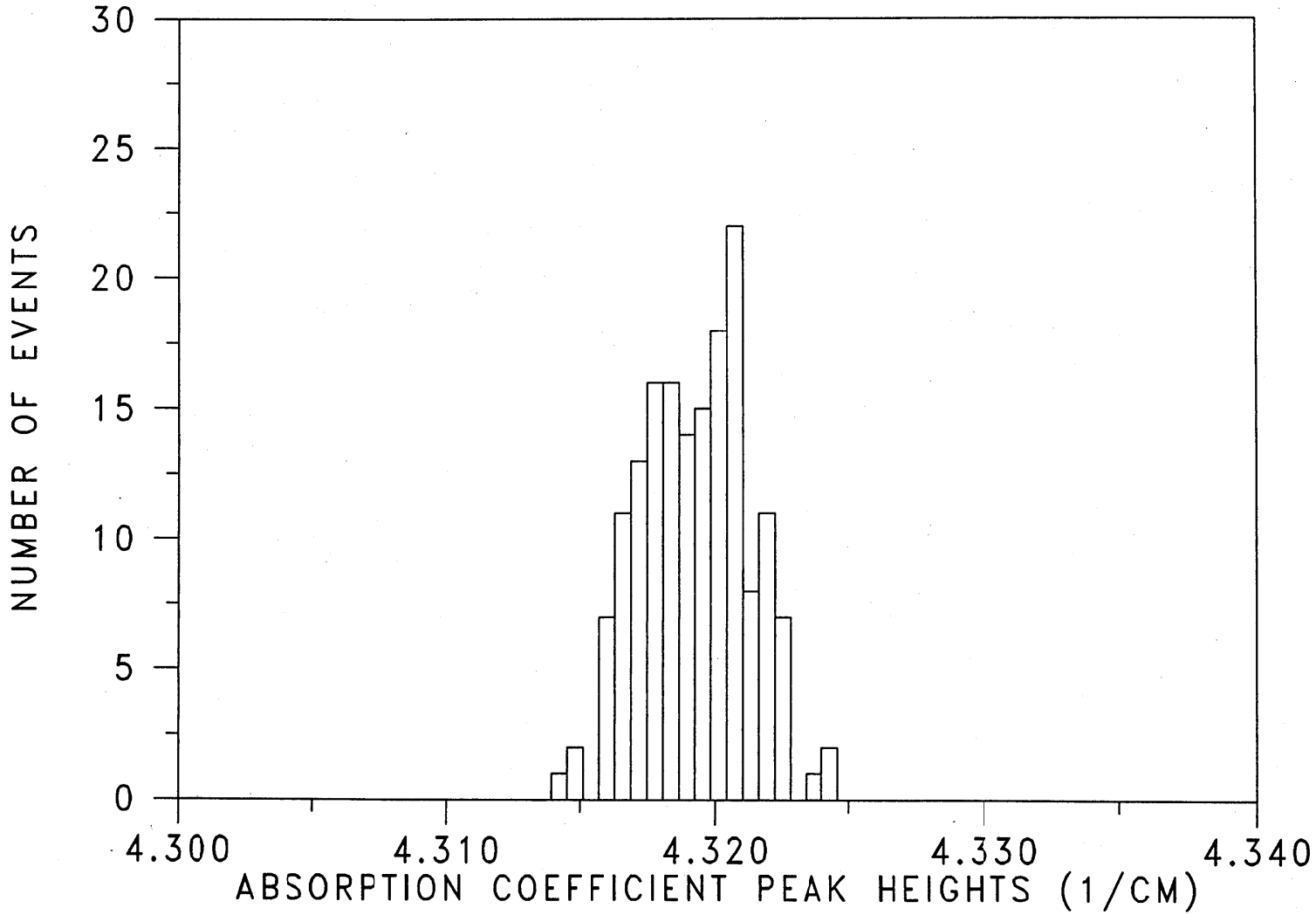

Figure 20. Histogram for time plots of absorption coefficient peak heights for the high-oxygen specimen of the performance evaluation set. The mean value is 4.319, and the percent standard deviation is 0.046%.

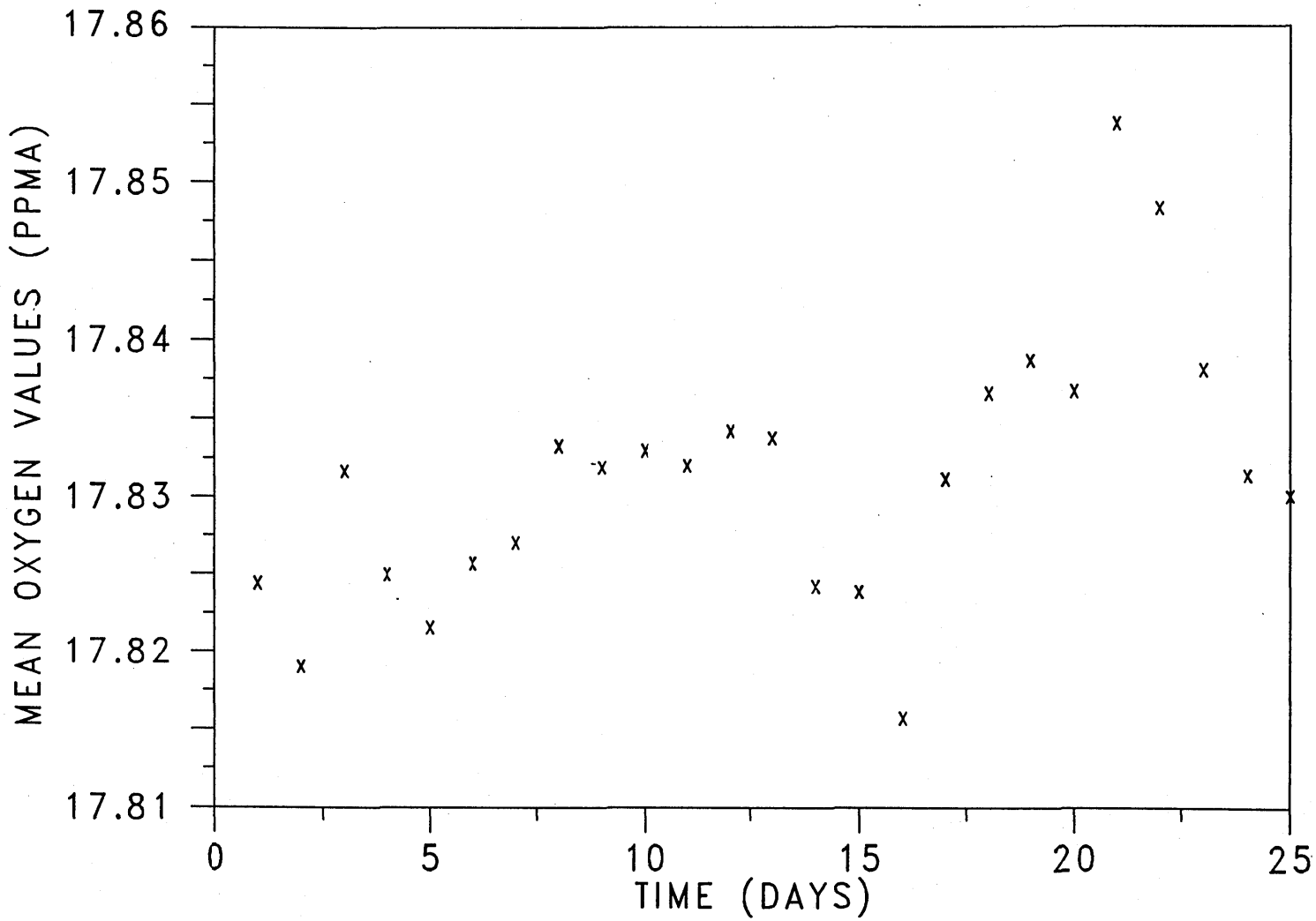

Figure 21. Time plots of mean values, over a daily run, of oxygen concentration for the low-oxygen specimen of the performance evaluation set. These points are drift compensated, and the percent standard deviation is 0.0100 ppma or 0.0055%.

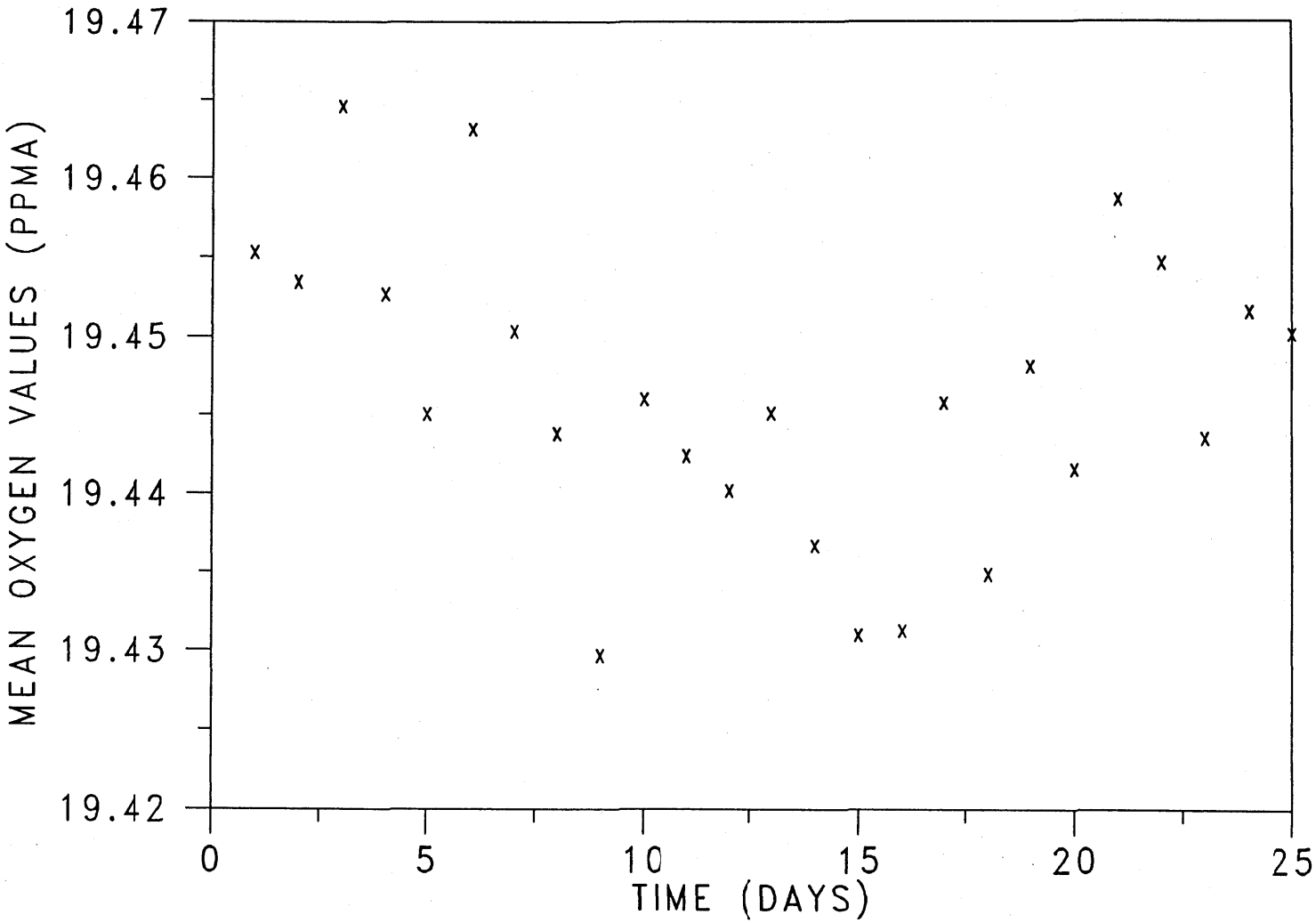

Figure 22. Time plots of mean values, over a daily run, of oxygen concentration for the medium-oxygen specimen of the performance evaluation set. These points are drift compensated, and the percent standard deviation is 0.0093 ppma or 0.0047%.

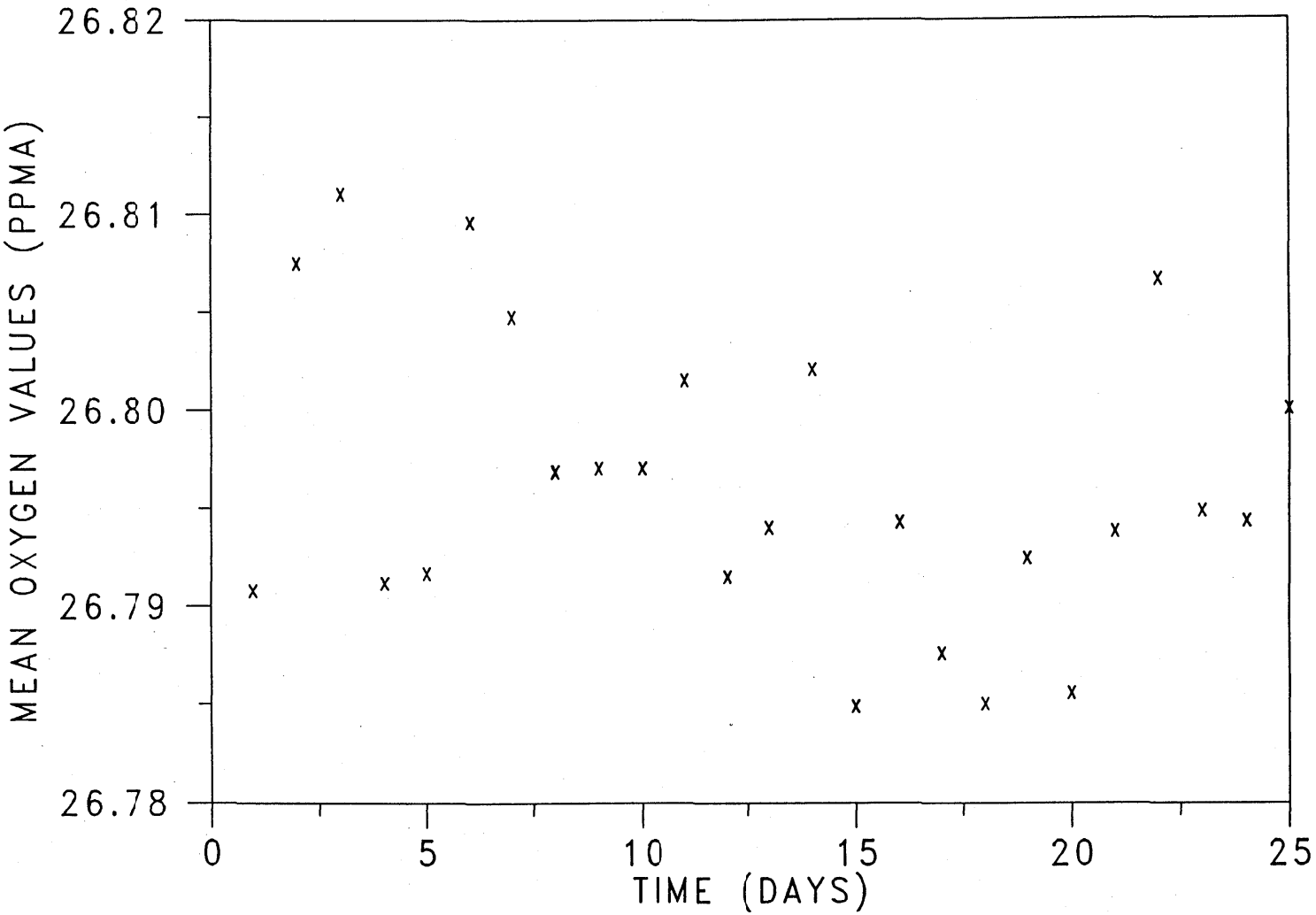

Figure 23. Time plots of mean values, over a daily run, of oxygen concentration for the high-oxygen specimen of the performance evaluation set. These points are drift compensated, and the percent standard deviation is 0.0075 ppma or 0.0028%.

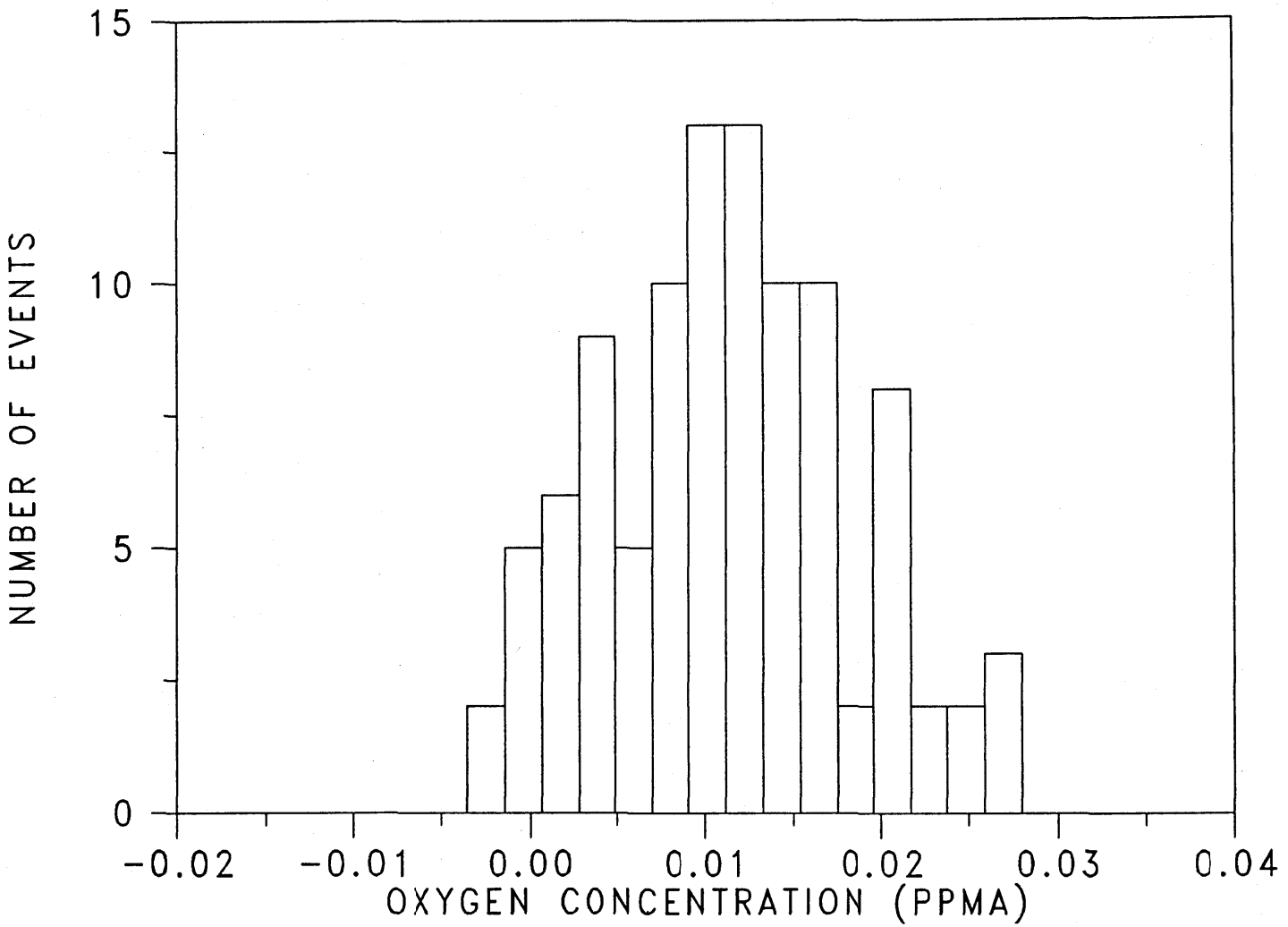

Figure 24. Histogram comparing measured oxygen concentrations among all SRM float-zone specimens. The mean difference from the comparison GRR float-zone specimen is 0.0112 ppma, and the standard deviation is 0.007 ppma.

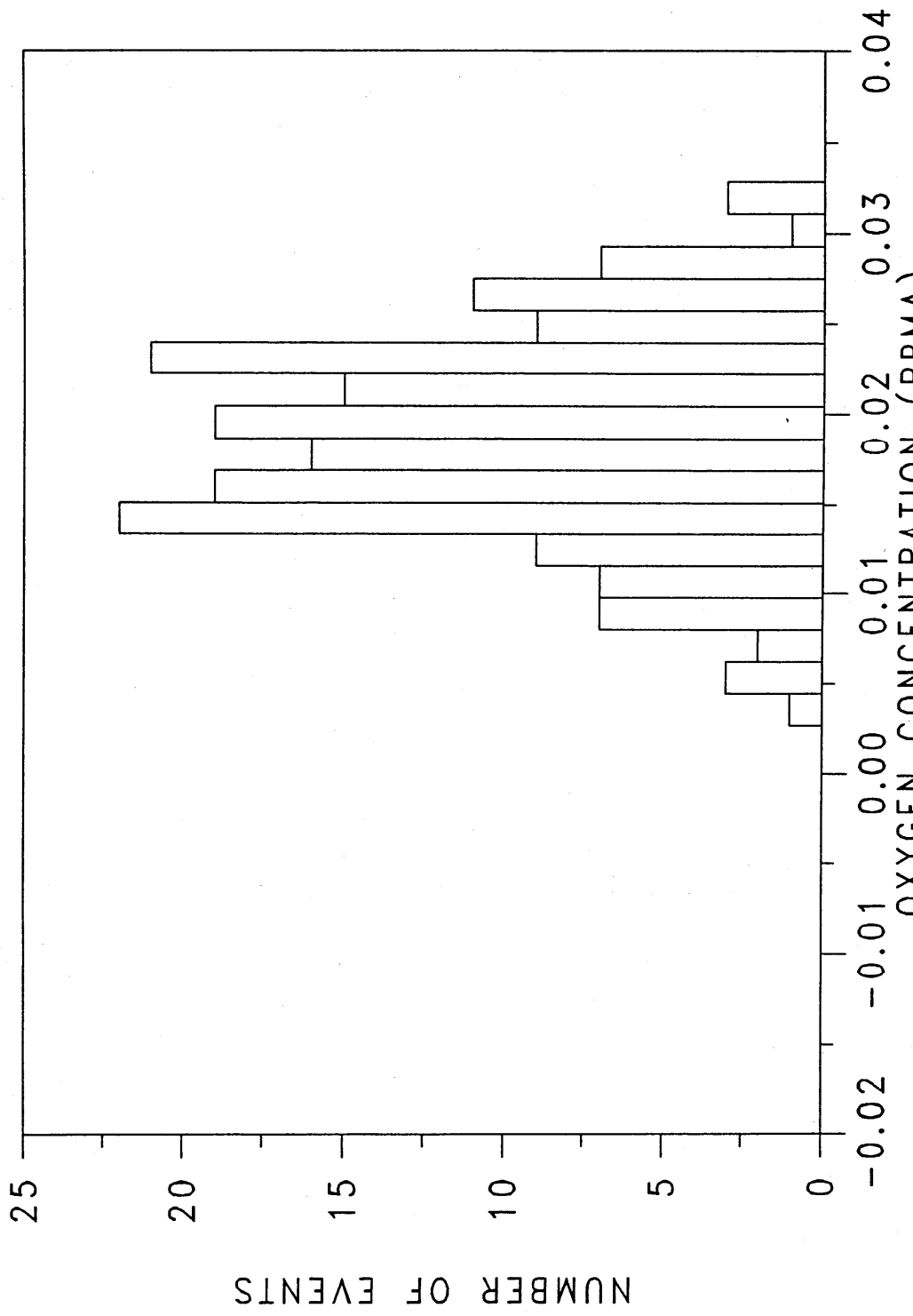

Figure 25. Histogram for repeated measurements of oxygen concentration on a single float-zone specimen. The mean difference from the GRR reference float-zone specimen is 0.019 ppma, and the standard deviation is 0.006 ppma.

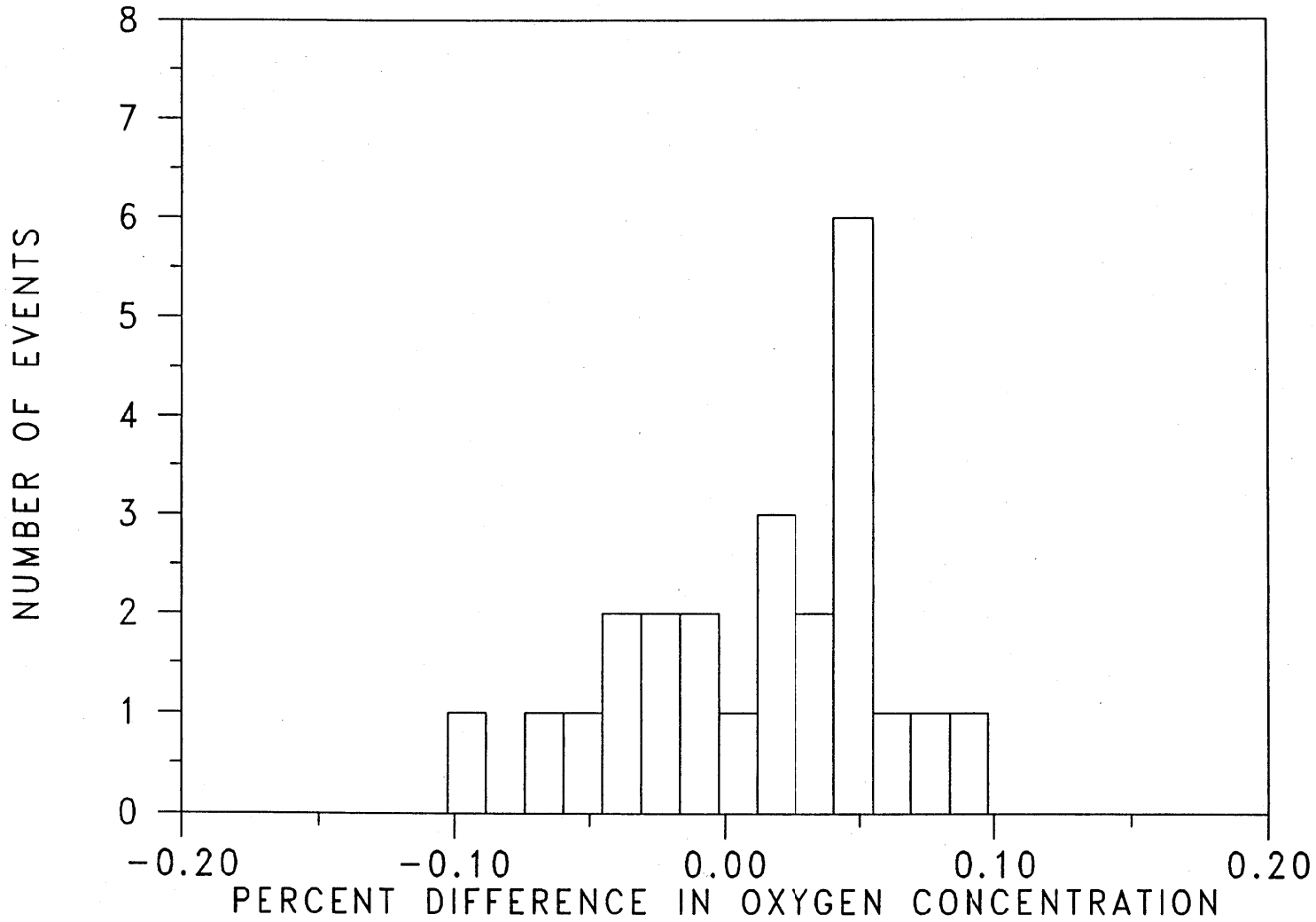

Figure 26. Histogram for a material uniformity study of percent difference values in measured oxygen concentration for positional offsets of 2 mm. The standard deviation is 0.048%.

TABLE 1. SRM 2551 conversion coefficient data using absolute oxygen concentration data from the GRR and absorption coefficient data from the NIST FTIR

specimen code from GRR [1]	oxygen concentration (ppma)*	absorption coefficient (cm^{-1})
210101	8.678	1.4431
210201	12.334	1.8983
210301	14.593	2.2560
210401	17.325	2.8752
210501	20.356	3.1340
210701	23.524	3.8646
210801	26.821	4.3172
210901	28.721	4.7014

* After adjustment of 0.072% to agree with the full GRR specimen set [sec. III].

TABLE 2. Percent difference in absorption coefficient peak height due to positional shifts of 2 mm from center position

α (cm^{-1})	% change of α	% standard deviation	beam position
2.6842	reference value	0.051	center
2.6841	0.004	0.034	2-mm shift
2.6832	0.040	0.033	2-mm shift
2.6996	reference value	0.027	center
2.7015	-0.070	0.037	2-mm shift
2.6970	0.100	0.035	2-mm shift
3.6293	reference value	0.019	center
3.6266	0.070	0.024	2-mm shift
3.6325	-0.090	0.040	2-mm shift
3.5109	reference value	0.023	center
3.5126	-0.050	0.035	2-mm shift
3.5119	-0.030	0.021	2-mm shift
4.1906	reference value	0.029	center
4.1890	0.040	0.037	2-mm shift
4.1909	-0.007	0.017	2-mm shift
4.1683	reference value	0.042	center
4.1703	-0.050	0.018	2-mm shift
4.1676	0.020	0.033	2-mm shift
2.7022	reference value	0.031	center
2.7034	0.044	0.036	2-mm shift
2.7029	0.026	0.027	2-mm shift

TABLE 2. (continued)

α (cm^{-1})	% change of α	% standard deviation	beam position
3.6346	reference value	0.039	center
3.6326	-0.055	0.029	2-mm shift
3.6363	0.047	0.039	2-mm shift
4.1971	reference value	0.025	center
4.1963	-0.019	0.031	2-mm shift
4.1979	0.019	0.032	2-mm shift
2.6818	reference value	0.041	center
2.6828	0.038	0.033	2-mm shift
2.6824	0.023	0.030	2-mm shift
3.4924	reference value	0.018	center
3.4941	0.049	0.032	2-mm shift
3.4920	-0.011	0.029	2-mm shift
4.1659	reference value	0.017	center
4.1682	0.056	0.026	2-mm shift
4.1678	0.046	0.023	2-mm shift

TABLE 3. Summary of uncertainty estimates

source of uncertainty	oxygen level	1σ (%)	2σ (%)
standard deviation due to FTIR reproducibility	low	0.068	0.136
	medium	0.050	0.100
	high	0.044	0.088
standard deviation due to SRM float-zone oxygen variability	low	0.041	0.082
	medium	0.030	0.060
	high	0.027	0.054
standard deviation estimate related to material uniformity	low	0.030	0.060
	medium	0.030	0.060
	high	0.030	0.060
total SRM uncertainty	low	0.086	0.17
	medium	0.067	0.13
	high	0.060	0.12

TABLE 4. Percent difference in absorption coefficient peak height after later repeats

SRM set #	oxygen level	% difference	difference in ppma
1	low	-0.017	-0.0029
1	medium	0.035	0.0080
1	high	0.003	0.0008
15	low	0.042	0.0071
15	medium	0.062	0.0143
15	high	0.002	0.0005
17	low	0.050	0.0085
17	medium	0.082	0.0189
17	high	0.038	0.0100
18	low	0.097	0.0165
18	medium	-0.007	-0.0016
18	high	0.017	0.0044
53	low	0.131	0.0223
53	medium	0.117	0.0257
53	high	0.017	0.0044
77	low	0.092	0.0156
77	medium	0.129	0.0271
77	high	0.065	0.0169
100	low	0.070	0.0110
100	medium	0.044	0.0092
100	high	0.070	0.0182

TABLE 5. Percent difference in absorption coefficient peak height for three remeasurements with different locations of the specimens in their holder

SRM set #	oxygen level	% difference	difference in ppma
15	low	0.060	0.0102
15	medium	0.035	0.0080
15	high	0.026	0.0068
15	low	0.034	0.0058
15	medium	0.006	0.0014
15	high	0.019	0.0049
15	low	0.042	0.0071
15	medium	0.062	0.0143
15	high	0.002	0.0005
77	low	-0.051	-0.0087
77	medium	0.004	0.0009
77	high	-0.094	-0.0207
77	low	0.016	0.0027
77	medium	0.034	0.0102
77	high	-0.058	-0.0151
77	low	-0.024	-0.0041
77	medium	0.080	0.0176
77	high	0.098	0.0255

TABLE 6. Certified interstitial oxygen values for the 100 SRM sets (ppma)

set #	low oxygen	medium oxygen	high oxygen
1	16.837	22.781	26.250
2	16.752	22.778	26.267
3	16.809	22.833	26.303
4	16.758	22.771	26.316
5	16.878	22.702	26.334
6	16.853	22.711	26.327
7	16.868	22.784	26.368
8	16.869	22.762	26.312
9	16.727	22.648	26.323
10	16.744	22.621	26.262
11	16.727	22.684	26.267
12	16.732	22.637	26.233
13	16.933	22.576	26.050
14	16.943	22.650	26.033
15	16.910	22.583	26.128
16	16.946	22.595	26.108
17	16.777	22.539	26.058
18	16.757	22.578	26.012
19	16.773	22.605	26.062
20	16.785	22.596	26.071
21	16.826	22.824	26.052
22	16.824	22.819	26.028
23	16.809	22.822	26.058
24	16.865	22.830	26.062
25	16.667	22.526	26.001

TABLE 6. (continued)

set #	low oxygen	medium oxygen	high oxygen
26	16.654	22.557	25.983
27	16.646	22.581	26.041
28	16.646	22.539	26.056
29	16.851	22.437	25.892
30	16.829	22.411	25.890
31	16.848	22.473	25.920
32	16.854	22.445	25.915
33	16.843	22.319	26.169
34	16.888	22.261	26.174
35	16.849	22.346	26.160
36	16.894	22.372	26.159
37	16.823	22.119	26.109
38	16.832	22.101	26.083
39	16.831	22.109	26.096
40	16.817	22.084	26.083
41	17.005	22.157	25.948
42	17.032	22.158	25.937
43	16.998	22.165	26.032
44	17.017	22.151	26.045
45	16.852	22.136	25.945
46	16.887	22.103	25.946
47	16.925	22.133	25.955
48	16.937	22.129	25.938
49	16.938	22.116	25.883
50	16.941	22.114	25.866

TABLE 6. (continued)

set #	low oxygen	medium oxygen	high oxygen
51	16.990	22.083	25.897
52	16.984	22.107	25.894
53	16.957	22.125	25.608
54	16.865	21.956	25.946
55	16.866	22.021	25.903
56	16.846	22.004	25.926
57	16.814	21.998	25.922
58	16.904	22.013	25.908
59	16.831	22.017	25.898
60	16.873	22.008	25.894
61	16.823	21.924	25.950
62	16.789	21.885	25.986
63	16.841	21.895	26.033
64	16.827	21.917	26.018
65	16.736	21.802	26.060
66	16.755	21.804	26.007
67	16.752	21.856	26.003
68	16.764	21.851	26.021
69	16.620	21.790	25.896
70	16.607	21.882	25.868
71	16.625	21.830	25.890
72	16.647	21.811	25.876
73	16.746	21.738	25.752
74	16.716	21.776	25.797
75	16.768	21.803	25.879

TABLE 6. (continued)

set #	low oxygen	medium oxygen	high oxygen
76	16.764	21.766	25.888
77	16.632	21.713	25.879
78	16.673	21.724	25.840
79	16.670	21.721	25.849
80	16.664	21.699	25.858
81	16.915	21.500	25.822
82	16.900	21.485	25.839
83	16.948	21.532	25.852
84	16.970	21.539	25.891
85	16.844	21.303	25.803
86	16.786	21.292	25.891
87	16.810	21.395	25.873
88	16.818	21.300	25.810
89	16.822	21.199	25.820
90	16.780	21.246	25.765
91	16.823	21.275	25.853
92	16.841	21.284	25.860
93	16.814	20.964	25.867
94	16.794	20.991	25.876
95	16.803	20.929	25.814
96	16.824	20.891	25.765
97	16.912	20.999	25.875
98	16.881	21.042	25.843
99	16.935	21.053	25.923
100	16.903	21.117	25.945

TABLE 7. Center thickness values for the 100 SRM sets (mm)

set #	low oxygen	medium oxygen	high oxygen	float-zone
1	2.0726	2.0347	2.0775	2.1207
2	2.0716	2.0331	2.0824	2.1213
3	2.0714	2.0323	2.0802	2.1244
4	2.0743	2.0296	2.0857	2.1233
5	2.0553	2.0824	2.0718	2.1150
6	2.0558	2.0829	2.0699	2.1207
7	2.0583	2.0834	2.0778	2.1132
8	2.0599	2.0830	2.0749	2.1206
9	2.0722	2.0687	2.1021	2.1203
10	2.0719	2.0684	2.1026	2.1192
11	2.0720	2.0711	2.0945	2.1180
12	2.0713	2.0732	2.0963	2.1160
13	2.0589	2.0638	2.0568	2.1140
14	2.0589	2.0669	2.0550	2.1153
15	2.0599	2.0656	2.0525	2.1131
16	2.0566	2.0666	2.0521	2.1172
17	2.0728	2.0726	2.0701	2.1174
18	2.0718	2.0720	2.0728	2.1206
19	2.0760	2.0737	2.0670	2.1165
20	2.0753	2.0750	2.0677	2.1184
21	2.0841	2.0901	2.0573	2.1279
22	2.0830	2.0897	2.0673	2.1243
23	2.0724	2.0879	2.0517	2.1297
24	2.0720	2.0888	2.0596	2.1249
25	2.0633	2.0814	2.0404	2.1205

TABLE 7. (continued)

set #	low oxygen	medium oxygen	high oxygen	float-zone
26	2.0631	2.0851	2.0419	2.1248
27	2.0693	2.0765	2.0372	2.1188
28	2.0674	2.0791	2.0395	2.1232
29	2.0759	2.0895	2.0697	2.1284
30	2.0776	2.0819	2.0711	2.1310
31	2.0779	2.0910	2.0604	2.1314
32	2.0783	2.0852	2.0611	2.1325
33	2.0760	2.0779	2.1013	2.1161
34	2.0739	2.0814	2.1037	2.1167
35	2.0770	2.0815	2.0956	2.1155
36	2.0755	2.0843	2.0970	2.1150
37	2.0570	2.0724	2.0455	2.1195
38	2.0602	2.0752	2.0426	2.1233
39	2.0564	2.0765	2.0452	2.1158
40	2.0572	2.0798	2.0432	2.1204
41	2.0515	2.0795	2.0703	2.1306
42	2.0503	2.0767	2.0709	2.1376
43	2.0498	2.0764	2.0764	2.1331
44	2.0480	2.0746	2.0750	2.1401
45	2.0412	2.0708	2.0609	2.1186
46	2.0406	2.0670	2.0628	2.1226
47	2.0417	2.0683	2.0660	2.1176
48	2.0430	2.0621	2.0688	2.1225
49	2.0461	2.1008	2.0739	2.1106
50	2.0436	2.0885	2.0721	2.1144

TABLE 7. (continued)

set #	low oxygen	medium oxygen	high oxygen	float-zone
51	2.0437	2.1017	2.0760	2.1078
52	2.0415	2.0904	2.0732	2.1114
53	2.0515	2.1012	2.0519	2.1350
54	2.0512	2.0956	2.0511	2.1347
55	2.0434	2.0972	2.0526	2.1399
56	2.0441	2.0912	2.0526	2.1391
57	2.0484	2.0721	2.0621	2.1296
58	2.0459	2.0773	2.0619	2.1248
59	2.0435	2.0773	2.0603	2.1294
60	2.0431	2.0796	2.0604	2.1211
61	2.0440	2.0561	2.0771	2.1184
62	2.0444	2.0661	2.0747	2.1211
63	2.0369	2.0620	2.0796	2.1237
64	2.0394	2.0685	2.0800	2.1272
65	2.0495	2.0817	2.0855	2.1252
66	2.0504	2.0820	2.0862	2.1283
67	2.0400	2.0799	2.0856	2.1242
68	2.0410	2.0796	2.0845	2.1243
69	2.0173	2.0910	2.0962	2.1269
70	2.0164	2.0955	2.0984	2.1265
71	2.0157	2.0892	2.0868	2.1274
72	2.0159	2.0918	2.0887	2.1258
73	2.0448	2.0863	2.0860	2.1333
74	2.0466	2.0839	2.0829	2.1351
75	2.0409	2.0921	2.0849	2.1330

TABLE 7. (continued)

set #	low oxygen	medium oxygen	high oxygen	float-zone
76	2.0410	2.0894	2.0839	2.1336
77	2.0413	2.0818	2.0845	2.1202
78	2.0419	2.0793	2.0836	2.1194
79	2.0363	2.0840	2.0832	2.1143
80	2.0376	2.0791	2.0839	2.1134
81	2.0122	2.0770	2.0838	2.0504
82	2.0153	2.0736	2.0817	2.0547
83	2.0105	2.0757	2.0856	2.0545
84	2.0132	2.0715	2.0823	2.0569
85	2.0161	2.0661	2.0884	2.0535
86	2.0176	2.0688	2.0910	2.0546
87	2.0165	2.0695	2.0883	2.0485
88	2.0173	2.0716	2.0899	2.0496
89	2.0157	2.0829	2.0874	2.0461
90	2.0164	2.0786	2.0926	2.0488
91	2.0168	2.0775	2.0875	2.0471
92	2.0168	2.0758	2.0899	2.0510
93	2.0200	2.0684	2.1344	2.0462
94	2.0228	2.0675	2.1361	2.0535
95	2.0173	2.0663	2.1335	2.0420
96	2.0200	2.0679	2.1348	2.0482
97	2.0113	2.0794	2.1372	2.0554
98	2.0123	2.0767	2.1389	2.0587
99	2.0062	2.0791	2.1349	2.0721
100	2.0061	2.0788	2.1359	2.0730

APPENDIX A. SAMPLE CERTIFICATE

National Institute of Standards & Technology

Certificate of Analysis

Standard Reference Material 2551

Oxygen Concentration in Silicon Standard

SRM Set No.: 1

This Standard Reference Material (SRM) is intended for calibration of infrared spectrophotometers used to measure the 1107 cm^{-1} interstitial oxygen peak in silicon. Certified oxygen concentrations are given for low, medium, and high oxygen level Czochralski specimens. Each SRM unit is a set of four specimens comprising a float-zone specimen [with minimal oxygen concentration less than 0.1 parts per million atomic (ppma)], and the three Czochralski specimens which cover a range of roughly 8.5-17 mg/kg (15-30 ppma - (IOC-88)). [1-3] Each specimen has been individually measured and bears an SRM set number and a letter identification for each oxygen level (L, M, or H). Each specimen is nominally 25-mm square and 2-mm thick and has been polished on both sides. The specimen materials, which were obtained from Wacker Siltronic, Portland, OR, have resistivities greater than 3 ohm•cm.

CERTIFIED VALUES OF OXYGEN CONCENTRATION

Units	Low Level (L)	Medium Level (M)	High Level (H)
ppma	16.837	22.781	26.250
mg/kg	9.591	12.978	14.954
10^{17} atoms/cm^3	8.408	11.377	13.109

UNCERTAINTY OF CERTIFICATION (ppma)*

Low Level	Medium Level	High Level
0.029 (0.17 %)	0.030 (0.13 %)	0.031 (0.12 %)

NON-CERTIFIED THICKNESS VALUES (mm)

Float-Zone	Low Level	Medium Level	High Level
2.1207	2.0726	2.0347	2.0775

* The stated uncertainty is the 2σ precision with which the oxygen scale obtained from the eight-specimen calibration set is reproduced in each of the SRM sets. This does not include the uncertainty of the absolute values of oxygen for the calibration specimens. The certified portion of the SRM specimen is the central 6-mm diameter circle. Thickness values are not certified and are given as useful information only. To convert from ppma to mg/kg, multiply by 0.56967; to convert from ppma to atoms/cm^3, multiply by 0.49939 × 10^{17}.

Certification measurements were made by B.G. Rennex and sample preparation was done by J.M. Thomas, both of the NIST Semiconductor Electronics Division. The work was supported by the Materials Technology Group of this Division. Review of the statistical analyses was performed by J.J. Filliben of the NIST Statistical Engineering Division.

The preparation, certification, and issuance of this SRM were coordinated through the Standard Reference Materials Program by N.M. Trahey.

Gaithersburg, MD 20899
March 1, 1994

Thomas E. Gills, Acting Chief
Standard Reference Materials Program

(over)

Certification Apparatus: Power spectra were measured in the wavenumber vicinity of 1107 cm^{-1}, the location of the room temperature peak for interstitial oxygen, by a Fourier Transform Infrared (FTIR) spectrophotometer. The detector system comprised a gold-plated light-cone and a 2 mm-diameter, room temperature deuterated-triglycine-sulfate (DTGS) detector. The beam diameter at the specimen was 5 mm, and it was located at the specimen center to within $\pm$ 1 mm. The wavenumber resolution was 4 cm^{-1}. During the measurement, the sample chamber of the FTIR instrument was maintained at a temperature of 27.8 $\pm$ 0.5 °C. No detectable spurious blackbody radiation was found. [4]

Certification Measurement Protocol: In general, a certification measurement determination consisted of the following steps:

1a. Two SRM sets of four specimens each were mounted on a sample holder, along with a control specimen of known, medium oxygen concentration. After specimen loading, it was necessary to wait about an hour for transient thermal effects to reach steady state. Then, power spectra were measured in a test run in the following sequence: open beam; control specimen; first set (float-zone, low oxygen, medium oxygen, and high oxygen); open beam; control specimen; and second set (float-zone, low oxygen, medium oxygen, and high oxygen).

1b. Each power spectrum in the above test sequence was based on 90 scans, which took about five minutes, and at least four repeats of this sequence were made for each run. Thus, a certified oxygen value is computed using the average of four 5-min measurements spaced over a period of roughly 8 h.

2. The transmission spectrum for each specimen was calculated as the ratio of the specimen power spectrum over the open-beam power spectrum.

3. Absorption (coefficient) spectra were calculated for each test specimen and for each float-zone specimen. [1] The float-zone spectrum was then subtracted from the test specimen spectrum to arrive at the spectrum due to oxygen only.

4. The oxygen peak height was obtained as follows. A Gaussian curve fit to the absorption spectrum was made to determine the peak height and wavelength. A baseline was constructed, and the baseline value at the peak wavelength was subtracted from the peak height to calculate the net oxygen peak height.

5. Data on the control specimen were used to make a linear compensation for instrument drift over time; this improved instrument reproducibility by about a factor of three. Measurements were made on a separate four-specimen set (comprising a float-zone specimen and specimens at three oxygen levels) between each SRM run. These runs were made using the same procedure, including the use of a control specimen, as for the SRM runs, and they provided an estimate of the random uncertainty, or reproducibility, of the instrument over the entire period of SRM measurements.

Calibration of the NIST FTIR instrument was based on measurements of a subset of eight reference specimens from a larger set of specimens previously used in an international study called the Grand Round Robin (GRR). [2,3] The bias of the eight-specimen subset with respect to the complete GRR specimen set is -0.72%, as established by the GRR data. The measurements made to certify the SRM have been adjusted to eliminate this bias. These calibration measurements allowed a determination of an SRM conversion coefficient (from α to oxygen concentration) specific to the NIST FTIR instrument. The certified SRM oxygen concentration values are based on this SRM conversion coefficient, not on the GRR conversion coefficient. [4,5]

Also, a study was made to ascertain that no additional error was observed when repeated points were taken after a specimen had been removed from and replaced back into the sample holder. Initially, a significant offset occurred due to removal and replacement of a specimen, perhaps because of non-uniformities in the beam and detector at this level of precision. This error was eliminated when a light-cone was used in the detector assembly. [4]

Uncertainties: The SRM uncertainty is based on the precision of the NIST FTIR spectrophotometer and on uncertainties due to non-uniformity of thickness and oxygen concentration over the central 6-mm area of the SRM specimen sampled by the FTIR beam. Standard deviations were estimated for the various contributing factors (all of which are ISO Type A) and added in quadrature. [6] This sum was multiplied by a factor of two to get a 2σ value for the expanded uncertainty. The first contributing factor is instrument reproducibility, as estimated by the standard deviation for data taken on the NIST FTIR for the four-specimen set. The standard deviation of the reproducibility, as determined in a series of measurements independent of and concurrent with the certification measurements, is 0.0115 ppma for all three oxygen levels. The second contributing factor is variability of both thickness and oxygen concentration from one area to another over the specimen surface. The standard deviation for this factor is 0.0051 ppma for low oxygen, 0.0069 ppma for medium oxygen, and 0.0078 ppma for high oxygen specimens. The third contributing factor is variability of oxygen among the float-zone, or "zero-oxygen," SRM specimens. The standard deviation for this variation is 0.007 ppma, for all three oxygen levels.

Adding these three values of standard deviation in quadrature, and multiplying by two, gives the following 2σ estimates of total SRM precision: 0.029 ppma (0.17%) for low oxygen specimens, 0.030 ppma (0.13%) for medium oxygen specimens, and 0.031 ppma (0.12%) for the high oxygen specimens. These values of total SRM precision are intended to be of practical use for current IC industrial requirements. They are much smaller than the uncertainty values of an absolute measurement of oxygen concentration. They are also much smaller than the interlaboratory variability of 2.7% (1σ) from the GRR report, and this interlaboratory variability is an indication of the interlaboratory agreement expected without an SRM. [2,3]

The certified oxygen concentration values are independent of temperature and are internally consistent from any one SRM specimen or set to any other, to within the above-stated total SRM precision. And, if two distinct instruments calibrated by two different SRM sets were to have the same precision as the certifying spectrometer, the agreement between their values for identical specimens would be described by a precision equal to roughly twice the total SRM precision. That is, four separate σ values - one for each SRM and one for each instrument - would be added in quadrature to estimate the total comparison standard deviation.

RECOMMENDED CALIBRATION AND HANDLING INSTRUCTIONS FOR SRM 2551

Calibration Procedure: The detailed procedure for calibration of a user instrument will depend on the particular application. For guidance, a user should refer to standard test methods for measurement of oxygen in silicon. [1,7] More information is contained in the SRM certification report and in documents which explain the SRM experiment and the statistical methodology in greater detail. [4,5,8]

It is recommended that both the open beam and float-zone specimen be measured every time a calibration is made, unless a user can demonstrate that this is unnecessary. Such a demonstration would involve a statistical comparison of results with the open beam and float-zone spectra measured every time against results where this is not the case.

To obtain the best agreement with the certified SRM values, a user must use a 5-mm beam and must locate this beam at the center of the SRM specimen, to within 1 mm. Also, the user should make sure that the temperatures of the specimens to be measured are as close as possible to the temperatures of the SRM specimens. This is because the user calibration factor is temperature dependent even though the certified oxygen value is not. [7] That is, the measured absorption coefficient peak height varies with temperature in this range with a coefficient of 0.0016 K^{-1}, while the actual oxygen concentration remains constant. This means that the certified estimate of oxygen concentration can be used without adjustment even if a user's measurement temperature is different from the value used in the SRM 2551. However, the user must expect his own oxygen conversion coefficient to vary with temperature according to the just-quoted temperature coefficient.

The certified quantity is the interstitial oxygen concentration, OX_{srm}, for the low, medium, and high oxygen specimens. This oxygen concentration is proportional to the height of the 1107 cm^{-1} peak of the absorption coefficient spectrum, with the constant of proportionality being the conversion coefficient. Without an SRM, a user calculates an oxygen value, OX_u, as a product of a measured absorption coefficient peak height and the internationally accepted conversion coefficient, C. [2,3] With the SRM, the instrument conversion coefficient must be adjusted by a calibration factor determined from the calibration. This calibration factor is equal to the ratio, R_u, of (OX_{srm}/OX_u), where OX_{srm} is the certified oxygen value for an SRM specimen, and OX_u is the measured oxygen value for that same SRM specimen using the international value of C.

The subscript j = l, m, or h, identifies each of the three SRM specimens. R_{uj} refers to the three calibration factor values obtained by the user, u, with the three SRM specimens. For the three SRM specimens, the ratios, $R_{uj}=(OX_{srmj}/OX_{uj})$ are the calibration factors for the user instrument, and the products, R_{uj} x C, are the conversion coefficients for the user instrument. These three conversion coefficients may now be used to calculate oxygen values for unknown specimens.

In general, a user should evaluate the three calibration factors for the low, medium, and high level oxygen SRM specimens, but then must choose which value to use in a particular measurement. If the three values are close (e.g. within the reproducibility of the user instrument), the average of all three values should be used. If there are larger differences in the three calibration factors, R_{uj}, the user may use the calibration factor of the SRM specimen with the closest value to that of the unknown specimen. Alternatively, a user can use an interpolation, an example of which is given below. This example is for an unknown specimen with an oxygen value between those of the low and medium level SRM specimens.

Let OX_{ul}, OX_{um}, and OX_x be the user-measured, peak-height values for the low and medium SRM specimens, and for the unknown specimen, respectively. And, let R_{ul} and R_{um} be the previously determined calibration factors for the same SRM specimens. The interpolated value of the calibration factor, R_x, is then:

$$R_x = R_{ul} + (OX_x - OX_{ul})\,(R_{um} - R_{ul}) / (OX_{um} - OX_{ul})$$

An interpolation in the range between the mid-oxygen specimen and the high-oxygen specimen can be made in an equivalent manner.

Handling Procedures: The SRM specimens are mounted on aluminum templates. Do not touch the polished surfaces of the SRM specimens with the fingers or with any hard or abrasive material. Handle the specimens by holding the aluminum templates. If it should be necessary to remove specimens from these templates, please follow the instructions below:

1. Gradually warm the template to approximately 70 °C or until the mounting wax begins to flow. Carefully remove the specimen with non-metallic tweezers or with a vacuum wand, taking care not to scratch the specimen surface.

2. While the specimen is still warm, flush it with tepid methyl alcohol, or an alternative solvent, until all wax is removed. Clean cotton may be used with the alcohol.

3. After all traces of wax have been removed with the alcohol, wash with a warm solution of liquid detergent and de-ionized water to ensure that all wax residue has been removed. Then, rinse with de-ionized water to remove all traces of detergent.

4. Make a final rinse with methyl alcohol and blow dry with nitrogen to avoid spotting.

5. To replace a specimen into the aluminum templates, put four dabs of mounting wax on the four inside corners of the template. Slowly heat the template until the wax begins to flow. Place the specimen (at room temperature) squarely into the recesses of the template and continue to press it against the template with a cotton swab until the wax begins to flow again. Finally, allow the template to cool.

ADDENDUM

The following additional information is given here in view of a recent publication [8]: All SRM 2551 specimens are n-type. This means that there is no measurable error due to free-carrier absorption in the vicinity of the 1107 cm^{-1} oxygen peak [9].

REFERENCES

[1] ASTM Standard F1188, Standard Test Method for Interstitial Atomic Oxygen Content of Silicon by Infrared Absorption," Annual Book of ASTM Standards, Vol. 10.05, ASTM, Philadelphia, PA, 1991.

[2] Baghdadi, A., Bullis, W.M., Croarkin, M.C., Li, Yue-zhen, Scace, R.I., Series, R.W., Stallhofer P., and Watanabe, M., "Interlaboratory Determination of the Calibration Factor for the Measurement of Interstitial Oxygen Content of Silicon by Infrared Absorption," J. Electrochem. Soc. 136, 2015-2024, 1989.

[3] Baghdadi, A., Scace, R.I., and Walters, E.J., Semiconductor Measurement Techology: "Database for and Statistical Analysis of the Interlaboratory Determination of the Conversion Coefficient for the Measurement of the Interstitial Oxygen Content of Silicon by Infrared Absorption," NIST Special Publication 400-82 , 1989.

[4] Rennex, B.J., NIST Special Publication 260-121, Standard Reference Materials: "The certification of a Standard Reference Material for the Determination of Interstitial Oxygen Concentration in Semiconductor Silicon by Infra-Red Spectrophotometer," (in prep).

[5] Rennex, B.J. and Ehrstein, J.R., "Methodology for the Utilization of High-Precision/Reduced-Absolute-Accuracy Measurements in Standard Reference Materials," (to be published in the NIST J. of Res., 1994).

[6] "*Guide to the Expression of Uncertainty in Measurement*," ISO, Geneva, Switzerland, 1993. Available from Bureau International des Poids et Mesures, Pavilon de Breteuil, F-92312 Sevres Cedex, France.

[7] DIN Standard 50 438/1, "Determination of Impurity Content in Semiconductors by Infrared Absorption; Oxygen in Silicon," Beuth Verlag, Berlin (1993) [in German. An English translation is published in the Annual Book of ASTM Standards, Vol. 10.05, ASTM, Philadelphia, PA (1993).]

[8] Kitagawara, Y., Tamatsuka, M., Takenaka, T., "Accurate Evaluation of Interstitial Oxygen Concentrations in Medium-Resistivity Si Crystals," J. Electrochem. Soc. 141 (5), 1362-1364, May 1994.

[9] Gladden, W.K., Baghdadi, A., "Free Carrier Absorption and Interstitial Oxygen Measurements, "Emerging Semiconductor Technology, ASTM STP 960, D.C. Gupta and P.H. Langer, Eds., American Society for Testing and Materials, 1986.

APPENDIX B. CALCULATION OF ABSORPTION COEFFICIENT PEAK HEIGHT

The following derivation expresses the absorption coefficient, α, in terms of the measured transmittance, T, through a double-side-polished wafer. These are spectral quantities which have peaks due to impurities. The goal is to calculate an oxygen peak height. Equation (1) expresses T in terms of α and x, the wafer thickness. T is actually a ratio of a test specimen power spectrum over an open-beam power spectrum. Figure 2 shows transmittance for the oxygen specimen and a float-zone specimen (nominally with zero oxygen content) at the oxygen peak. Figure 3 shows absorption coefficient spectra for the same, as well as their difference, which is the peak due to oxygen only.

$$T = \frac{(1 - R)^2 \, e^{-\alpha x}}{1 - R^2 \, e^{-2\alpha x}} . \tag{1}$$

The numerator incorporates the fact that there is a reflection at both surfaces and there is absorption across the thickness of the wafer. The denominator results from multiple reflections within the specimen.

$$let \; z = e^{-\alpha x} .$$

$$define \; C_1 = \frac{(1-R)^2}{2R^2} .$$

$$define \; C_2 = \frac{4R^2}{(1 - R)^4} .$$

Solving the quadratic equation in z gives

$$z = \frac{C_1}{T}\left(\left(1 + C_2 T^2\right)^{\frac{1}{2}} - 1\right) . \tag{2}$$

$$\alpha = -\left(\frac{1}{x}\right) \ln(z) . \tag{3}$$

Note that T refers to a ratio of power spectra with and without a specimen in the spectrophotometer beam; that is, T describes the loss due only to the specimen.

For the "oxygen in silicon" measurement, α is the sum of the following two terms: α_{ox} is the absorption coefficient due to interstitial oxygen and α_{si} is the absorption coefficient due to silicon. That is, the measured T_s for a silicon specimen with oxygen enables one to calculate α_s via eq (3), and $\alpha_s = \alpha_{ox} + \alpha_{si}$. What is really needed is α_{ox}, and this requires an independent measurement of α_{si}, which is measured on a float-zone, or zero-oxygen specimen. Then, α_{ox} = the measured value of α_s minus the measured value of α_{si}.

The peak height of α_{ox} is calculated by subtracting the value at the peak wave number of a baseline, which is a straight line between the curve values on either side of the 1107 cm^{-1} oxygen peak. Ideally, the baseline should be a constant zero; in practice it is not. A certain robustness is inherent to the method since errors due to optics are cancelled to some extent by two features of the calculation. First, the float-zone spectrum is subtracted from the unknown oxygen specimen; next, the baseline level of oxygen is subtracted from the peak level. To the extent that errors in the measured T values are multiplicative, they cancel. If these errors are additive, they cancel only partially, because of the nonlinearity of the expression for α in terms of T.

The following is a step-by-step explanation of the computer algorithm for calculation of oxygen concentration in silicon.

1. Measure a power spectrum, P, for the following cases:

   P_{open} - air reference (open beam)
   P_{fz} - silicon reference (floatzone, zero oxygen, or silicon background)
   P_s - oxygen specimen (silicon plus oxygen structure)

2. Calculate transmission spectra for the silicon reference and oxygen specimens.

   $T_r = P_{fz}/P_{open}$
   $T_s = P_s/P_{open}$

3. Calculate the absorption coefficient spectra, α_r and α_s using eq (3) in this appendix.

4. Calculate the absorption coefficient due to interstitial oxygen.

   $\alpha_{ox} = \alpha_s - \alpha_r$

5. Perform the curve fitting on the 1107 cm^{-1} oxygen peak as follows.

The baseline value is the average of two average values -- of points between 1030 and 1050 cm^{-1} on one side and between 1160 and 1180 cm^{-1} on the other side. The peak value is the result of a gaussian fit to points between 1096 and 1119 cm^{-1}. The difference of these values is the absorption coefficient peak height. Multiplication of this peak height by the conversion coefficient gives the oxygen concentration.

This method follows that of ASTM Method F1188 [6] except that the curve fitting is done on α_{ox} rather than on T_s and the range of values for baseline averaging is slightly different.

APPENDIX C. ISSUES RELATED TO THE CONVERSION COEFFICIENT

One goal of the SRM was to arrive at oxygen values which are consistent with the earlier GRR work [1,2]. The discussion below shows in mathematical terms that the use of the SRM conversion coefficient, C_i, determined with the NIST FTIR for SRM 2551, avoids any bias between the values of the SRM 2551 specimens and the values of the GRR specimens. On the other hand, if another conversion coefficient, e.g., the GRR value, were used, such a bias would occur.

The GRR study determined the GRR conversion coefficient, C, which was based on averages over many specimens and many laboratories and which was based on both spectrometer and absolute measurements. The combined results showed an interlab variability, which means that each instrument had a bias with respect to the average for all instruments.

Let Ci be a set of N conversion coefficients for N instruments (laboratories) in a study in which absolute measurements, A_{is}, have been made on a set of specimens, "s," along with relative instrument measurements, R_{is}. C_i is the average of R_{is}/A_{is} for a particular instrument, "i." In the case of the oxygen SRM, A_{is} is a value of oxygen concentration, and R_{is} is a peak height for the optically determined absorption coefficient. A_s is the average value for all instruments for specimen "s" (i.e., $C = \sum C_s/N$).

Each C_i has a difference from C, $D_i = C_i - C$. Assume that sufficient measurement points have been taken to ensure that the average of the D_i points is primarily due to the "i" instrument. This average value, D_i, represents a systematic instrument bias which must be duly considered and used to achieve the correct absolute value as estimated by the GRR study.

If a specimen is measured by instrument "i," and if C (the GRR average value) is used to calculate each A_{is}, the value of A_{is} will be wrong by an amount equal to $-D_i$. That is, if only one instrument were used to estimate each A_{is}, and if it used C instead of C_i, the value would be wrong by $-D_i$. This situation applies only when an instrument uses specimens for which each A_{is} (absolute oxygen value) was measured in the GRR.

If an instrument does not have access to the specimens used for absolute determinations, then C (i.e., the GRR mean value) conversion coefficient should be used, and the relevant precision for that measurement is the interlab precision in the GRR study. For the GRR study, the interlab precision, as estimated by 1-sigma, was 2.7%; the comparable value for the NIST precision was approximately 0.05%. Thus, the achievable internal consistency among high precision users of the NIST SRM can be about 50 times better than the internal consistency without an SRM (when a user must use the GRR coefficient). Also, if independent SRM studies were to be made by two different standards laboratories, the difference between their conversion coefficients would be the sum of any systematic difference in the absolute measurements and the bias between the two optical instruments.

A related issue is how to handle differences between different standards which depend on an absolute measurement with large uncertainties. The systematic difference in the absolute measurements would result in a systematic difference between the two standard reference materials. Such a difference could cause confusion among the various users of one or both of these standards. A practical solution which may be considered for future cases where more than one standard is developed, would be to thoroughly characterize the total systematic difference between two different standards and to report it to SRM users.

APPENDIX D. PRODUCTION RUN PROTOCOL

The measurement protocol was the following. Two sets of four wafers were placed in a 3 x 3 position specimen holder. Although there was originally room for only nine specimens, it was necessary to measure ten positions in all - eight specimens for the two production sets and a control specimen and a location for an open beam. For this reason, the center position of the specimen holder contained a control specimen with one quadrant of its area removed. When this empty quadrant was in the beam, an open beam spectrum was measured. When the opposite quadrant was in the beam, the control specimen spectrum was measured. Before the quadrant was removed, a comparison was made between the measured peak height at the center of the control specimen and at the quadrant to be used for the oxygen measurement. The reason was that the optical measurements in the GRR had been made on the center of this specimen. The comparison between these two peak height values was within 0.01%. For this reason, the fact that the center is not used does not result in a significant error in the slope determination discussed in section IV.

The measurement sequence was the following:

FIRST SET

1. open beam
2. control specimen
3. float-zone specimen
4. "level 1" specimen
5. "level 2" specimen
6. "level 3" specimen

SECOND SET

7. open beam
8. control specimen
9. float-zone specimen
10. "level 1" specimen
11. "level 2" specimen
12. "level 3" specimen

This sequence was repeated four times, without reloading, to give four oxygen values with respect to the float-zone specimen, for each of the three levels of oxygen peak height, for two complete specimen sets. Thus, each reported value of oxygen peak height is an average of four repeated measurements or points. Having an average reduces the chance of outliers. Also, the use of time plots over 8 h for each production run made it possible to verify that the curves for the various specimens were tracking in terms of any drift that may have been present. This was a necessary requirement to ensure that spurious transient effects were not present which might have affected the drift compensation.

Each spectrum was the result of 90 scans which took 4.5 min each. Spectra were checked for each run to ensure that the transmission at 2000 cm^{-1} was within $\pm 2\%$ of 53.8%, the expected value in nonabsorbing regions of the spectrum. The numbers of scans and repetitions were chosen as a compromise between achieving good averages for each point versus detailed information regarding drift.

The entire protocol required 8 h, and this resulted in measurement of two SRM sets. A wait period of an hour was required after loading of specimens, due to thermal transients caused by opening the instrument cover. The spectrometer was housed in a room with a temperature control good to $\pm 0.5°C$. Two of these protocols were performed in a day; thus, four SRM sets were measured per day. The remaining portion of the 24-h period was used to measure repeats of a set of performance evaluation specimens. The protocol for these tests was similar to that for the production run sets except that only one set (of three oxygen specimens plus a float-zone specimen) was measured in sequence instead of two sets. Control specimen measured values were used for drift compensation of the measured values for the three specimens in each SRM set, and each report value was the average of four measured values.

APPENDIX E. UNIT CONVERSIONS

There are three units of oxygen number fraction (concentration) commonly used: parts per million by weight (a mass fraction), ppm (wt) or mg/kg; parts per million atomic (a number fraction) or (ppma); and number per cm^3 times 10^{17} (a concentration within bulk silicon). The conversions between these are the following. Since ppm by itself is ambiguous, the (a) or (wt) are included.

$$O(10^{17}\ cm^{-3}) = (d_{Si} * N_A / A_O) * (ppm\ (wt)/10^6)$$

$$= 0.876633 * ppm\ (wt)$$

$$O(ppm\ (wt)) = (A_O / A_{Si}) * O\ ppm\ (a)$$

$$= 0.569668 * O\ ppm\ (a)$$

$$O(10^{17}\ cm^{-3}) = 0.876633 * 0.569668 * O\ ppm\ (a)$$

$$= 0.499389 * O\ ppm\ (a)$$

where

d_{Si} = density of silicon = 2.328995 g/cm^3 [10]
N_A = Avogadro's Number = $6.022169 * 10^{23}$ atoms/mol
A_O = atomic weight of oxygen = 15.9994 g/mol
A_{Si} = atomic weight of silicon = 28.0855 g/mol